

FOAM DRILLING SIMULATOR

A Thesis

by

AMIR SAMAN PAKNEJAD

Submitted to the Office of Graduate Studies of
Texas A&M University
in partial fulfillment of the requirements for the degree of

MASTER OF SCIENCE

December 2005

Major Subject: Petroleum Engineering

FOAM DRILLING SIMULATOR

A Thesis

by

AMIR SAMAN PAKNEJAD

Submitted to the Office of Graduate Studies of
Texas A&M University
in partial fulfillment of the requirements for the degree of

MASTER OF SCIENCE

Approved by:

Chair of Committee,	Jerome J. Schubert
Committee Members,	Hans Juvkam-Wold
	Reza Langari
Head of Department,	Stephen A. Holditch

December 2005

Major Subject: Petroleum Engineering

ABSTRACT

Foam Drilling Simulator.

(December 2005)

Amir Saman Paknejad, B.S., Petroleum University of Technology (PUT)

Chair of Advisory Committee: Dr. Jerome Schubert

Although the use of compressible drilling fluids is experiencing growth, the flow behavior and stability properties of drilling foams are more complicated than those of conventional fluids. In contrast with conventional mud, the physical properties of foam change along the wellbore. Foam physical and thermal properties are strongly affected by pressure and temperature. Many problems associated with field applications still exist, and a precise characterization of the rheological properties of these complex systems needs to be performed. The accurate determination of the foam properties in circulating wells helps to achieve better estimation of foam rheology and pressure.

A computer code is developed to process the data and closely simulate the pressure during drilling a well. The model also offers a detailed discussion of many aspects of foam drilling operations and enables the user to generate many comparative graphs and tables. The effects of some important parameters such as: back-pressure, rate of penetration, cuttings concentration, cuttings size, and formation water influx on pressure, injection rate, and velocity are presented in tabular and graphical form.

A discretized heat transfer model is formulated with an energy balance on a control volume in the flowing fluid. The finite difference model (FDM) is used to write the governing heat transfer equations in discretized form. A detailed discussion on the determination of heat transfer coefficients and the solution approach is presented.

Additional research is required to analyze the foam heat transfer coefficient and thermal conductivity.

DEDICATION

To my parents, brother, and Parisa

ACKNOWLEDGEMENTS

I wish to express my sincere thanks and appreciation to the chairman of my graduate advisory committee, Dr. Jerome J. Schubert, for his continuous guidance, enthusiasm and support throughout my graduate research. His knowledge and his invaluable assistance on my thesis were essential.

I also wish to thank Dr. Hans Juvkam-Wold and Dr. Reza Langari for serving on my graduate advisory committee.

I would like to express my highest gratitude to the faculty and staff at the Department of Petroleum Engineering at Texas A&M University for providing me the opportunity to pursue my studies at Texas A&M University.

Finally, thanks to my mother and father for their encouragement and to my fiancé for her support and love.

TABLE OF CONTENTS

	Page
ABSTRACT.....	iii
DEDICATION.....	iv
ACKNOWLEDGEMENTS.....	v
TABLE OF CONTENTS.....	vi
LIST OF FIGURES	viii
LIST OF TABLES	xi
 CHAPTER	
I INTRODUCTION	1
Foam Rheology	2
Foam Pressure Analysis.....	7
Heat Transfer	9
 II FUNDAMENTALS.....	 12
Foam Quality	12
Foam Specific Weight.....	14
Foam Velocity.....	15
Foam Friction Factor.....	15
Foam Hydrostatic and Friction Loss Analysis.....	16
Cuttings Removal Phenomena.....	17
Pressure Drop Across Bit Nozzles.....	18
Heat Capacity.....	19
 III FOAM DRILLING SIMULATOR.....	 21
Assumptions.....	21
Data Input.....	23
Run.....	25
Output Data.....	27
Features	40

CHAPTER	Page
IV HEAT TRANSFER	92
Development of Model	92
Bit Mechanical Energy	98
Solution	99
V CONCLUSIONS AND RECOMMENDATIONS	101
Conclusions	101
Recommendations	101
NOMENCLATURE	103
REFERENCES	107
VITA	111

LIST OF FIGURES

FIGURE	Page
3.1 Simulator Main Menu	22
3.2 Wellbore Geometry Input Data.....	23
3.3 Operative Input Data.....	24
3.4 Output Data Form	28
3.5 Output Data Graph Form	29
3.6 Bottom-hole Pressure vs. Depth	33
3.7 Liquid Injection rate vs. Depth	34
3.8 Liquid Injection Rate vs. Pressure	34
3.9 Gas Injection Rate vs. Depth	35
3.10 Gas Injection Rate vs. Pressure.....	35
3.11 Foam Quality vs. Depth	36
3.12 Foam Quality vs. Pressure	37
3.13 Foam Viscosity vs. Depth.....	38
3.14 Foam Viscosity vs. Foam Quality.....	38
3.15 Foam Velocity vs. Depth	39
3.16 Foam Velocity vs. Pressure.....	39
3.17 Back-pressure vs. Depth	40
3.18 Simulator Features	41
3.19 Bottom-hole Pressure vs. Depth at Different Back-pressures	43
3.20 Foam Quality vs. Depth at Different Back-pressures	44
3.21 Gas Injection Rate vs. Depth at Different Back-pressures	45
3.22 Minimum Required Injection Rates vs. Depth at Different Back-pressures ...	46
3.23 Flow Properties vs. Depth at Different Back-pressures	47
3.24 Deviation of Bottom-hole Pressure vs. Depth (Different Back-pressures).....	49
3.25 Deviation of Gas Injection Rate vs. Depth (Different Back-pressures).....	49
3.26 Deviation of Velocity vs. Depth (Different Back-pressures).....	50

FIGURE	Page
3.27	Deviation of Viscosity vs. Depth (Different Back-pressures)51
3.28	Deviation of Moody Friction Factor vs. Depth (Different Back-pressures)51
3.29	Deviation of Quality vs. Depth (Different Back-pressures)52
3.30	Bottom-hole Pressure vs. Depth at Different Rates of Penetration54
3.31	Minimum Injection Rates vs. Depth at Different Rates of Penetration55
3.32	Foam Flow Properties vs. Depth at Different Rates of Penetration.....56
3.33	Deviation of Bottom-hole Pressure vs. Depth (Different ROP)57
3.34	Deviation of Injection Rates vs. Depth (Different ROP)58
3.35	Deviation of Flow Properties vs. Depth (Different ROP).....59
3.36	Bottom-hole Pressure vs. Depth at Different Cuttings Concentrations61
3.37	Minimum Injection Rates vs. Depth at Different Cuttings Concentrations62
3.38	Flow Properties vs. Depth at Different Cuttings Concentrations63
3.39	Deviation of Bottom-hole Pressure vs. Depth (Different Concentrations).....64
3.40	Deviation of Injection Rates vs. Depth (Different Concentrations)65
3.41	Deviation of Flow Properties vs. Depth (Different Concentrations)66
3.42	Bottom-hole Pressure vs. Depth at Different Cuttings Diameters68
3.43	Minimum Injection Rates vs. Depth at Different Cuttings Diameters.....69
3.44	Foam Flow Properties vs. Depth at Different Cuttings Diameters70
3.45	Deviation of Bottom-hole Pressure vs. Depth (Different Diameters).....71
3.46	Deviation of Injection Rates vs. Depth (Different Diameters)72
3.47	Deviation of Flow Properties vs. Depth (Different Diameters).....73
3.48	Bottom-hole Pressure vs. Depth at Different Water Influx Rates75
3.49	Flow Properties vs. Depth at Different Water Influx Rates.....76
3.50	Minimum Injection Rates vs. Depth at Different Water Influx Rates77
3.51	GLR vs. Depth at Different Water Influx Rates78
3.52	Gas Injection Rate vs. Depth at Different Water Influx Rates79
3.53	Flow Properties vs. Depth at Different Water Influx Rates.....80
3.54	Deviation of Flow Properties vs. Depth (Different Influx Rates).....81
3.55	Bottom-hole Pressure vs. Depth at Different Injection Rates.....83
3.56	Foam Quality vs. Depth at Different Injection Rates83

Figure		Page
3.57	Gas Injection Rate vs. Depth at Different Injection Rates	84
3.58	Deviation of Gas Injection Rate vs. Depth (Different Injection Rates)	84
3.59	Flow Properties vs. Depth at Different Injection Rates	85
3.60	Deviation of Bottom-hole Pressure vs. Depth (Different Injection Rates)	86
3.61	Deviation of Quality vs. Depth (Different Injection Rates)	87
3.62	Deviation of Flow Properties vs. Depth (Different Injection Rates)	88
4.1	Control Volume in the Flowing Fluid	92

LIST OF TABLES

TABLE	Page
3.1 Output Results.....	30
3.2 Summary of Results (Deviations for Back-pressure)	53
3.3 Summary of Results (Deviations for ROP)	60
3.4 Summary of Results (Deviations for Cuttings Concentration)	67
3.5 Summary of Results (Deviations for Cuttings Diameter).....	74
3.6 Summary of Results (Deviations for Water Influx Rate)	82
3.7 Summary of Results (Deviations for Injection Rate).....	89
3.8 Summary of Effects of Parameters on the Pressure.....	90
3.9 Summary of Effects of Parameters on the Gas Injection Rate.....	90

CHAPTER I

INTRODUCTION

Stable foam could be described as a special type of aerated drilling fluids. Foam is made up of a mixture of incompressible fluids injected with compressed air or other gases. In foam as a gas-liquid dispersion the incompressible fluid is the continuous phase and the gas is the discontinuous phase. The incompressible component is usually the mixture of treated fresh water and a surfactant foaming agent. Additives and foaming agents such as polymers, graphite, and asphalt can be added to the foam as viscosifiers, stabilizers, lubricants, and corrosion inhibitors. The compressible component is usually air, nitrogen, natural gases, and rarely CO₂.

Stable foam fluids were first used in workover operations back in 1969¹. Since the first use of foam as drilling fluid in the late 1980s, it has been proved that use of drilling fluids that have hydrostatic flowing pressures less than pore pressures of the potential producing rock formations would increase the drilling and production rates. Underbalanced drilling has proven its efficiency in numerous situations where serious problems were encountered with conventional drilling operations. Fractured formations and depleted or high permeability zones are ideal candidates for foam drilling. The effectiveness of stable foam in countering these problems would be between the effectiveness of air drilling and aerated drilling. The actual selection of stable foam drilling fluid over either air drilling or aerated drilling fluids is not a distinct analytic process. Such a selection is usually made after investigating the drilling problem experiences in drilled wells of that specific drilling area.

This thesis follows the style of *SPE Drilling & Completion*.

Major advantages provided by the foam drilling technique are reduction of lost circulation and differential sticking, prevention of formation damage, improvement in rate of penetration, improved economics and life cycle, continuous drill stem test, and the ability to produce reservoir fluids while drilling.

A DOE research study by Medley *et al.*² forecasted that by the year 2005, UBD in the United States would account for 10,000 to 12,000 wells per year, or up to 37% of all wells. This would increase the annual cost of UBD operations to about U.S. \$6 billion.

Although the use of compressible drilling fluids is experiencing growth, the flow behavior and stability properties of drilling foams are more complicated than those of conventional fluids. Many problems associated with field applications still exist, and a precise characterization of the rheological properties of these complex systems needs to be performed.

Foam Rheology

The concept of foam rheology was first discussed by Sibree³ in 1934. He found that the apparent viscosity of foam was higher than that of each its constituents. He also found that foam shows Newtonian behavior below of critical shear-stress value and plug flow behavior above of that.

The study of fire-fighting foam behavior by Grove *et al.*⁴ produced one of the earliest, most enlightening papers on foam rheology. By measuring the effects of pressure, shear stress, and foam quality on the apparent viscosity, they indicated that at high shear rates the apparent viscosity is independent of shear rate. They also found that at constant pressures viscosity highly depends on foam quality and varies directly with foam quality.

Fried's⁵ results with a modified rotational viscometer were also consistent with the previous works. He found that foam viscosity decreased with decreasing foam quality and increased with increasing tube diameters.

Raza and Marsden⁶ study of foams with qualities ranging 0.7 - 0.96 stated that foam shows pseudoplastic behavior below critical flow rates and plug flow behavior above that. They found that the critical flow rate is dependent on both foam quality and tube diameter. They did not correct their experiments for slippage at the tube wall and for the compressibility of the foam.

David and Marsden⁷ corrected the experimental results for the both semi-compressibility and slippage at the wall. They concluded that corrected viscosity for both slippage and compressibility is independent of foam quality. They also found that slip coefficient increased with shear stress, but the corrected apparent viscosity still increased with the tube diameter.

Einstein's⁸ theoretical development was the first mathematical treatment of rheological problems in foam. He considered the foam as a suspension of solids in liquid. Based on the energy balance criteria his two-phase viscosity for the foam quality ranging from 0 to 0.45 is given by;

$$\mu_F = \mu_u (1 + 2.5\Gamma), \dots\dots\dots(1.1)$$

Where;

μ_F = Foam viscosity

μ_u = Base liquid viscosity

Γ = Foam quality

Hatschek⁸ developed a similar foam rheology model based on Stoke's law for foam quality ranging from 0 to 0.74 as;

$$\mu_F = \mu_u (1 + 4.5\Gamma), \dots\dots\dots(1.2)$$

He also described the viscosity of foam for qualities between 0.74 and 0.99. It was based on conservation of energy during interference, deformation, and packed bubbles within a flow boundary. His proposed model for the foam viscosity is;

$$\mu_F = \mu_u \left(\frac{1}{1 - \Gamma^{\frac{1}{3}}} \right), \dots\dots\dots(1.3)$$

This equation is only applicable in high shear rates, where the foam viscosity is almost independent of shear rate.

Mitchell⁹ developed his model based on Rabinowitsch's theory. He proposed two empirically derived equations for foam viscosity. The equations of foam viscosity for foam qualities from 0 to 0.54 and 0.54 to 0.97 are expressed respectively as;

$$\mu_F = \mu_u (1 + 3.6\Gamma), \dots\dots\dots(1.4)$$

$$\mu_F = \mu_u \left(\frac{1}{1 - \Gamma^{0.49}} \right), \dots\dots\dots(1.5)$$

In contradiction with previous models that pertained only to capillary tubes, Beyer *et al.*¹⁰ were the first to present a model based on both laboratory and pilot-scale tests. They followed Mooney's procedure to correlate slip velocity with liquid volume fraction and wall shear stress. The authors stated that the accuracy of their model in large diameter wells may be increased by accounting for liquid buildup. Using yield shear stress obtained in pilot-scale experimental data, the viscosity is given as;

For $0.02 < \text{LVF} < 0.1$;

$$\mu_o = \frac{1}{(7200\text{LVF} + 267)}, \dots\dots\dots(1.6)$$

For $0.1 < \text{LVF} < 0.25$;

$$\mu_o = \frac{1}{(2533LVF + 733)}, \dots\dots\dots(1.7)$$

where;

LVF = Liquid Volume Fraction

μ_o = Bingham Viscosity

Blauer *et al.*⁸ proposed to use effective viscosity, density, average velocity, and pipe diameter to calculate Reynolds number and Fanning friction factor for foam fluids. They found the relationship between Reynolds number and Fanning friction factor for foam was the same as that of single-phase fluid. They assumed that foam behaves like a Bingham plastic fluid and foam plastic viscosity and yield strength experimentally determined as a function of foam quality.

Their proposed equation for effective viscosity of Bingham plastic foam is given as;

$$\mu_e = \mu_p + \frac{g_c \tau_y D}{6v}, \dots\dots\dots(1.8)$$

where;

μ_e = Effective Viscosity

μ_p = Plastic Viscosity

$g_c = 32.2$

τ_y = Yield strength

D = Tube inside diameter

v = Velocity

Reidenbach *et al.*¹¹ performed experimental work with water foams using nitrogen as an internal phase. They proposed a Herschel-Bulkely model to describe a laminar foam flow through pipes. They found that substitution of CO₂ for N₂ as the internal phase gives similar laminar rheology. A modified scale-up relationship was used to describe

compressibility in turbulent flow. They defined a correlation for apparent viscosity that is used as a Newtonian viscosity in standard pressure drop calculations. Apparent viscosity is defined as;

$$\mu_a = \tau_{yp} \left(\frac{8v}{d} \right)^{-1} + K \left(\frac{8v}{d} \right)^{n-1}, \dots\dots\dots (1.9)$$

where;

μ_a = Apparent Viscosity

τ_{yp} = True yield point stress

d = Pipe inside diameter

v = Bulk velocity

K = Consistency index

Sanghani ¹² set up an experiment with a concentric annular viscometer to closely simulate actual wellbore conditions. He found that the Power-Law model was statistically superior to the Bingham model in correlating their data. He concluded that foam is pseudoplastic at low shear rates and Bingham plastic at high shear rates. He also provided experimental data to correlate pseudoplastic parameters K and n , as a function of foam quality as below;

$$K = -.15626 + 56.147\Gamma - 312.77\Gamma^2 + 576.65\Gamma^3 + 63.960\Gamma^4 - 960.46\Gamma^5 - 154.68\Gamma^6 + 1670.2\Gamma^7 - 937.88\Gamma^8, \dots\dots\dots (1.10)$$

$$n = 0.095932 + 2.3654\Gamma - 10.467\Gamma^2 + 12.955\Gamma^3 + 14.467\Gamma^4 - 39.673\Gamma^5 + 20.625\Gamma^6, \dots\dots\dots (1.11)$$

And;

$$\mu_e = K \left(\frac{2n+1}{3n} \right)^n \left(\frac{12v_f}{D_H} \right)^{n-1}, \dots\dots\dots (1.12)$$

where;

D_H = Hydraulic diameter

Recently Ozbayoglu *et al.*¹³ conducted a rheological study for foam. They conclude that wall slip effect is not negligible and should be considered to establish the true flow behavior of foam in pipes. Their experimental data indicated that foam rheology was best characterized by the Power-Law model for foam qualities ranging 0.7 to 0.8 and the Bingham plastic model gives better fit for higher foam qualities. By using the Rabinowitch-Mooney equation the rate of shear at the tube wall is given as follows;

$$\gamma_w = \frac{8v}{D} \frac{3n+1}{4n}, \dots\dots\dots(1.13)$$

where;

$$n = \frac{d \ln(\tau_w)}{d \ln\left(\frac{8v}{D}\right)}, \dots\dots\dots(1.14)$$

where;

γ = Wall shear rate

τ_w = Wall shear stress

Foam Pressure Analysis

The study of static and dynamic behavior of foam has been a subject of interest to many investigators. In drilling with conventional incompressible drilling fluids, it is possible to calculate frictional and hydrostatic pressures separately and then to determine the overall pressure drop. In drilling with foam such a method is not possible because the frictional and hydrostatic pressure components influence each other. Iterative methods seem to be the best approach when dealing with compressible fluids.

Krug and Mitchell¹⁴ were the first to develop charts for finding volume and injection-pressure requirements for foam drilling operations. They developed a numerical model

based on modified Buckingham-Reiner equations. They assumed incremental pipe lengths with fixed pressure drop along the wellbore and pressure-dependent variables were averaged over each pressure increment.

Beyer *et al.*¹⁰ developed a finite-difference approach for predicting injection pressures during foam circulation. Their model was found to be valid for foam qualities greater than 0.75. For foam qualities below 0.75 they proposed that frictional gradients be interpolated between that of 0.75-quality foam and the value for flowing water of the same velocity.

Blauer *et al.*⁸ proposed a method in which an effective Newtonian viscosity and foam density are calculated and hydraulic analysis proceeds as if the fluid were an incompressible Newtonian fluid. They assumed gas-phase density to be negligible. To revise this assumption Blauer and Kohlhaas¹⁵ proposed another model that iterates on length. To monitor the changes in quality, velocity, viscosity, and pressure, the wellbore was divided into length segments. The real gas law was used to account for gas compressibility.

Okpobiri and Ikoku¹⁶ developed an iterative semi-empirical method for the prediction of frictional losses caused by the solid-liquid phase of foam. Foam flow in this method was mathematically modeled as Ostwald-de Waele Power-Law fluid and solutions were obtained by iterating on pipe/annulus segments length.

Guo *et al.*¹⁷ presented a trial and error method to estimate the frictional and hydrostatic pressures. They coupled the pressure components through the pressure-dependent fluid density. Foam was treated a power law fluid.

Lord¹⁸ was the first who used a different more sophisticated approach. He developed an equation of state based on the real gas law and mass balance conservation. He assumed an average friction factor for the entire system and numerically solved the mechanical

energy balance equation for compressible fluid flow. To produce good results with this method one needs to estimate the best appropriate value of friction factor.

Spoerker *et al.*¹⁹ proposed a new two-phase flow equation to modify Lord's solution. Instead of the real gas equation of state they suggested the use of the virial equation. They solved the differential mechanical energy balance equation and presented an explicit expression for pressure loss of foam flow.

Liu and Medley²⁰ modified the previous work with accounting for formation fluids influx.

Gardiner *et al.*²¹ proposed an alternative approach by combining the "Volume Equalized Power Law" model and Hagen-Poiseuille equation. They also derived an explicit expression for foam flow pressure losses.

Guo *et al.*²² recently presented a closed form hydraulics equation for predicting bottomhole pressure for foam drilling operations. Their analytical model couples the frictional and hydrostatic pressure components in vertical and inclined wellbores. In this newly developed model foam, is considered to have the Power-law behavior.

Heat Transfer

Unlike conventional mud, foam physical and thermal properties are strongly affected by temperature. Wellbore temperature plays an essential role in the prediction of foam rheological properties.

Foam thermal properties are the function of pressure and foam quality. Pressure on the other hand is a function of thermal properties and temperature, which makes the situation a little complicated especially in deep well drilling.

The accurate determination of the temperature in circulating wells helps to achieve better estimation of foam rheology and pressure. Several authors have proposed different models to predict the wellbore temperature during drilling operations.

Farris²³ was the first who showed a direct relation between well depth and circulating bottom-hole temperature. He developed a chart showing the circulating bottom-hole temperatures during cement jobs and his chart has formed a basis for calculation of bottom-hole temperatures during drilling operations.

Edwardson *et al.*²⁴ developed a method to compute the changes in formation temperature caused by circulation of mud during drilling. The Basis of their method was the analytical solution of the differential equation for heat conduction. The solution of the heat conduction equation was presented in a series of graphs that were used to determine formation temperature disturbance at various radii.

Crawford *et al.*²⁵ developed a model based on the Edwardson *et al.*²⁴ method to calculate wellbore temperatures during mud circulation. Their calculation technique provided temperatures, as function of time, wellbore geometry, and mud rate at varying depths in both the casing and annulus. Their method represented a numerical solution for the transient heat transfer at a given depth.

Holmes and Swift²⁶ proposed a simple analytical method for prediction of mud temperature in the drill pipe and annulus during drilling at any depth. Their mathematical model was based on the steady-state equation for heat transfer between the fluid in the annulus and the fluid in the drill pipe, combined with an approximate equation for the transient heat transfer between the fluid in the annulus and the wellbore formation. As a solution for heat transfer equations, temperatures were calculated as a function of well depth, mud rate, mud characteristics, and wellbore geometry.

Keller *et al.*²⁷ were the first to use the finite difference method (FDM) in their model. They developed a two-dimensional transient heat transfer model to predict the wellbore

temperatures at any depth. They also concluded that external heat sources such as frictional heating, rotational energy, and drill bit energy have significant influence on wellbore temperature.

Marshall and Lie²⁸ have developed a model to calculate both the transient and steady-state temperatures in the wellbore during drilling. A computer code based on FDM was developed to solve all the heat transfer equations simultaneously. The energy source terms were included in the model.

All of the earlier models are developed based on drilling with conventional mud, however, no model is yet developed for foam.

CHAPTER II

FUNDAMENTALS

Foam Quality

Foam quality is the volumetric ratio of gas-phase to gas/liquid-phase. The foam quality index Γ can be defined as;

$$\Gamma = \frac{V_g}{V_g + V_l + V_f}, \dots\dots\dots(2.1)$$

where;

V_g = Gas volume

V_l = Liquid volume

V_f = Formation fluid influx volume

The foam quality is a function of the pressure in the annulus. Most foams are stable when foam quality is between 0.6 - 0.97. In stable foam drilling operations the lower limit of foam quality is usually found at the bottom of the annulus and the higher limit at the top of the annulus. Qualities greater than 0.97 would cause the continuous cellular foam structure, that entraps the gaseous phase to become unstable and the foam turns into mist. When quality is less than 0.6, gas forms isolated bubbles that are independent of the liquid-phase and two phases can move with different velocities which breaks down the foam structure.

The ideal gas law gives;

$$\frac{P_s V_s}{T_s} = \frac{PV}{T}, \dots\dots\dots(2.2)$$

where;

P = Pressure at any point

P_s = Pressure at surface

T = Temperature at any point

T_s = Temperature at surface

V = Gas volume at any point

V_s = Gas volume at surface

Eq. 2.2 can be rearranged to;

$$V = \frac{P_s T}{P T_s} V_s, \dots\dots\dots (2.3)$$

Substituting **Eq. 2.3** into **Eq. 2.1** yields;

$$\Gamma = \frac{\frac{P_s T}{P T_s} Q_{gs}}{\frac{P_s T}{P T_s} Q_{gs} + Q_l + Q_f}, \dots\dots\dots (2.4)$$

where;

Q_{gs} = Gas injection rate

Q_l = Liquid injection rate

Q_f = Formation fluid influx rate

Gas-liquid ratio (GLR) is defined as;

$$GLR = \frac{Q_{gs}}{Q_l}, \dots\dots\dots (2.5)$$

In order to maintain the surface foam quality at the desired value, we need to set an appropriate gas-liquid injection ratio at surface. Based on the maximum allowable foam quality at surface without backpressure, the GLR is calculated as;

$$GLR = \frac{\Gamma_{\max}}{1 - \Gamma_{\max}} \left[\frac{1}{7.48} + \frac{5.615Q_f}{60Q_l} \right], \dots\dots\dots(2.6)$$

By substituting **Eq. 2.5** and **Eq. 2.6** into **Eq. 2.4**, the correlation for foam quality at any point can be expressed as;

$$\Gamma = \frac{\frac{P_s T}{PT_s} GLR}{\frac{P_s T}{PT_s} GLR + \frac{1}{7.48} + \frac{5.615Q_f}{60Q_l}}, \dots\dots\dots(2.7)$$

Foam Specific Weight

The specific weight of foam can be expressed as;

$$\gamma_f = \Gamma \gamma_g + (1 - \Gamma) \gamma_l, \dots\dots\dots(2.8)$$

where;

γ_g = Specific weight of gas phase

γ_l = Specific weight of liquid phase

The ideal gas law gives;

$$\gamma_g = \frac{S_g P}{53.3T}, \dots\dots\dots(2.9)$$

where;

S_g = Specific gravity of gas

Introducing **Eq. 2.9** into **Eq. 2.8** results in;

$$\gamma_f = \gamma_l - \left[\gamma_l - \frac{S_g P}{53.3T} \right] \Gamma, \dots\dots\dots(2.10)$$

Foam Velocity

Foam velocity can be expressed as;

$$v_f = \frac{Q_g + Q_l + Q_f}{A}, \dots\dots\dots(2.11)$$

where;

A = Cross sectional area of flow path

Introducing **Eq. 2.5** and **Eq. 2.6** into **Eq. 2.11**, the velocity of foam at any point is given by;

$$v_f = \frac{\frac{P_s T}{P T_s} GLR + \frac{1}{7.48} + \frac{5.615 Q_f}{60 Q_l}}{A} \left(\frac{144}{60} Q_l \right), \dots\dots\dots(2.12)$$

Foam Friction Factor

Determining friction factor is crucial for foam flow calculations. Assuming that stable foam flow falls into a laminar flow regime, the theoretical approach for the Moody friction factor is expressed as a function of Reynolds number:

$$f = \frac{64}{Re}, \dots\dots\dots(2.13)$$

With Reynolds number calculated as;

$$Re = \frac{\bar{v} D_H \bar{\rho}}{\mu_e}, \dots\dots\dots(2.14)$$

where;

f = Moody friction factor

Re = Reynolds number

\bar{v} = Average foam velocity

$\bar{\rho}$ = Average foam density

μ_e = Effective viscosity

It has been reported in several cases that the friction factor given by **Eq. 2.13** has been too high. Guo²⁹ developed an empirical correlation derived from two-phase flow regimes that gives good results for foam flow in conditions commonly encountered in foam drilling. This empirical approach which uses the weight flow rate is expressed as;

$$\dot{w} = 0.0765 S_g Q_g + 8.33 S_l Q_l, \dots\dots\dots(2.15)$$

where;

\dot{w} = Mass flow rate

$$D\rho v = 0.02173 \frac{\dot{w}}{D_H}, \dots\dots\dots(2.16)$$

$$f = 4 \times 10^{1.444 - 2.5 \log(D\rho v)}, \dots\dots\dots(2.17)$$

Foam Hydrostatic and Friction Loss Analysis

Consider foam flow in a vertical conduit section under steady-state conditions. Based on the first law of thermodynamics, the governing equation for flow is;

$$dP = \gamma_f \left[1 + \frac{f v_f^2}{2g D_H} \right] dL, \dots\dots\dots(2.18)$$

where;

P = Pressure

γ_f = Specific weight of foam

f = Moody friction factor

v_f = Foam velocity

D_H = Conduit hydraulic diameter

L = Conduit length

$g = 32.2$

Cuttings Removal Phenomena

In foam drilling operations volumetric injection rates of gas and liquid must meet the requirements of cuttings transport capacity and foam stability.

In contrast with air drilling, the minimum kinetic energy criterion for cuttings transport should not be used in foam drilling. The mixture of foam and cuttings can not be treated as a homogeneous system. Significant differences between foam and cuttings velocities may exist in the annulus. Therefore, the minimum drag force criterion is the best applicable option. Considering the laminar foam flow in normal foam drilling operations, the following equation is suggested by Moore³⁰ to estimate cuttings settling velocity in foam:

$$v_{sl} = 1.56 \frac{D_s (\rho_s - \rho_f)^{0.667}}{\rho_f^{0.333} \mu_e^{0.333}}, \dots\dots\dots (2.19)$$

where;

v_{sl} = Cuttings settling velocity

D_s = Cuttings equivalent diameter

ρ_f = Foam density

μ_e = Effective foam viscosity

The equation above is proposed for non-Newtonian Power-law fluids.

However, the required cuttings transport velocity depends on how fast the cuttings are generated by the drill bit and the amount of cuttings concentration allowed in the borehole during drilling.

When solid particles are settling down in a steady and still fluid of lower density, they first accelerate under the force of gravity and then decelerate due to the increasing drag force between the cuttings and the fluid. After a certain time, the velocity of the cutting reaches a constant value, known as terminal velocity. The cuttings terminal velocity is given by³¹;

$$v_{tr} = \frac{\pi d_h^2}{4 C_p A} \left[\frac{R_p}{3600} \right], \dots\dots\dots (2.20)$$

where;

v_{tr} = Terminal velocity

d_h = Hole diameter

C_p = Cuttings concentration

A = Annulus area

R_p = Rate of penetration

Finally, the foam velocity required to transport the cuttings to the surface is;

$$v_{foam} = v_{sl} + v_{tr}, \dots\dots\dots (2.21)$$

Pressure Drop Across Bit Nozzles

A nozzle is a device that causes the interchange of kinetic and internal energy of a fluid as a result of change in cross section of flow conduit. Nozzles are often installed into the orifices at the drill bit for better removal of cuttings. Pressure loss across the nozzles is usually very significant. There is no universal equation for predicting pressure loss across

bit nozzles for all types of drilling fluids. Based on gas fraction of fluids and flow regimes, different nozzle flow models are available.

One of the best models for estimating bit pressure drop for foam has been developed by Okpobiri and Ikoku¹⁶. The equation for pressure drop across bit nozzles is expressed as;

$$\Delta P_b = \frac{\bar{A}}{B} \left(\ln \frac{P_{bh}}{P_{bh} + \Delta P_b} + E V_n^2 \right), \dots\dots\dots (2.22)$$

$$\bar{A} = \frac{m_g \bar{z} RT}{M(m_g + m_l)}, \dots\dots\dots (2.23)$$

$$B = \frac{m_l}{\rho_l(m_g + m_l)}, \dots\dots\dots (2.24)$$

$$E = \frac{1}{2\bar{A}g_c}, \dots\dots\dots (2.25)$$

where;

ΔP_b = Pressure drop across the bit

P_{bh} = Bottom-hole pressure

v_n = Nozzle velocity

M = Gas molecular weight

m_g = Mass of gas

m_l = Mass of liquid

Heat Capacity

Like any two-phase mixture, heat capacity of foam is the average weighted heat capacity of each phase. Heat capacity of liquid-phase which is usually water, is a constant known value, however, heat capacity of gas-phase varies with temperature and pressure. Variation of gas specific heat with pressure is negligible, hence gas specific heat is usually considered as a function of only temperature. Heat capacity of foam can be calculated as;

$$C_{P_{Foam}} = \Gamma C_{P_{Gas}} + (1 - \Gamma) C_{P_{Water}}, \dots\dots\dots (2.26)$$

where;

$C_{P_{Foam}}$ = Heat capacity of foam

$C_{P_{Gas}}$ = Heat capacity of gas

$C_{P_{Water}}$ = Heat capacity of water

Suppose that the gas-phase is air, Memarzadeh and Miska³² have expressed the heat capacity of air as a function of temperature as below;

$$C_{P_{Air}} = 0.238 - 0.899 \times 10^{-5} T + 0.268 \times 10^{-7} T^2 - 0.629 \times 10^{-11} T^3, \dots\dots\dots (2.27)$$

CHAPTER III

FOAM DRILLING SIMULATOR

This chapter explains how the foam drilling model is developed and offers a detailed discussion of many aspects of foam drilling operations. This model is developed based on the fundamental equation for steady-state foam flow in vertical pipes, which had presented by **Eq. 2.18**.

Assumptions

Some basic assumptions in developing this foam drilling model are:

- It is assumed that compressible gasses can be approximated by the ideal gas law.
- Calculations are based on a constant wellbore geometry.
- The term bottom-hole is applied for the total depth just above the drill collars.
- Foam rheology is characterized by the Power-Law model.
- Wellbore temperature is assumed to be equal to the formation temperature.
- Gas expansion right below the drill bit (Joule-Thomson effect) is ignored.
- The minimum drag force criterion is used for cuttings transport analysis.
- The trouble free cuttings concentration is assumed to be 4%.
- Formation fluid influx is considered as an incompressible fluid which is known as water.

A computer code is developed to process the data and accurately simulate the pressure during drilling a well. The following explains the function of each key on the interface of the code. The interface of the simulator is shown in **Fig. 3.1**.

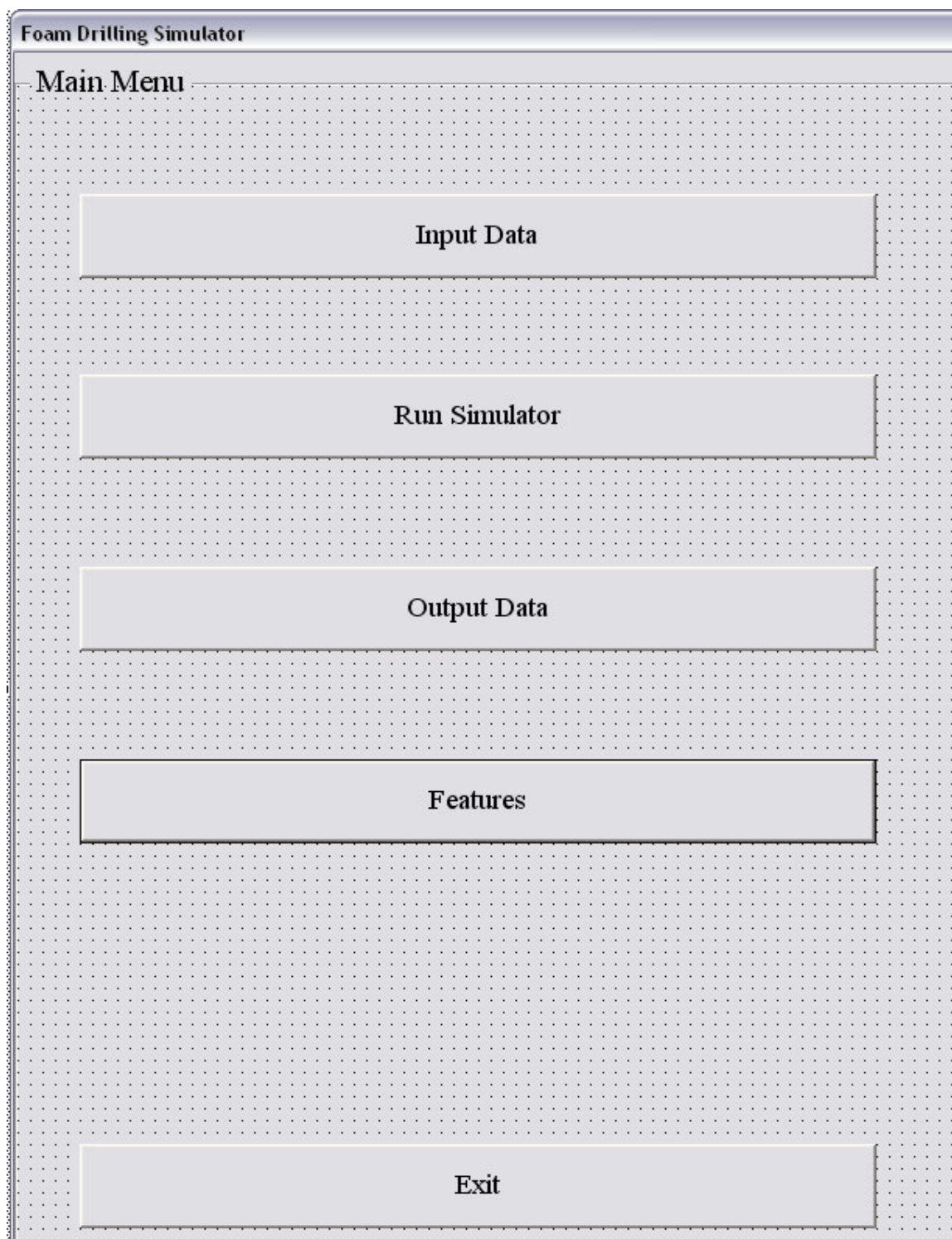


Fig. 3.1-Simulator Main Menu

Data Input

To begin the simulation we first need to collect the data. The, “Input Data”, button enables the user to enter the initial data. The initial data is collected through the program data input user form, **Fig. 3.2** shows the wellbore geometry input data.



The image shows a software interface for entering wellbore geometry data. It features a window with two tabs: "Wellbore Geometry" (selected) and "Operative Data". The background is a light gray grid. Five input fields are visible, each with a label, a text box, and a unit. The values entered are: Hole Diameter (7.875 in.), Pipe Outer Diameter (4.5 in.), Depth (9500 ft.), Wellbore Inclination (0 Degree), and Depth Intervals (100 ft.).

Parameter	Value	Unit
Hole Diameter :	7.875	in.
Pipe Outer Diameter :	4.5	in.
Depth :	9500	ft.
Wellbore Inclination :	0	Degree
Depth Intervals :	100	ft.

Fig. 3.2-Wellbore Geometry Input Data

The operative input data is shown in **Fig. 3.3**.

Wellbore Geometry		Operative Data	
Surface Temperature :	80	F	
Surface Pressure :	14.7	psi	
Thermal Gradient :	0.01	F/ft	
Max. Quality @ Surface :	0.95		
Min. Quality @ Bottom :	0.7		
Average Cuttings Concentration :	4	%	
Average Cuttings Size :	0.5	in.	
Cuttings Specific Gravity :	2.7	in.	
Formation Water Influx :	0	bbl/hr	
Rate of Penetration (ROP) :	60	ft/hr	
<div style="border: 1px solid black; padding: 5px; display: inline-block;">Submit Data</div>			

Fig. 3.3-Operative Input Data

Run

By clicking the, “Run”, button the following steps takes place:

Step 1

In order to maintain the surface foam quality at the desired maximum value, we need to set an appropriate gas-liquid injection ratio at surface. Based on the maximum allowable foam quality and no formation water influx, the GLR at surface pressure (no backpressure at the choke) is calculated by using **Eq. 2.6**.

Step 2

The second step is to calculate the foam properties at surface. Surface foam quality is known (maximum quality). Foam specific weight is first calculated by **Eq. 2.10** and then the hydrostatic pressure is calculated as;

$$P_{Bottom-hole} = \gamma_{foam} \times \Delta Depth + P_{surface}, \dots\dots\dots(3.1)$$

Since the bottom-hole pressure has been calculated, the foam quality and foam specific weight at bottom can be calculated. By taking the average for foam quality and foam specific weight over the length the new hydrostatic bottom-hole pressure is calculated. This procedure would repeat several times to obtain the accurate hydrostatic bottom-hole pressure.

Step 3

Foam consistency index K and flow behavior index n are calculated based on the foam quality at the bottom, to determine the viscosity of foam. In order to calculate foam required velocity to transport the cuttings to the surface given by **Eq. 2.21**, terminal velocity and cuttings settling velocity should first be determined. Considering the fact that cuttings settling velocity and viscosity are function of each other, the values of each should be determined by iteration. Once the required foam velocity is known the liquid injection rate should be determined to set the actual foam velocity, given by **Eq. 2.12**,

equal to the minimum required velocity. Finally, Reynolds number and Moody friction factor are calculated based on actual foam velocity and viscosity at bottom of the hole.

Now that required flow properties are determined, **Eq. 2.18** is used to calculate the total hydrostatic and frictional pressure at bottom.

Step 4

Using the bottom-hole pressure obtained in Step 3, the quality and specific weight of foam at bottom are calculated. Then the average pressure between the surface and the bottom is calculated. Using the average pressure; quality, specific weight, viscosity, velocity, and Moody friction are calculated and consequently **Eq. 2.18** yields a new bottom-hole pressure. At this point, Step 4 is repeated to update the value of minimum required injection rate.

Step 4 needs to be repeated several times to determine the accurate bottom pressure.

Step 5

As the drill-bit goes down, foam flow enters the next depth increment (ΔDepth) of the wellbore. In this step, instead of using the surface properties which were used in the previous step, the bottom-hole pressure, temperature, and foam properties of the previous step should be used as surface properties. Then the Step 3 and Step 4 are repeated again.

Step 6

The surface pressure used in Step 5, is independent of liquid injection rate calculated in that step. To consider the effect of new liquid injection rate on calculations of previous depth increments, all the calculations except determining the injection rates should be repeated again to find the most accurate value for bottom-hole pressure in the last depth increment.

Step 7

The foam quality obtained in Step 6 should be checked to make sure that, it is not lower than the required minimum foam quality. If the foam quality was lower than the required minimum foam quality, it means back-pressure is needed at the surface choke. The minimum required back-pressure to maintain the foam quality greater than the minimum limit is calculated.

Step 8

The Step 1 through Step 7 should be repeated until the bit reaches the total depth. Note that the calculated bottom-hole pressure is based on the minimum required back-pressure at the choke. This means that no lower values of back-pressure can be used. The effect of using the higher values of back-pressure can be evaluated in another part of the simulator.

Output Data

The “Output Data” button offers two choices. As it is shown in **Fig. 3.4**, the results can be seen either as a table or graphs.

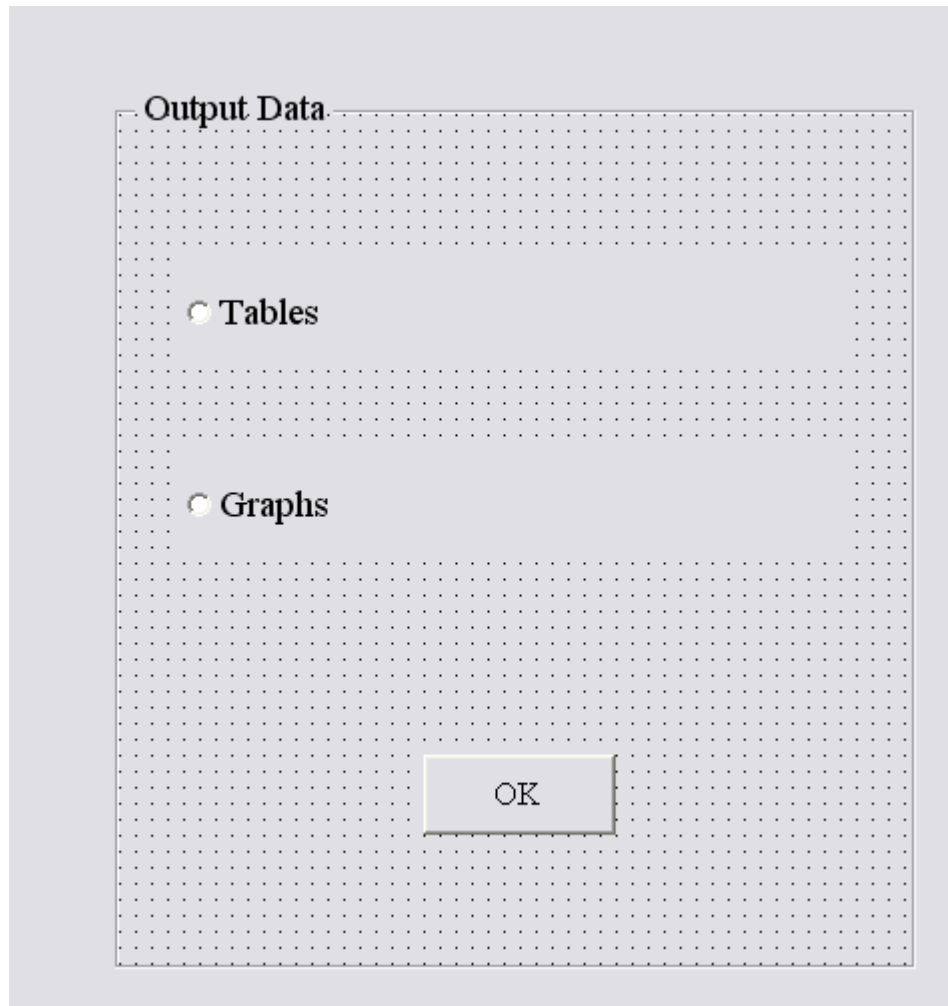
A screenshot of a software dialog box titled "Output Data". The dialog box has a light gray background and a dotted grid pattern. It contains two radio button options: "Tables" and "Graphs". Both radio buttons are currently unselected. At the bottom center of the dialog box is an "OK" button. The dialog box is set against a solid gray background.

Fig. 3.4-Output Data Form

The program has the ability to generate the graphs which are chosen by the user. The list of options is shown in **Fig. 3.5**.

Here is an example in which the input data shown in **Fig. 3.2** and **Fig. 3.3** is simulated and the output data is presented by both the table and figures.

Graphs

Vs. Depth

☐ Bottom-hole Pressure

☐ Liquid Injection Rate

☐ Gas Injection Rate

☐ Foam Quality

☐ Foam Velocity

☐ Foam Viscosity

Vs. Pressure

☐ Liquid Injection Rate

☐ Gas Injection Rate

☐ Foam Quality

☐ Foam Velocity

☐ Foam Viscosity

☐ Back-Pressure

Vs. **Depth**

OK

Fig. 3.5-Output Data Graph Form

Table 3.1-Output Results

Depth (ft)	Pressure (psia)	Foam Quality	Liquid Injection Rate (gal/min)	Gas Injection Rate (scf/min)	Foam Velocity (ft/sec)	Foam Viscosity (lb/ft-sec)	Moody Friction Factor
100	147.4798	0.947406	15.78	41.87851	10.40485	0.057512	0.324051
200	155.4484	0.944817	16.2	45.02509	9.904534	0.059446	0.334946
300	163.4721	0.942234	16.64	48.29128	9.451074	0.061319	0.345497
400	171.5536	0.939655	17.07	51.67406	9.038051	0.063135	0.355731
500	179.6959	0.93708	17.5	55.20311	8.660173	0.0649	0.365675
600	187.9013	0.934508	17.93	58.88136	8.313038	0.066618	0.375354
700	196.1727	0.931938	18.36	62.71141	7.992955	0.068293	0.38479
800	204.5124	0.929369	18.79	66.69589	7.696805	0.069928	0.394002
900	212.9229	0.926801	19.23	70.87446	7.421936	0.071527	0.403007
1000	221.4065	0.924233	19.67	75.21721	7.166078	0.073091	0.411823
1100	229.9654	0.921666	20.1	79.68584	6.927275	0.074625	0.420464
1200	238.6018	0.919097	20.54	84.35931	6.703836	0.07613	0.428943
1300	247.3178	0.916527	20.98	89.20596	6.494289	0.077608	0.437271
1400	256.1153	0.913956	21.42	94.22681	6.297346	0.079062	0.44546
1500	264.9963	0.911383	21.87	99.47042	6.111878	0.080492	0.453517
1600	273.9627	0.908808	22.31	104.8528	5.936889	0.0819	0.461452
1700	283.0161	0.90623	22.75	110.4156	5.771495	0.083288	0.469273
1800	292.1584	0.90365	23.2	116.2148	5.614913	0.084657	0.476984
1900	301.391	0.901066	23.64	122.1578	5.466445	0.086008	0.484593
2000	310.7157	0.89848	24.09	128.3434	5.325465	0.087341	0.492104
2100	320.1338	0.89589	24.53	134.6762	5.191412	0.088657	0.499521
2200	329.6468	0.893297	24.98	141.2608	5.063781	0.089958	0.506848
2300	339.2561	0.8907	25.42	147.9961	4.942116	0.091243	0.514089
2400	348.963	0.8881	25.87	154.9925	4.826004	0.092513	0.521245
2500	358.7688	0.885496	26.32	162.2049	4.715071	0.093769	0.52832
2600	368.6746	0.882888	26.76	169.5692	4.608977	0.09501	0.535315
2700	378.6816	0.880277	27.21	177.2089	4.50741	0.096238	0.542233
2800	388.791	0.877661	27.66	185.0753	4.410087	0.097452	0.549073
2900	399.0037	0.875042	28.11	193.1671	4.316747	0.098653	0.555838
3000	409.3208	0.87242	28.55	201.417	4.227152	0.09984	0.562529
3100	419.7433	0.869794	29	209.9622	4.141083	0.101015	0.569145
3200	430.2721	0.867164	29.45	218.7486	4.058336	0.102176	0.575689
3300	440.908	0.86453	29.89	227.6978	3.978727	0.103325	0.58216
3400	451.652	0.861893	30.34	236.9577	3.902081	0.104461	0.588559
3500	462.5049	0.859253	30.79	246.4698	3.82824	0.105584	0.594888
3600	473.4674	0.85661	31.23	256.1495	3.757054	0.106695	0.601145
3700	484.5403	0.853963	31.68	266.1555	3.688386	0.107793	0.607333
3800	495.7244	0.851314	32.12	276.339	3.622108	0.108879	0.613452
3900	507.0203	0.848661	32.57	286.8594	3.558101	0.109953	0.619503
4000	518.4287	0.846006	33.01	297.5607	3.496252	0.111015	0.625486

Table 3.1-Continued,

Depth (ft)	Pressure (psia)	Foam Quality	Liquid Injection Rate (gal/min)	Gas Injection Rate (scf/min)	Foam Velocity (ft/sec)	Foam Viscosity (lb/ft-sec)	Moody Friction Factor
4100	529.9502	0.843348	33.45	308.5174	3.436457	0.112065	0.631403
4200	541.5856	0.840688	33.9	319.835	3.37862	0.113104	0.637256
4300	553.3353	0.838026	34.34	331.3388	3.322648	0.114131	0.643045
4400	565.2	0.835361	34.78	343.1079	3.268456	0.115148	0.648772
4500	577.1803	0.832695	35.22	355.1542	3.215963	0.116154	0.65444
4600	589.2767	0.830026	35.66	367.4814	3.165094	0.11715	0.66005
4700	601.4898	0.827356	36.1	380.093	3.115778	0.118135	0.665604
4800	613.82	0.824685	36.54	392.9926	3.067948	0.119112	0.671105
4900	626.2679	0.822012	36.98	406.184	3.02154	0.120079	0.676555
5000	638.834	0.819338	37.41	419.5585	2.976495	0.121038	0.681957
5100	651.5188	0.816663	37.85	433.3315	2.932756	0.121989	0.687314
5200	664.3228	0.813987	38.28	447.3004	2.89027	0.122932	0.69263
5300	677.2463	0.811311	38.71	461.56	2.848986	0.123869	0.697907
5400	690.29	0.808634	39.14	476.1244	2.808858	0.124799	0.703149
5500	703.4542	0.805957	39.57	490.9971	2.769838	0.125724	0.708359
5600	716.7393	0.803279	40	506.1819	2.731886	0.126644	0.713542
5700	730.1458	0.800602	40.43	521.6824	2.694959	0.12756	0.718701
5800	743.6742	0.797925	40.85	537.3706	2.659019	0.128472	0.723839
5900	757.3249	0.795249	41.27	553.3642	2.624029	0.129381	0.728961
6000	771.0981	0.792573	41.69	569.6789	2.589954	0.130288	0.734071
6100	784.9945	0.789897	42.11	586.3182	2.556761	0.131193	0.739173
6200	799.0143	0.787223	42.52	603.144	2.524417	0.132098	0.74427
6300	813.1579	0.78455	42.93	620.2826	2.492894	0.133003	0.749367
6400	827.4258	0.781878	43.34	637.751	2.462161	0.133908	0.754467
6500	841.8183	0.779207	43.75	655.5527	2.432192	0.134815	0.759575
6600	856.3357	0.776538	44.16	673.6912	2.40296	0.135723	0.764693
6700	870.9784	0.773871	44.56	692.0147	2.37444	0.136634	0.769826
6800	885.7467	0.771206	44.96	710.6616	2.346607	0.137548	0.774977
6900	900.641	0.768543	45.36	729.6498	2.31944	0.138466	0.780149
7000	915.6616	0.765882	45.75	748.8192	2.292916	0.139388	0.785345
7100	930.8088	0.763223	46.14	768.3152	2.267014	0.140316	0.790568
7200	946.0829	0.760567	46.53	788.1568	2.241714	0.141248	0.795821
7300	961.4842	0.757914	46.91	808.175	2.216997	0.142186	0.801106
7400	977.0129	0.755263	47.29	828.5227	2.192844	0.14313	0.806425
7500	992.6693	0.752616	47.67	849.2198	2.169238	0.14408	0.811779
7600	1008.454	0.749972	48.05	870.2694	2.146162	0.145037	0.817171
7700	1024.366	0.747331	48.42	891.4908	2.123599	0.146001	0.822602
7800	1040.407	0.744694	48.79	913.0471	2.101535	0.146972	0.828072
7900	1056.576	0.74206	49.15	934.7689	2.079953	0.14795	0.833583
8000	1072.875	0.739431	49.51	956.8244	2.058841	0.148936	0.839134

Table 3.1-Continued,

Depth (ft)	Pressure (psia)	Foam Quality	Liquid Injection Rate (gal/min)	Gas Injection Rate (scf/min)	Foam Velocity (ft/sec)	Foam Viscosity (lb/ft-sec)	Moody Friction Factor
8100	1089.302	0.736805	49.87	979.2353	2.038183	0.149928	0.844725
8200	1105.858	0.734183	50.23	1002.005	2.017967	0.150927	0.850356
8300	1122.543	0.731566	50.58	1024.933	1.998179	0.151934	0.856027
8400	1139.357	0.728954	50.93	1048.199	1.978808	0.152947	0.861736
8500	1156.301	0.726345	51.27	1071.616	1.959842	0.153967	0.867481
8600	1173.374	0.723742	51.62	1095.581	1.94127	0.154993	0.873262
8700	1190.577	0.721144	51.96	1119.718	1.92308	0.156025	0.879076
8800	1207.908	0.718551	52.29	1143.977	1.905261	0.157062	0.884921
8900	1225.37	0.715963	52.63	1168.793	1.887805	0.158105	0.890794
9000	1242.96	0.71338	52.96	1193.774	1.870701	0.159152	0.896693
9100	1260.68	0.710803	53.29	1219.095	1.853939	0.160203	0.902614
9200	1278.529	0.708232	53.61	1244.549	1.837511	0.161257	0.908554
9300	1296.507	0.705667	53.93	1270.34	1.821408	0.162314	0.914509
9400	1314.614	0.703107	54.25	1296.495	1.80562	0.163373	0.920476
9500	1332.85	0.700554	54.57	1323.014	1.790141	0.164433	0.92645

Table 3.1 shows a sample output data. The values presented in the last row of the table express the bottom-hole pressure, quality, injection rates, and flow properties at the total depth.

Pressure

The variation of pressure along the wellbore is shown in **Fig. 3.6**. The value of pressure at the depth of zero (at surface) indicates the minimum required back-pressure. **Fig. 3.6** shows the changes in pressure at any depth along the wellbore.

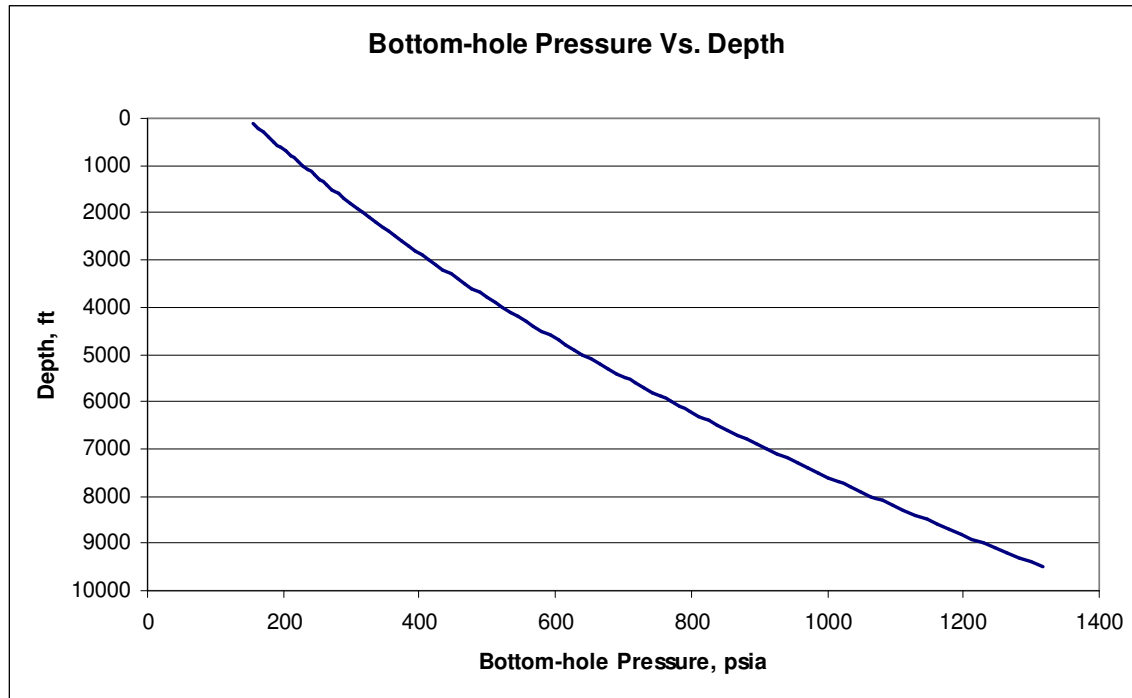


Fig. 3.6-Bottom-hole Pressure vs. Depth

Injection rate

While drilling with constant back-pressure at the choke, as the bit drills ahead successful removal of cuttings depends on the injection rate of foam. The minimum required liquid injection rates for successful cuttings transport at any depth along the wellbore are presented by the **Fig. 3.7** which shows that the minimum required liquid injection rate increases with depth. **Fig 3.8** shows that the minimum required liquid injection rate increases with pressure.

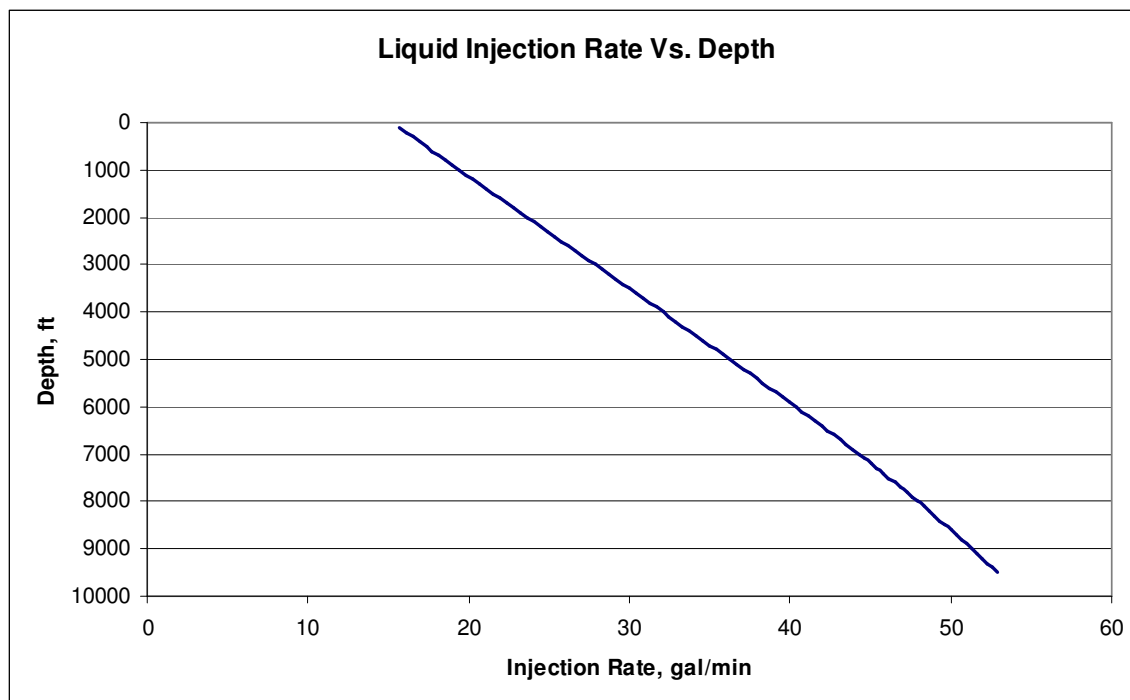


Fig. 3.7-Liquid Injection Rate vs. Depth

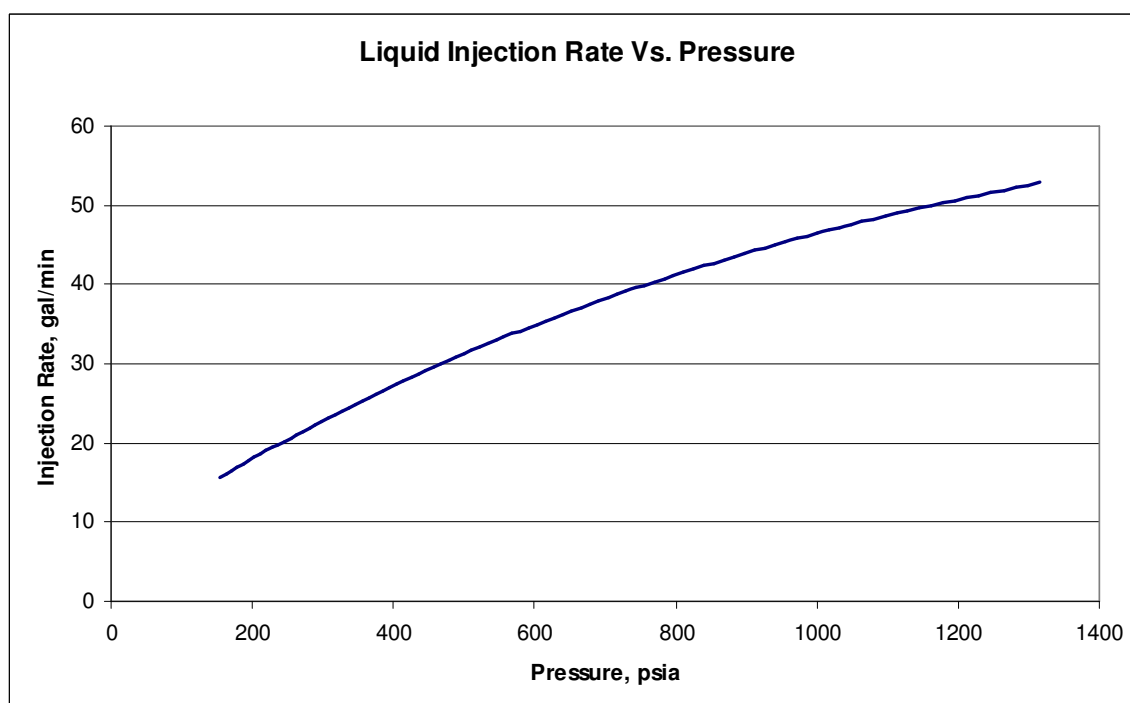


Fig 3.8-Liquid Injection Rate vs. Pressure

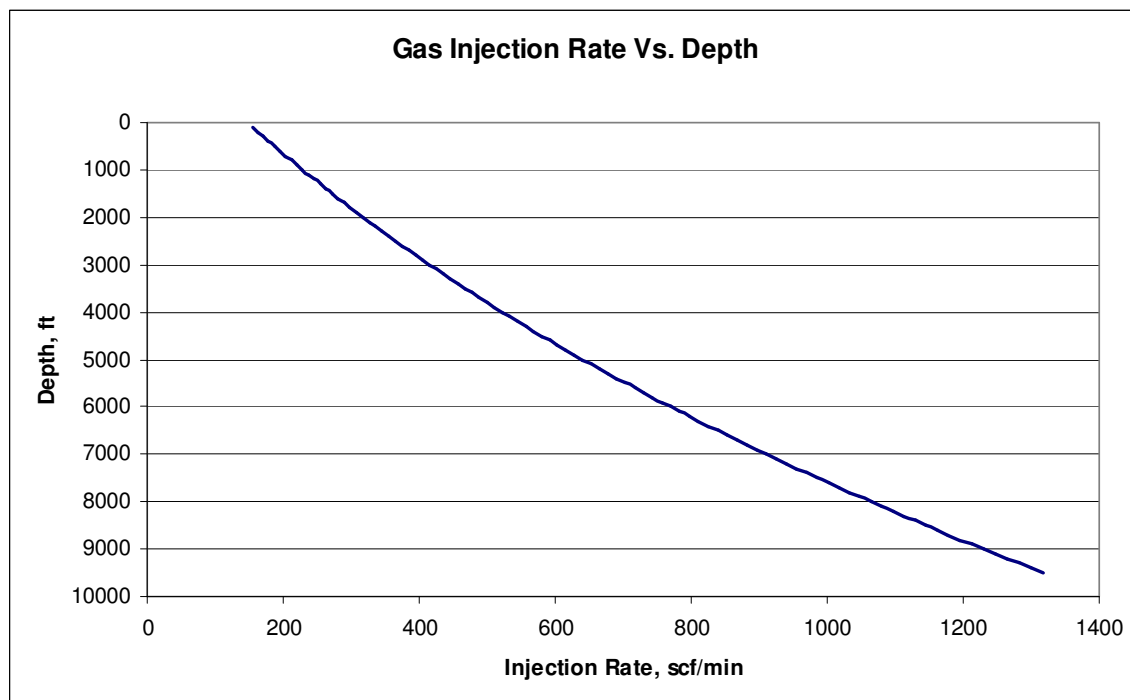


Fig 3.9-Gas Injection Rate vs. Depth

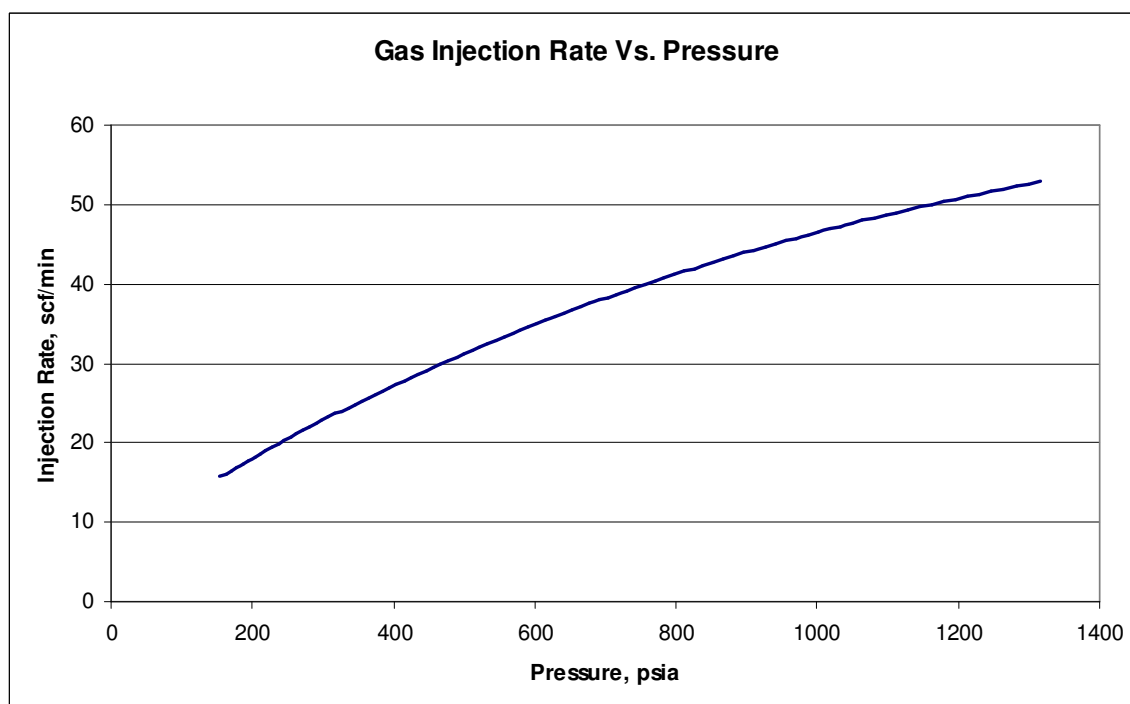


Fig 3.10-Gas Injection Rate vs. Pressure

The similar graphs are provided for gas injection rates and are presented in **Fig. 3.9** and **Fig. 3.10**. These figures indicate that minimum required gas injection rate increases with both the depth and pressure.

Foam quality

One of the major concerns of the foam drilling operations is to maintain the foam quality in a specific range. To monitor the changes in foam quality with respect to the depth and pressure the following graphs are provided. **Fig 3.11** shows that the quality of foam decreases with depth and **Fig 3.12** shows that the quality of foam decreases with pressure.

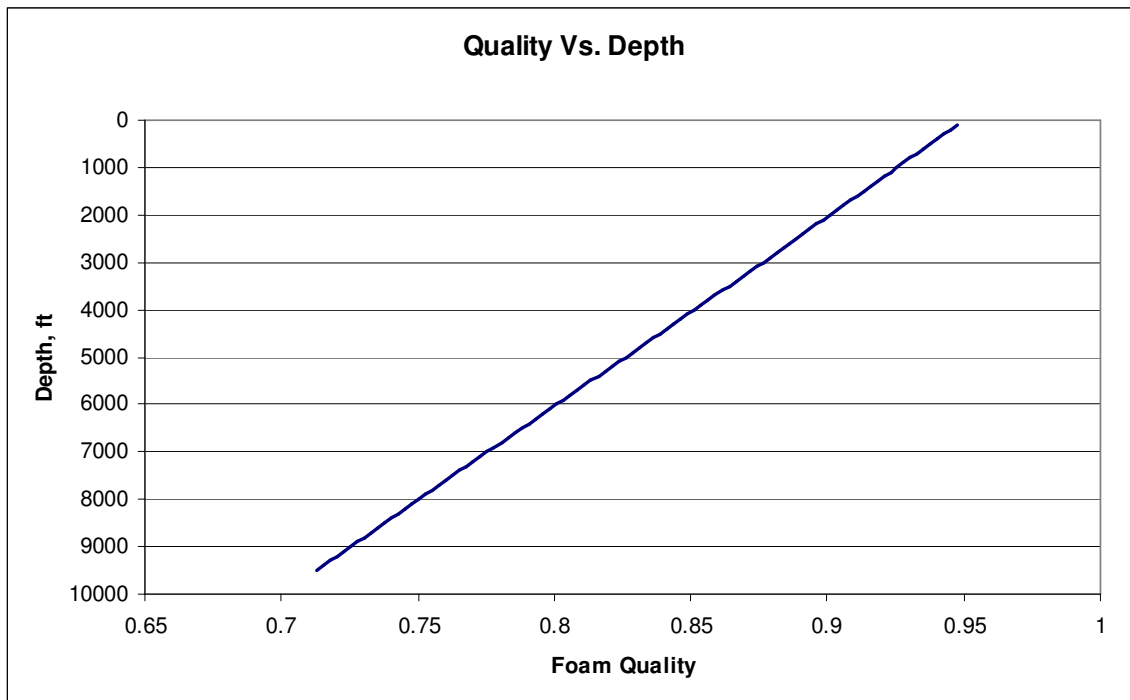


Fig 3.11-Foam Quality vs. Depth

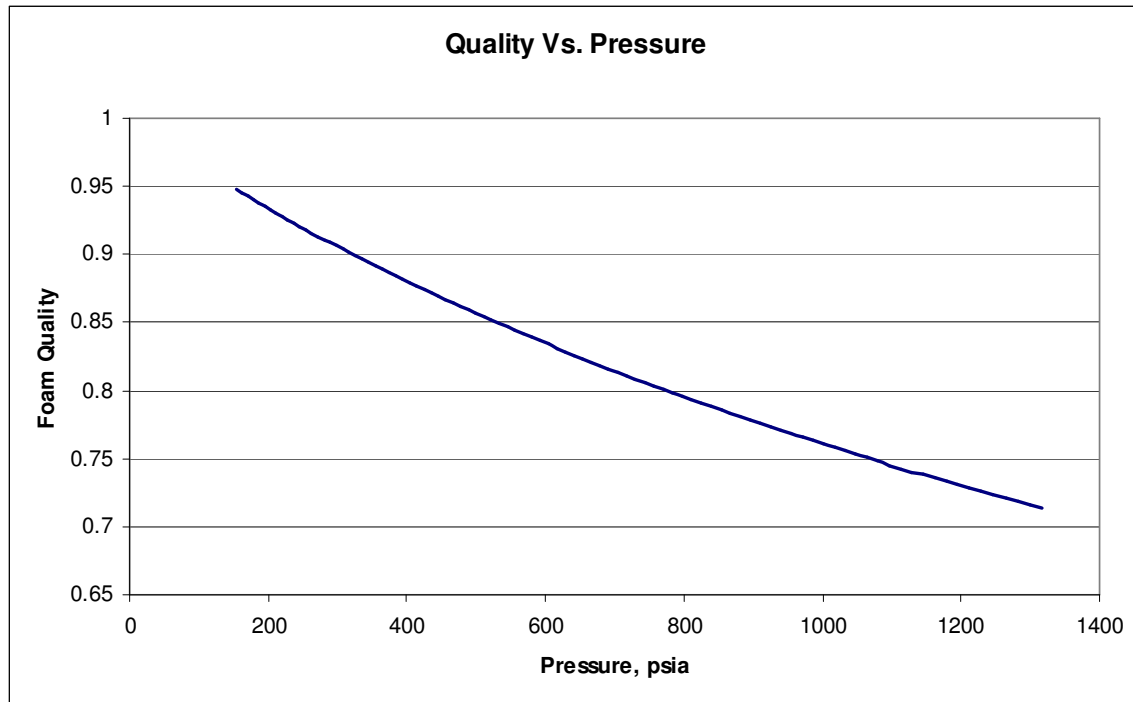


Fig 3.12-Foam Quality vs. Pressure

Foam viscosity

There has always been a debate about the rheology of the foam and many different models are developed to investigate this matter. The following graphs facilitate the comparison between the other methodologies and the one used in this research.

The increase in foam viscosity with depth is shown in **Fig 3.13**. The viscosity values used in this model are the function of both the foam quality and velocity. **Fig 3.14** shows that the foam viscosity decreases with increase in quality.

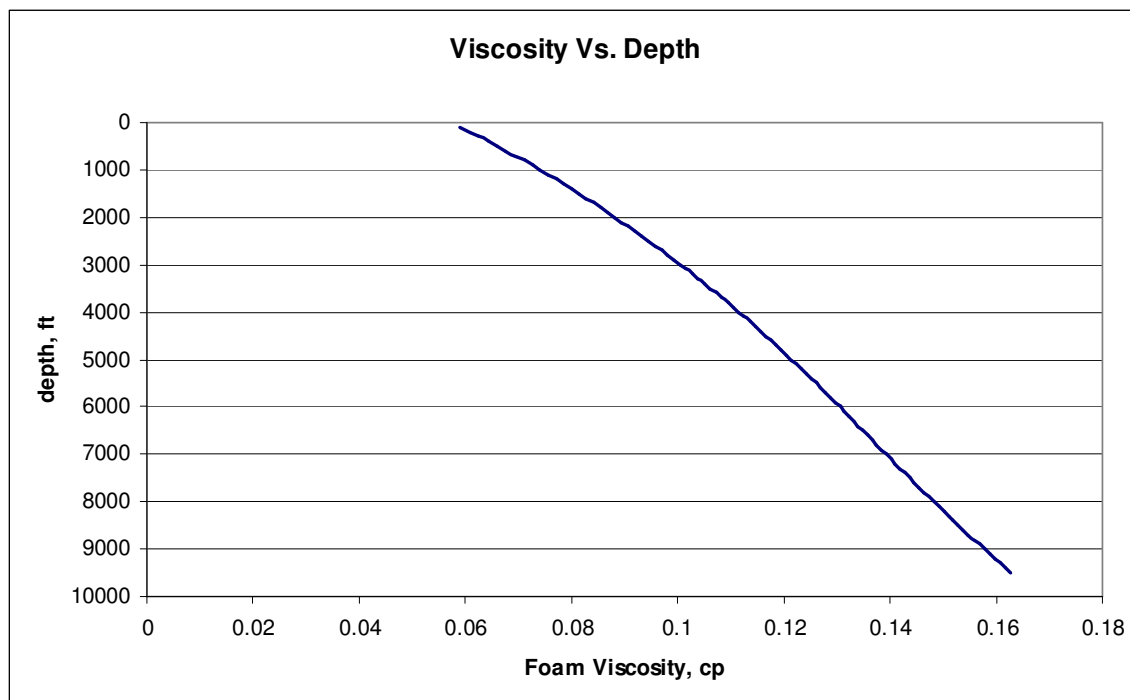


Fig 3.13-Foam Viscosity vs. Depth

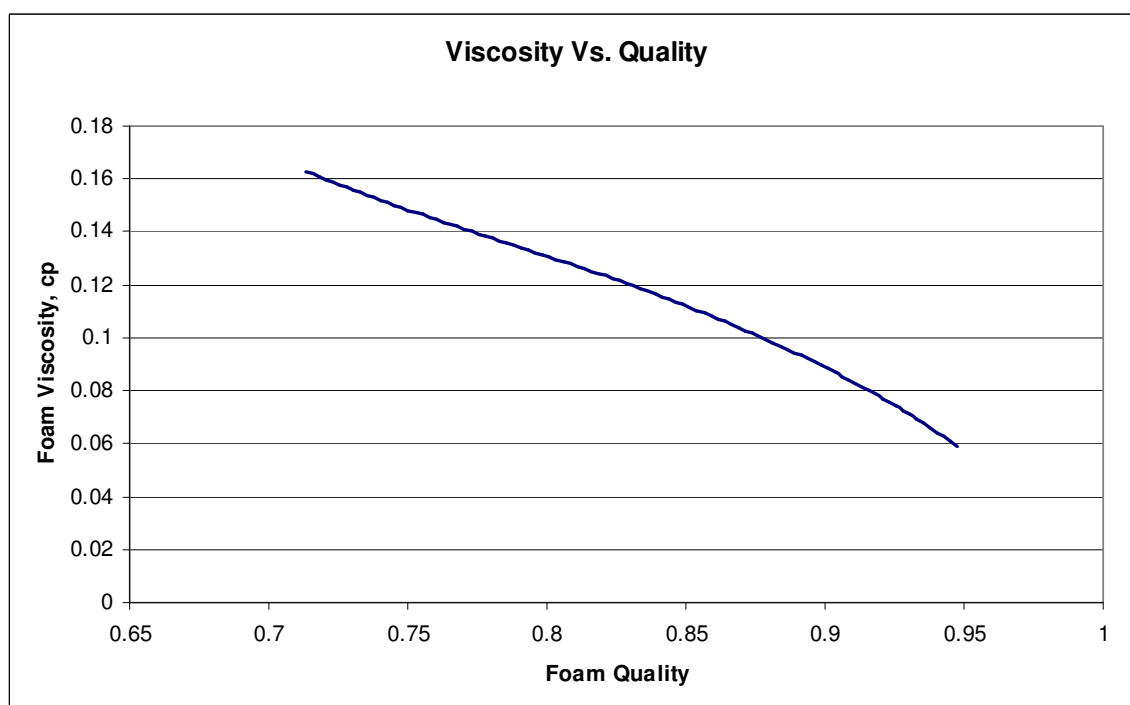


Fig 3.14-Foam Viscosity vs. Foam Quality

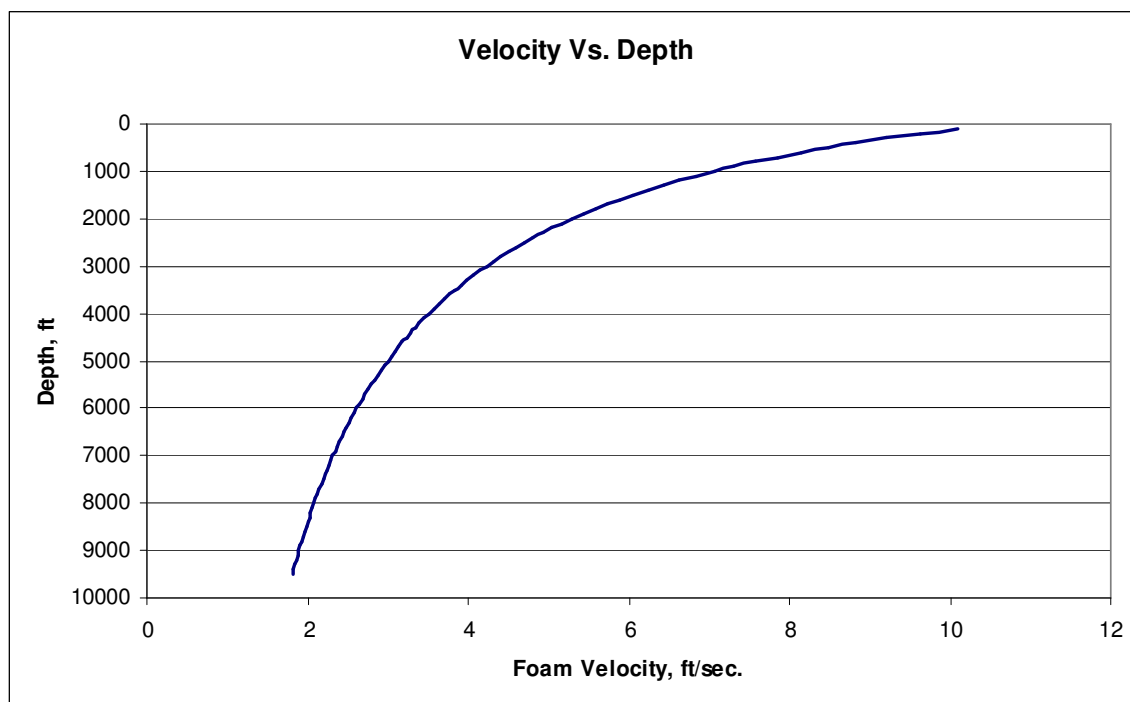
Foam velocity

Fig 3.15-Foam Velocity vs. Depth

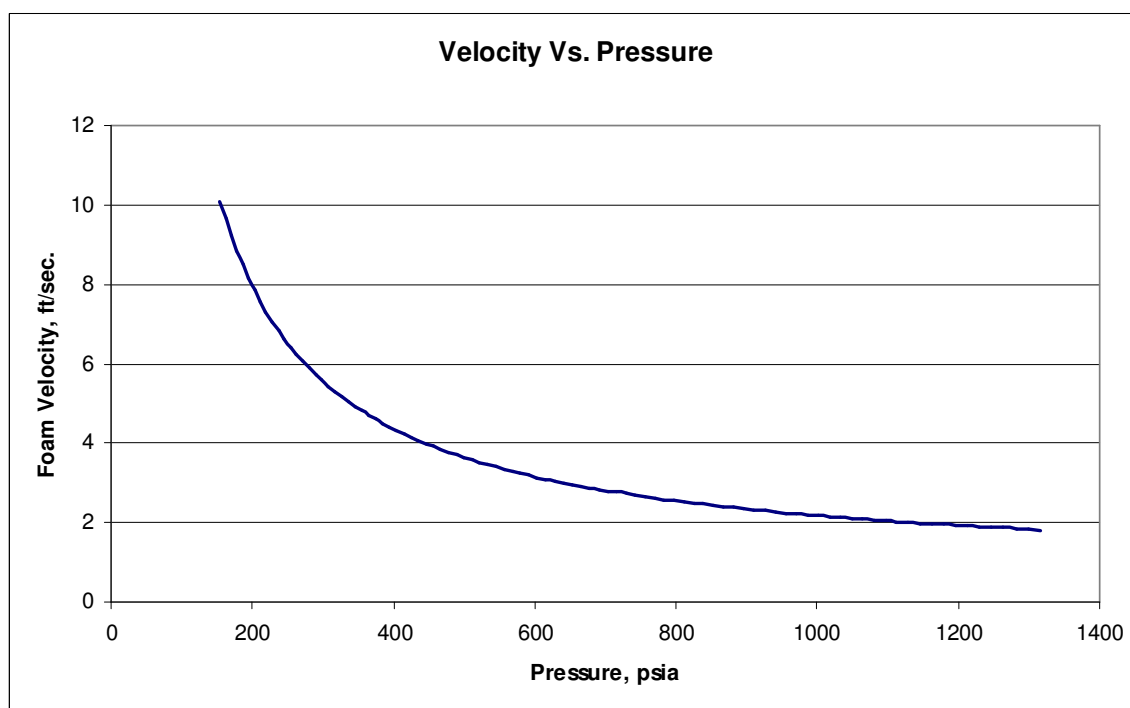


Fig 3.16-Foam Velocity vs. Pressure

As the foam viscosity increases along the wellbore, the decrease in the foam velocity is shown in **Fig. 3.15** and **Fig. 3.16**.

Minimum required back-pressure

Another critical aspect of foam drilling operations is the back-pressure determination. In order to maintain the foam stability, the surface choke should provide a sufficient back-pressure along the wellbore. The need to increase the surface back-pressure since the beginning to the end of a typical foam drilling operation is shown in **Fig. 3.17**.

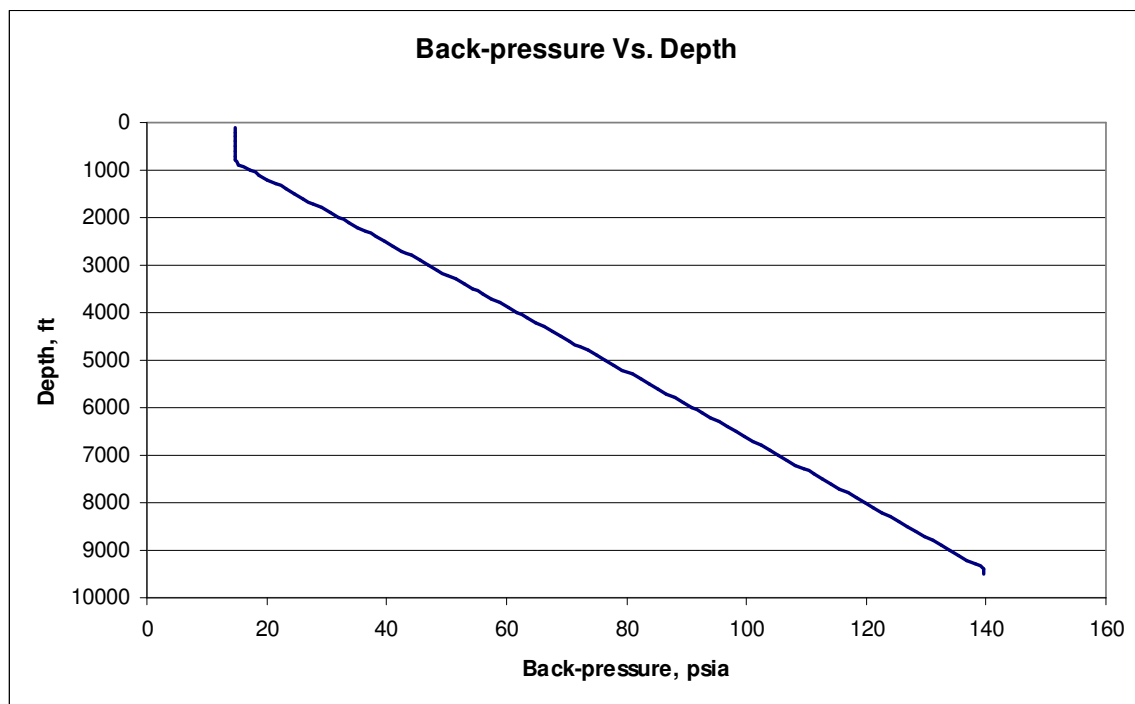


Fig 3.17-Back-pressure vs. Depth

Features

The button, “Features”, has been designed to offer the user several choices for generating comparative graphs. As it is shown in **Fig. 3.18**, there are five options to choose from.

Compare Results

☐ Back-Pressure

☒ Rate of Penetration (ROP)

☐ Cuttings Concentration

☐ Cuttings Size

☐ Formation Water Influx

☐ Injection Rate

☒ Variable Back-pressure ☒ Variable Injection Rate

ROP (1) ft/hr

Back-pressure psia

Injection Rate gal/min

ROP (2) ft/hr

Back-pressure psia

Injection Rate gal/min

ROP (3) ft/hr

Back-pressure psia

Injection Rate gal/min

OK

Fig. 3.18-Simulator Features

When a user chooses an option, that option is considered as a variable and the other options would remain constant. The user will be able to assign three different values to the variable. A program code simulates the model for the three values of the variable and generates the results in one graph. For better understanding of the foam flow behavior under different conditions, the simulator also shows the deviation of foam properties from the minimum value of the variable. A discussion about the properties is presented below;

Back-pressure

Considering the constant liquid injection rate of 75 (gal/min), three different values are assigned to the surface choke back-pressure. **Fig. 3.19A** shows that at the total depth, the bottom-hole pressure decreases with increase in the back-pressure. It is very important to remember that generally increasing the back-pressure increases the bottom-hole pressure. As it is shown in **Fig. 3.19B**, in this case increasing the back-pressure by more than 50% increases the bottom-hole pressure. Note that increasing the back-pressure by 50% decreases the bottom-hole pressure to its minimum limit (in this case).

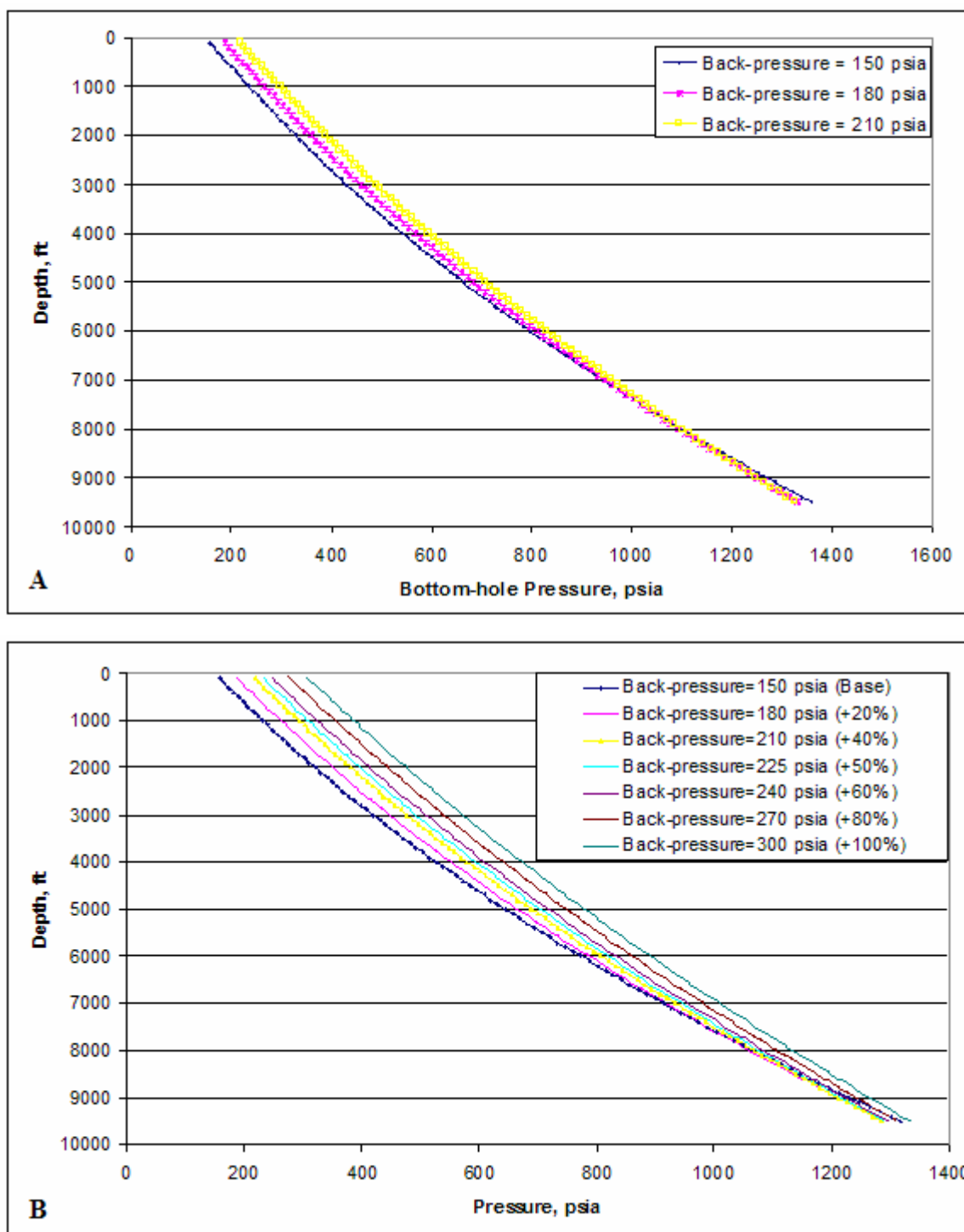


Fig. 3.19-Bottom-hole Pressure vs. Depth at Different Back-pressures. A. Bottom-hole Pressure Decreases with an Increase in Back-pressure. B. Bottom-hole Pressure Increases with an Increase in Back-pressure.

As it is shown in **Fig 3.20** the foam quality increases with an increase in back-pressure and consequently the bottom-hole pressure decreases. When the back-pressure is increased by more than 50%, the applied pressure at the surface and frictional pressure prevail over the hydrostatic pressure drop caused by the increase in foam quality and from this point any increase in the back-pressure increases the bottom-hole pressure.

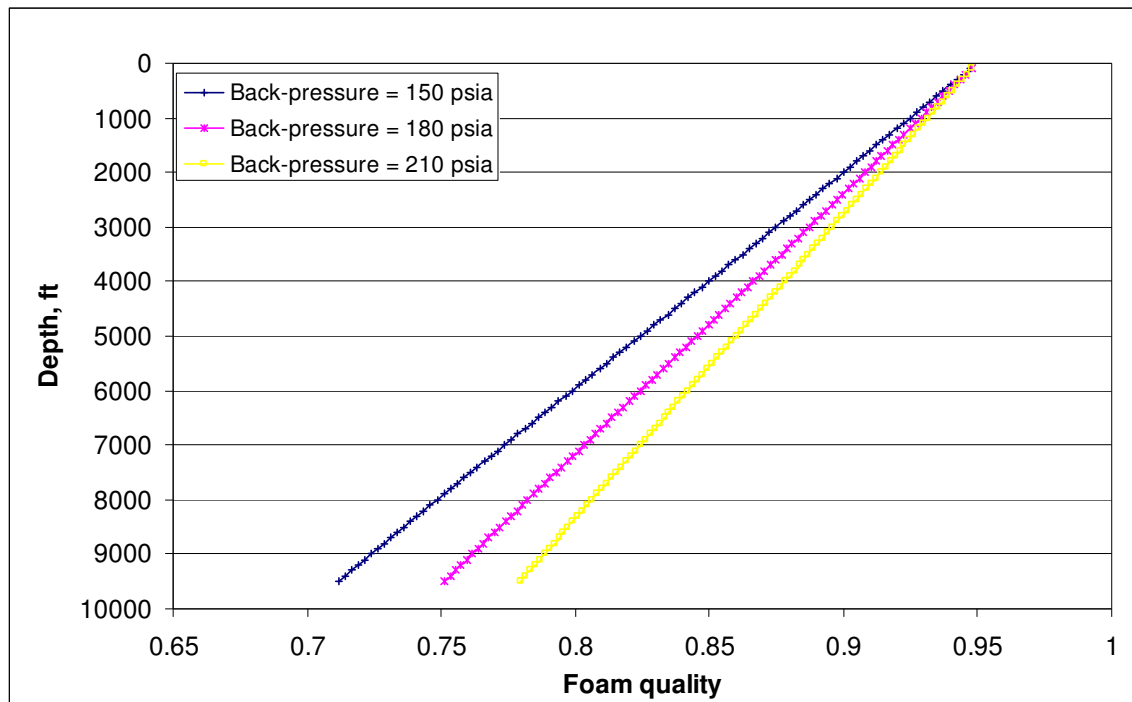


Fig. 3.20-Foam Quality vs. Depth at Different Back-pressures

It is shown in **Fig. 3.21** that at constant liquid injection rate an increase in back-pressure decreases the gas injection rate.

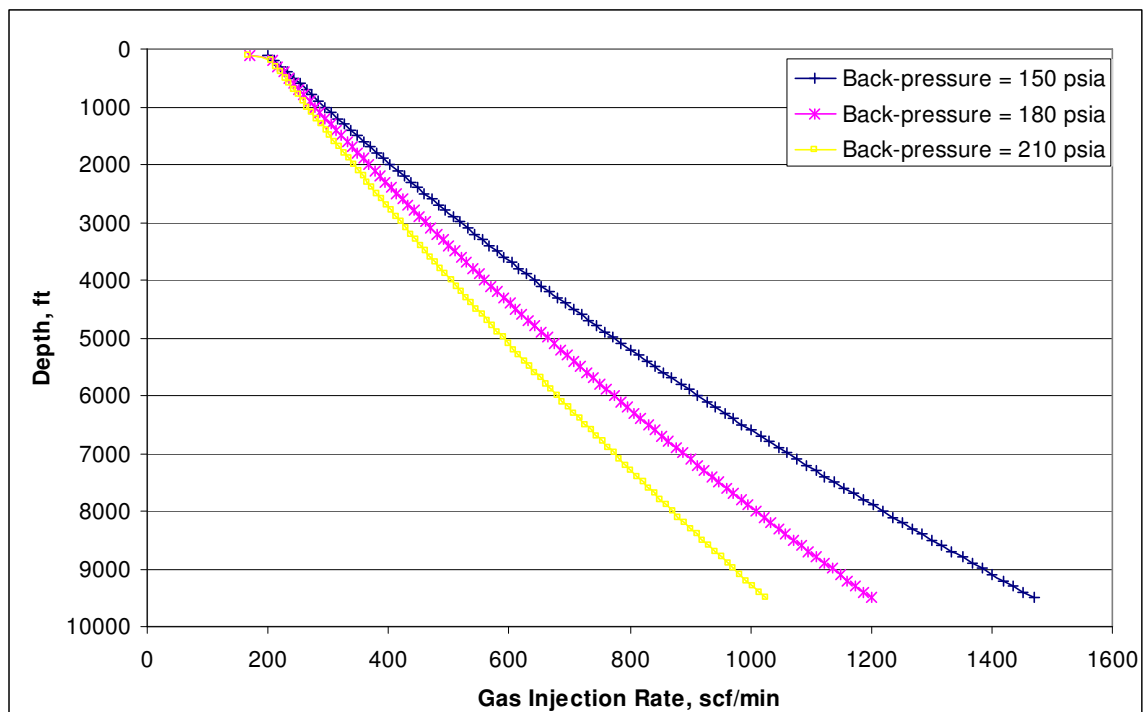


Fig. 3.21-Gas Injection Rate vs. Depth at Different Back-pressures

It should be noted as it is shown in **Fig 3.22**, increasing the back-pressure decreases the minimum required injection rates of the liquid and the gas.

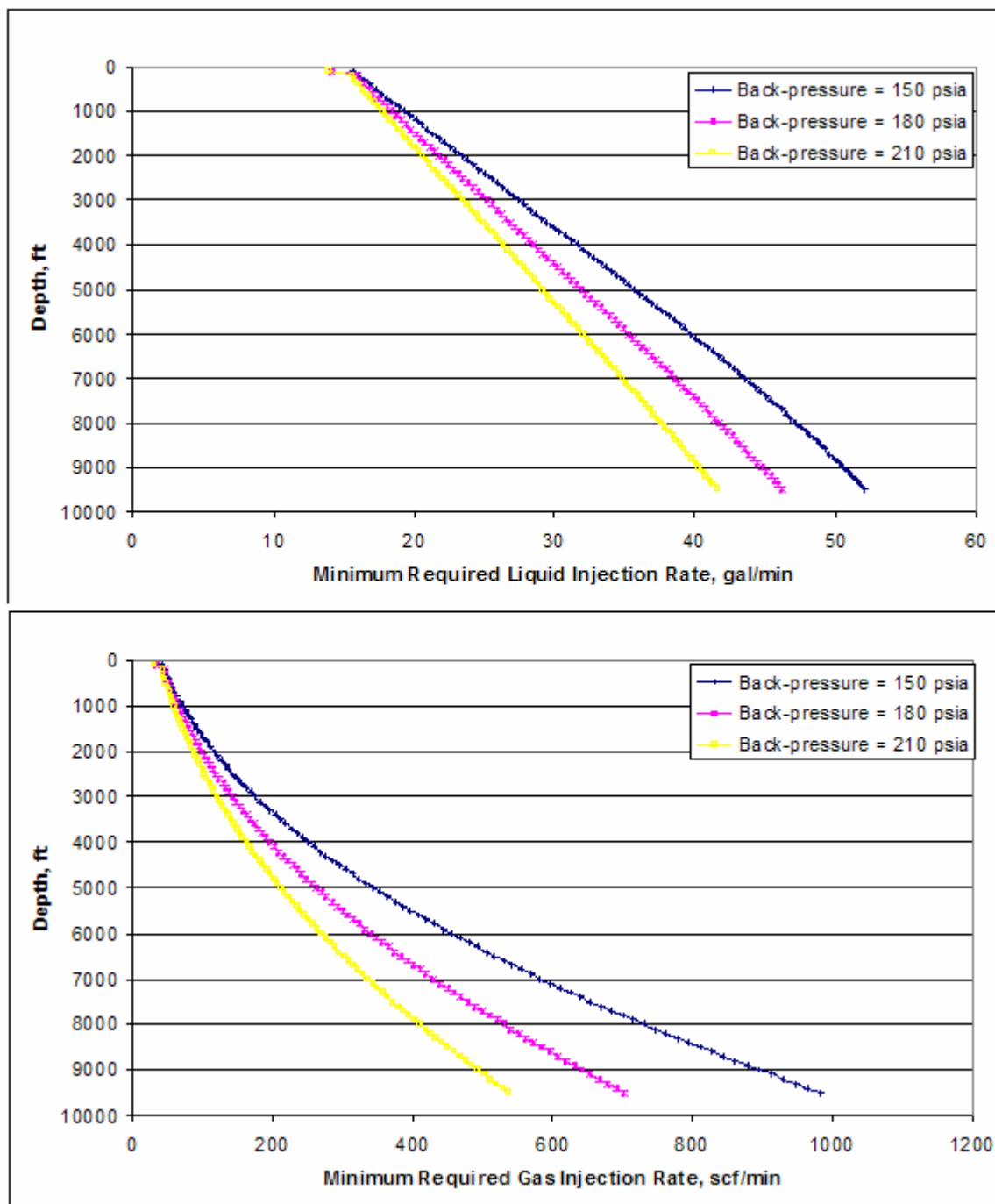


Fig. 3.22-Minimum Required Injection Rates vs. Depth at Different Back-pressures

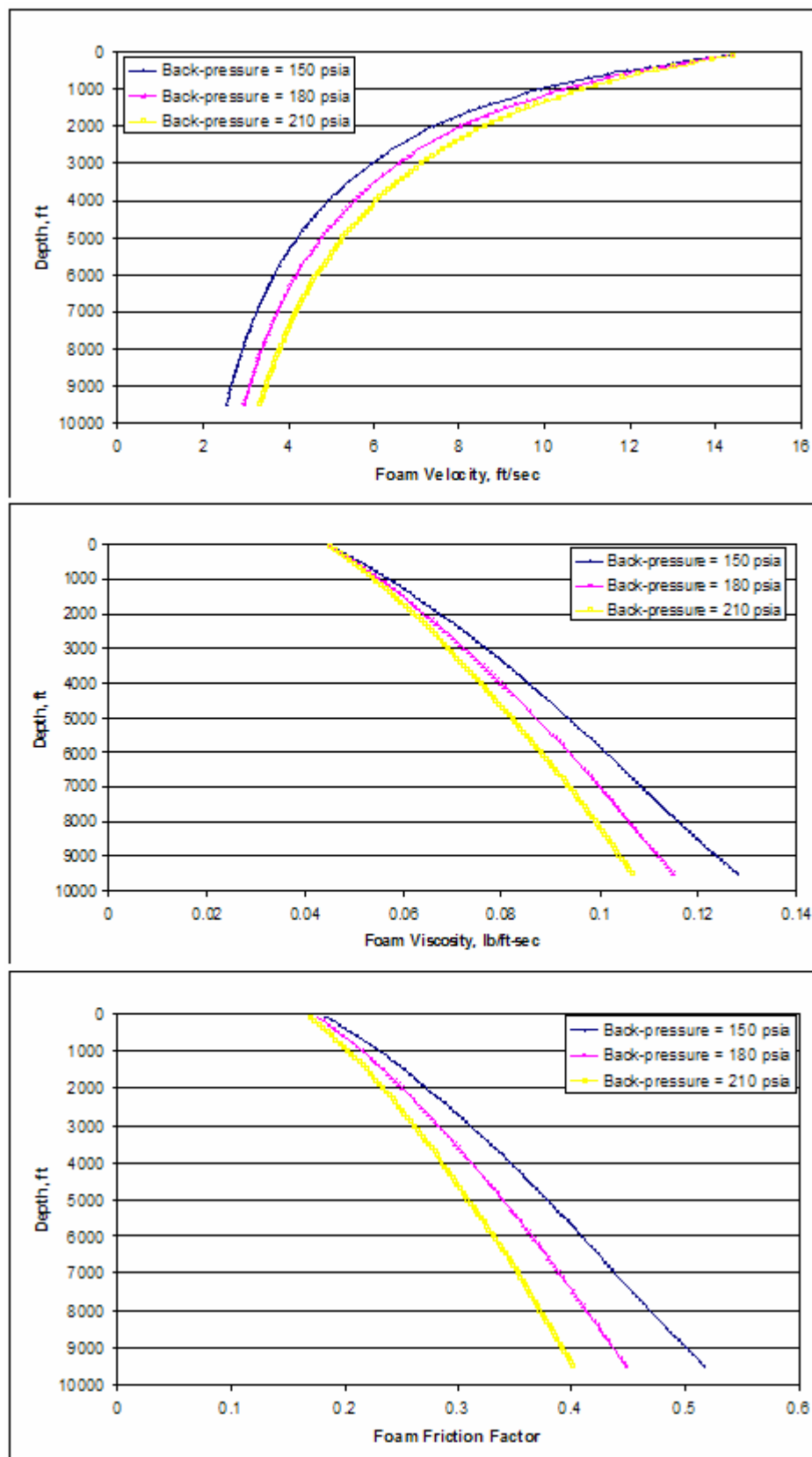


Fig. 3.23-Flow Properties vs. Depth at Different Back-pressures

Increasing the back-pressure increases the foam velocity and an increase in foam velocity decreases the foam viscosity and consequently the foam friction. **Fig 3.23** clearly shows the effect of increasing the back-pressure on the flow properties.

As the back-pressure increases, the effective magnitude of the relative changes of each parameter is investigated. At constant liquid injection rate of 75 (gal/min), a default value of 150 (psia) is assumed for the back pressure and then to make the comparison of the results easier, the default value is increased by 20% and 40% respectively. The deviations of properties in these two values are compared with the default value. The effect of increasing the back-pressure by 20% and 40% is indicated by the following figures;

Deviation of pressure in **Fig. 3.24**, suggests that increasing the back-pressure increases the bottom-hole pressure but at some depth (here at 8500-9000 ft) the bottom-hole pressure begins to decrease. As a result, increasing the back pressure by 20% and 40% decreases the pressure at the bottom by 2% and 2.5% respectively.

Fig. 3.25 shows that the gas injection rate decreases with an increase in back-pressure. Increasing the back-pressure by 20% and 40% decreases the gas injection rates at the total depth by 18% and 31% respectively. Remember that the liquid injection rate is assumed to be constant.

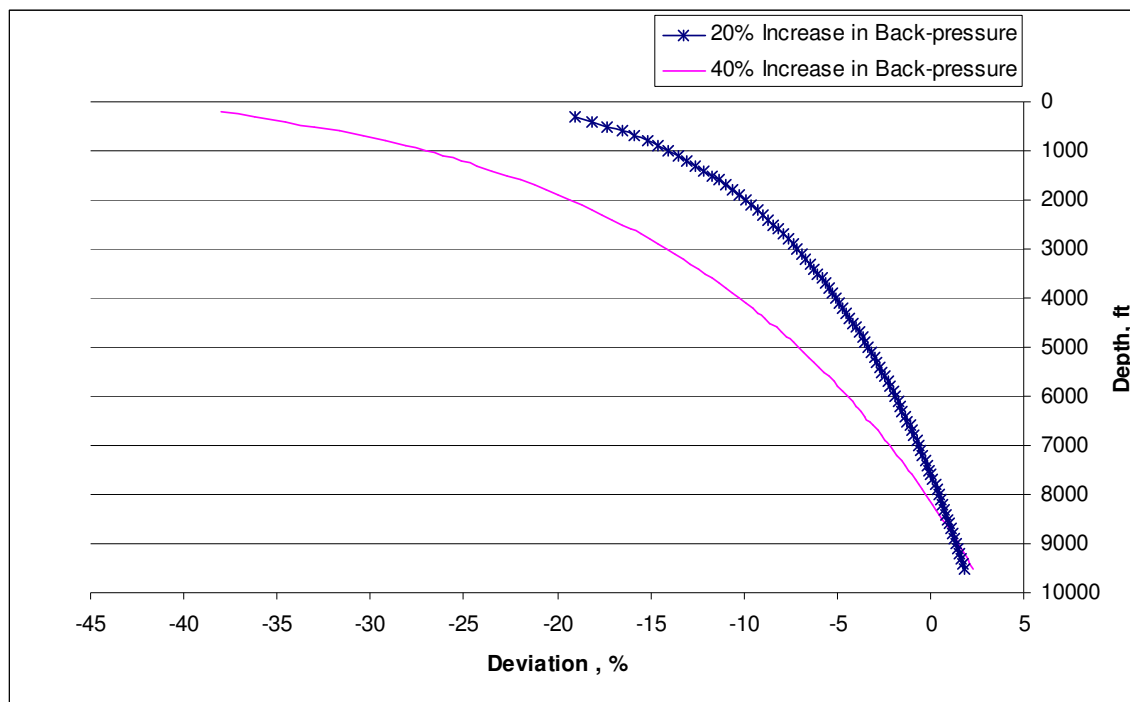


Fig. 3.24-Deviation of Bottom-hole Pressure vs. Depth (Different Back-pressures)

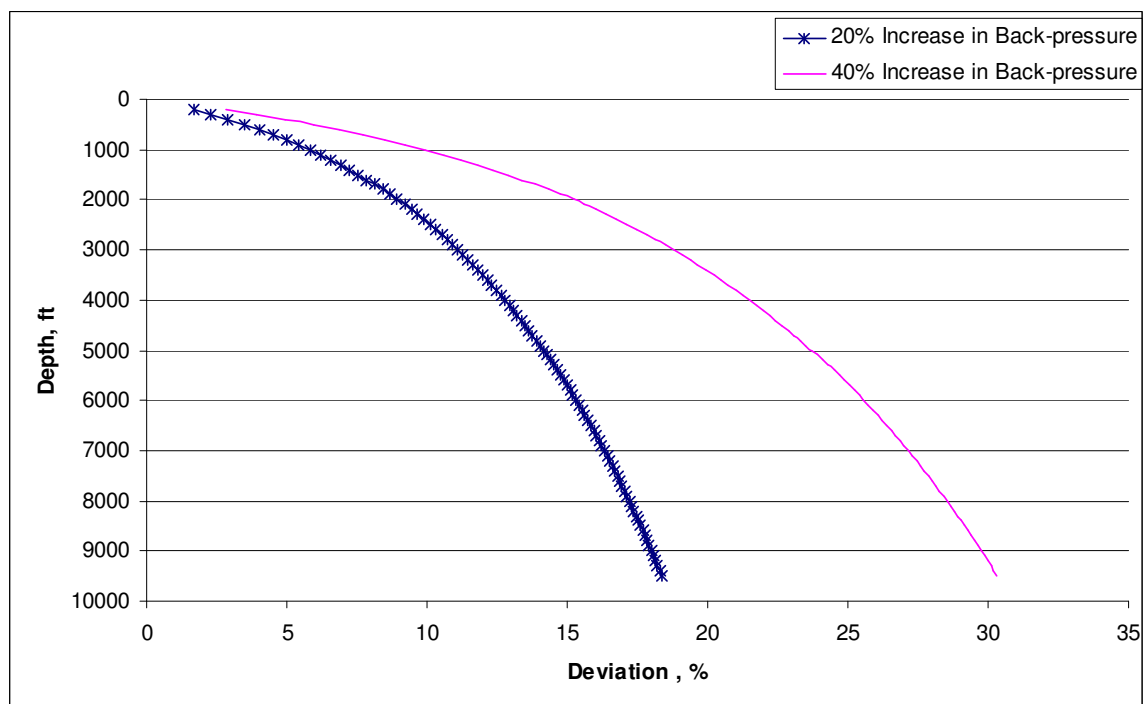


Fig. 3.25-Deviation of Gas Injection Rate vs. Depth (Different Back-pressures)

Fig. 3.26 shows that an increase in the back-pressure increases the velocity. The deviation of viscosity shown in **Fig. 3.27** indicates that, in contrast with the velocity, viscosity decreases with an increase in the back-pressure.

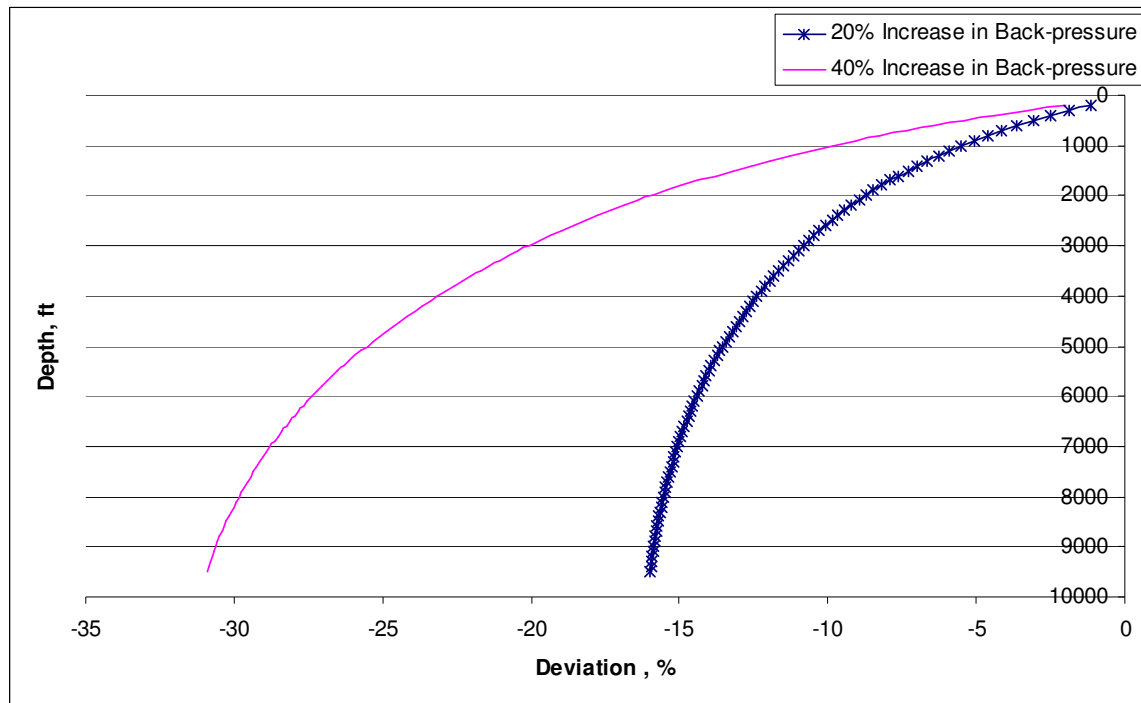


Fig. 3.26-Deviation of Velocity vs. Depth (Different Back-pressures)

Fig. 3.28 shows the decrease in the Moody friction with increasing the back-pressure.

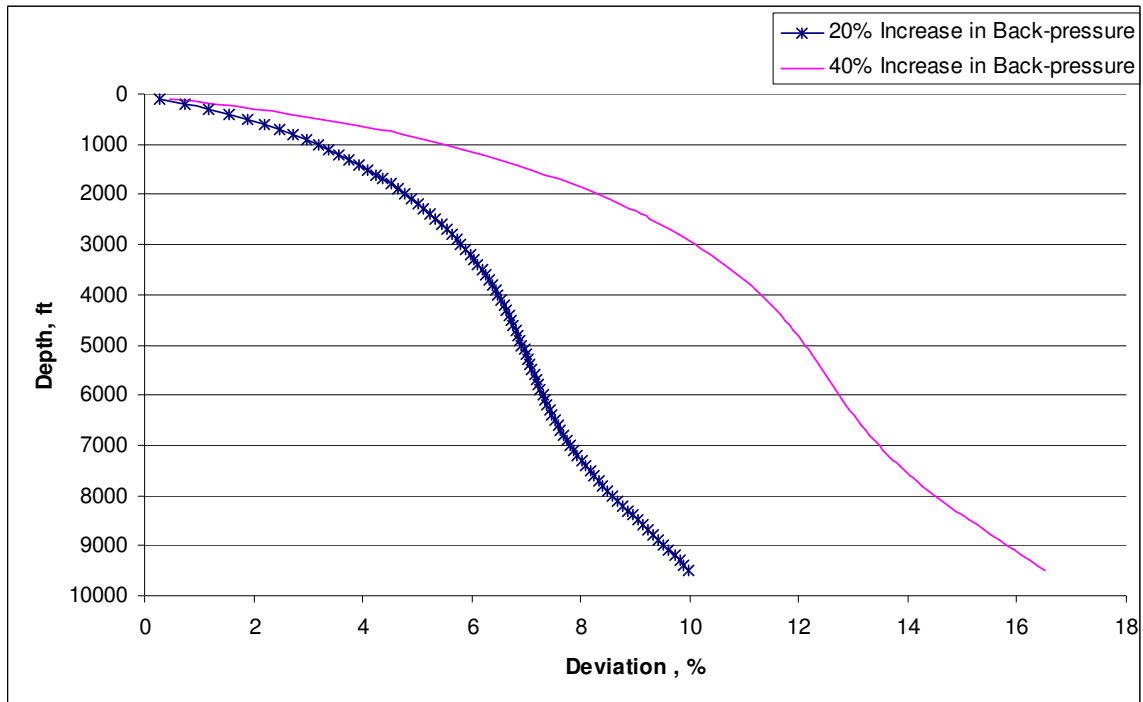


Fig. 3.27-Deviation of Viscosity vs. Depth (Different Back-pressures)

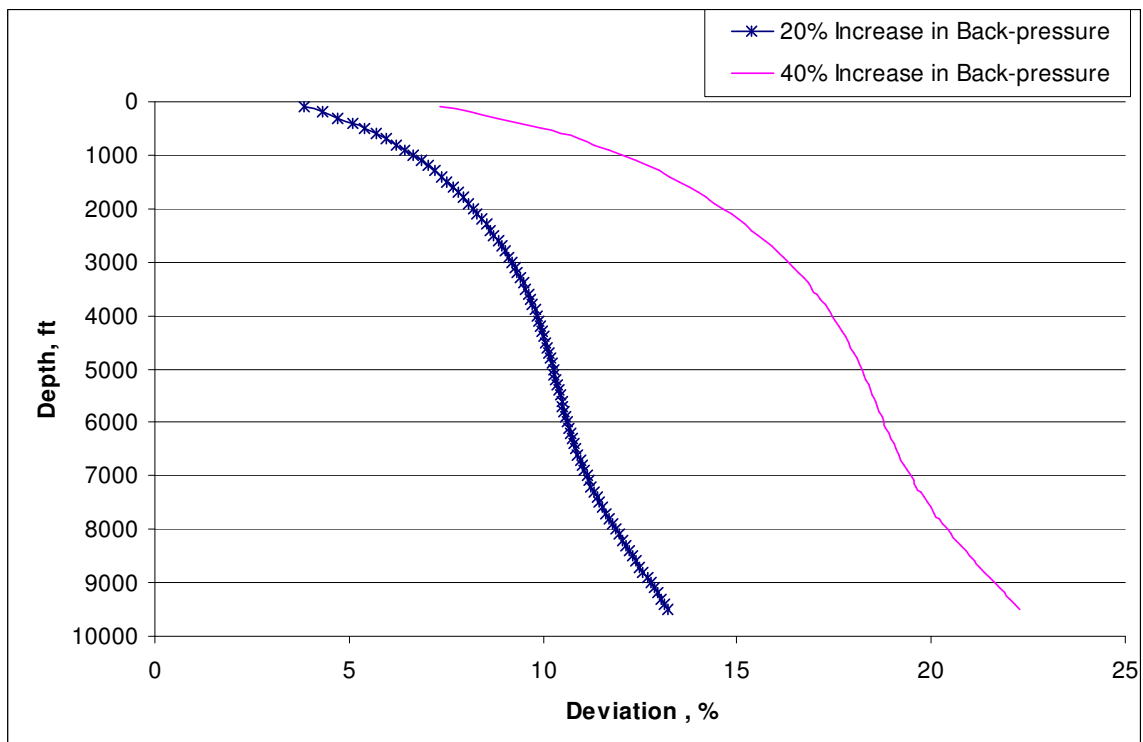


Fig. 3.28-Deviation of Moody Friction Factor vs. Depth (Different Back-pressures)

It was clearly predictable that the foam quality would increase with increasing the back-pressure. The deviation of foam quality is shown in **Fig. 3.29**.

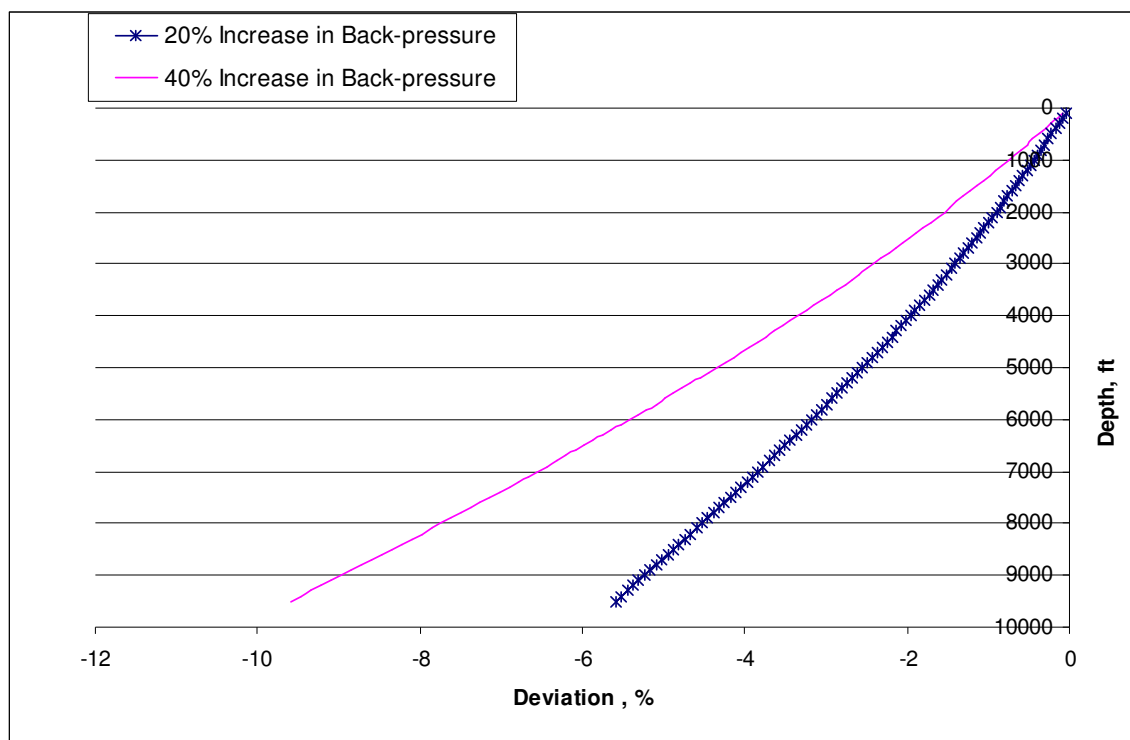


Fig. 3.29-Deviation of Quality vs. Depth (Different Back-pressures)

The summary of the deviation graphs is given in **Table 3.2**. The negative deviation represents an increase in the parameter.

Table 3.2-Summary of Results (Deviations for Back-pressure)

		Pressure	Gas Injection Rate	Velocity	Viscosity	Moody Friction	Quality
20% Increase in Back-pressure	% Deviation at Surface	-17	2	-1	1	5	0
	% Deviation at Bottom	2	18	-16	10	14	-5.5
40% Increase in Back-pressure	% Deviation at Surface	-38	3	-2	2	8	0
	% Deviation at Bottom	3	20	-32	17	22	-9.5

Rate of penetration (ROP)

Considering the constant back-pressure of 165 (psia), three different values are assigned to the rate of penetration. **Fig. 3.30** shows that the effect of ROP on the pressure is negligible.

All the graphs are plotted based on the minimum required liquid injection rates. The injection rate is not assumed to be constant because of, the direct effect of the ROP on the minimum required injection rates for successful removal of the cuttings.

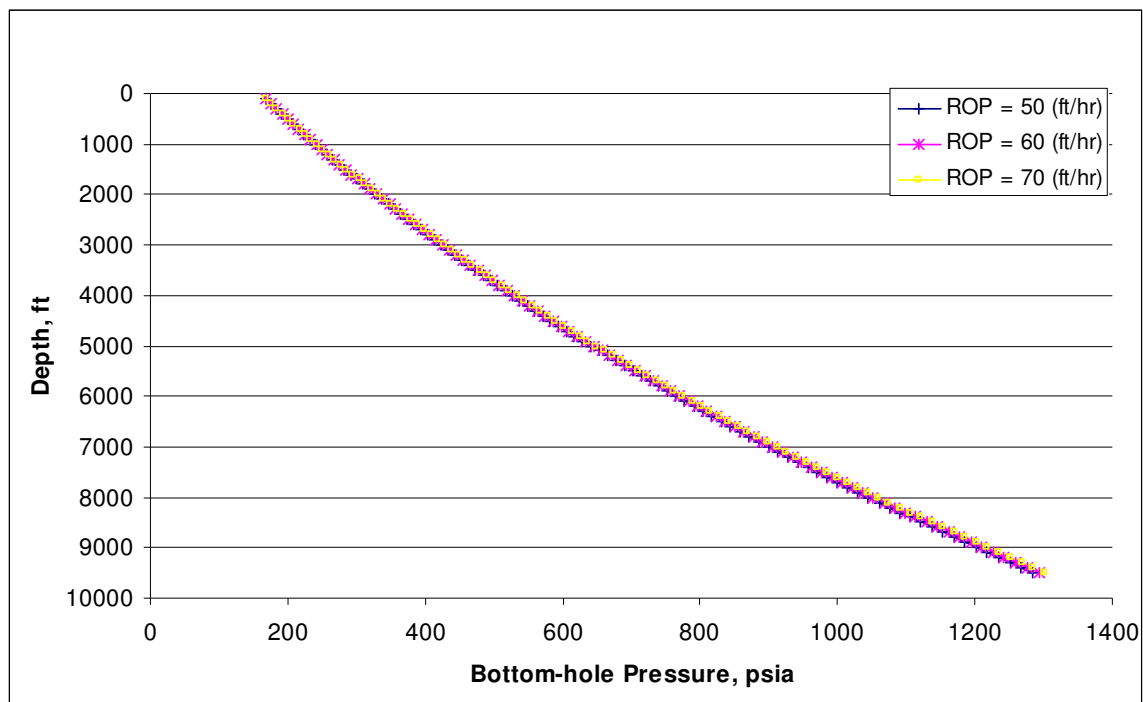


Fig. 3.30-Bottom-hole Pressure vs. Depth at Different Rates of Penetration

It is shown in **Fig. 3.31** that the increase in ROP increases the minimum required injection rates.

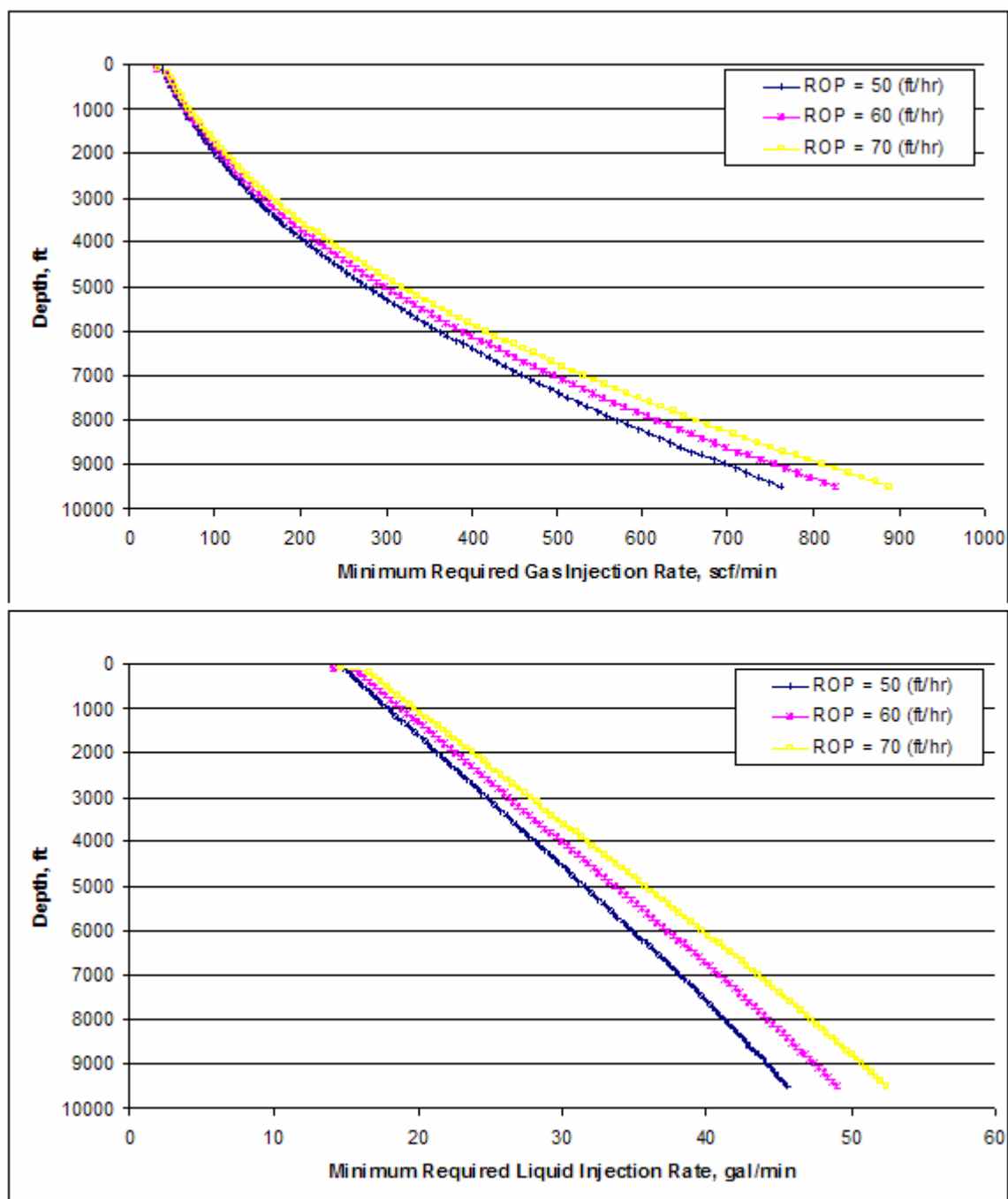


Fig. 3.31-Minimum Injection Rates vs. Depth at Different Rates of Penetration

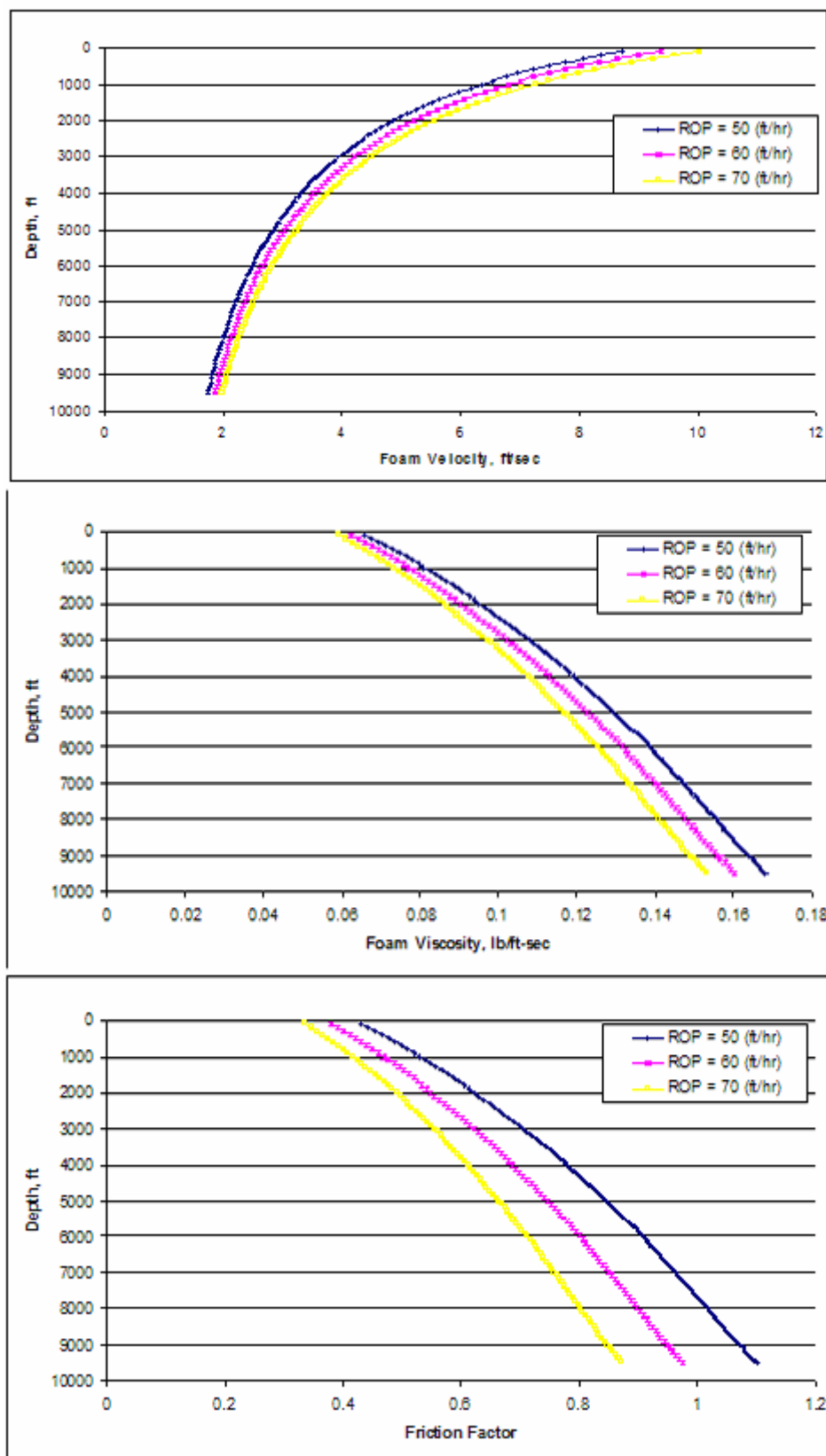


Fig. 3.32-Foam Flow Properties vs. Depth at Different Rates of Penetration

Increasing the back-pressure increases the foam velocity and an increase in foam velocity decreases the foam viscosity and consequently the foam friction. **Fig 3.32** clearly shows the effect of increasing the back-pressure on the flow properties.

A default value of 50 ft/hr is assumed for the ROP and then to make the comparison of the results easier, the default value is increased by 20% and 40% respectively. The deviations of properties in these two values are compared with the default value. The effect of increasing the ROP by 20% and 40% is indicated by the following figures;

Deviation of pressure in **Fig. 3.33**, suggests that increasing ROP increases the bottom-hole pressure. Since the graph shows a maximum deviation of 1.4% the increase in pressure is not considerable.

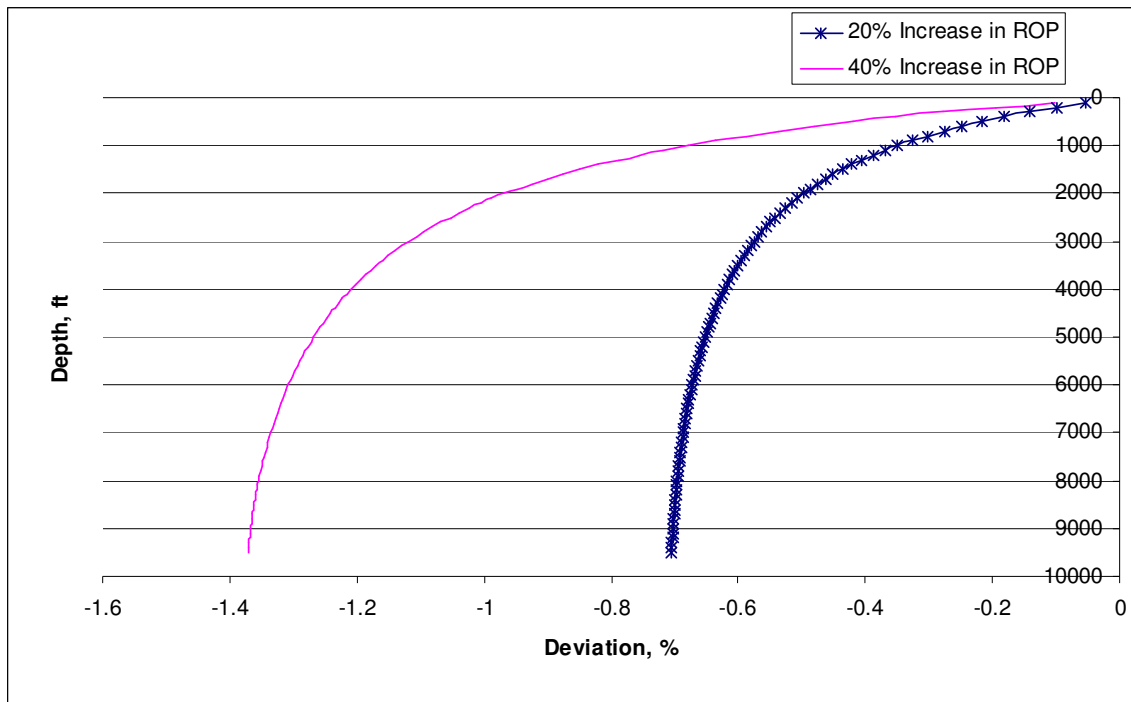


Fig. 3.33-Deviation of Bottom-hole Pressure vs. Depth (Different ROP)

Fig. 3.34 and **Fig. 3.35** show that the effect of increasing the rate of penetration on the minimum required injection rates and the velocity is approximately the same. It can be

concluded that ROP has much higher effect on the required injection rate than the pressure.

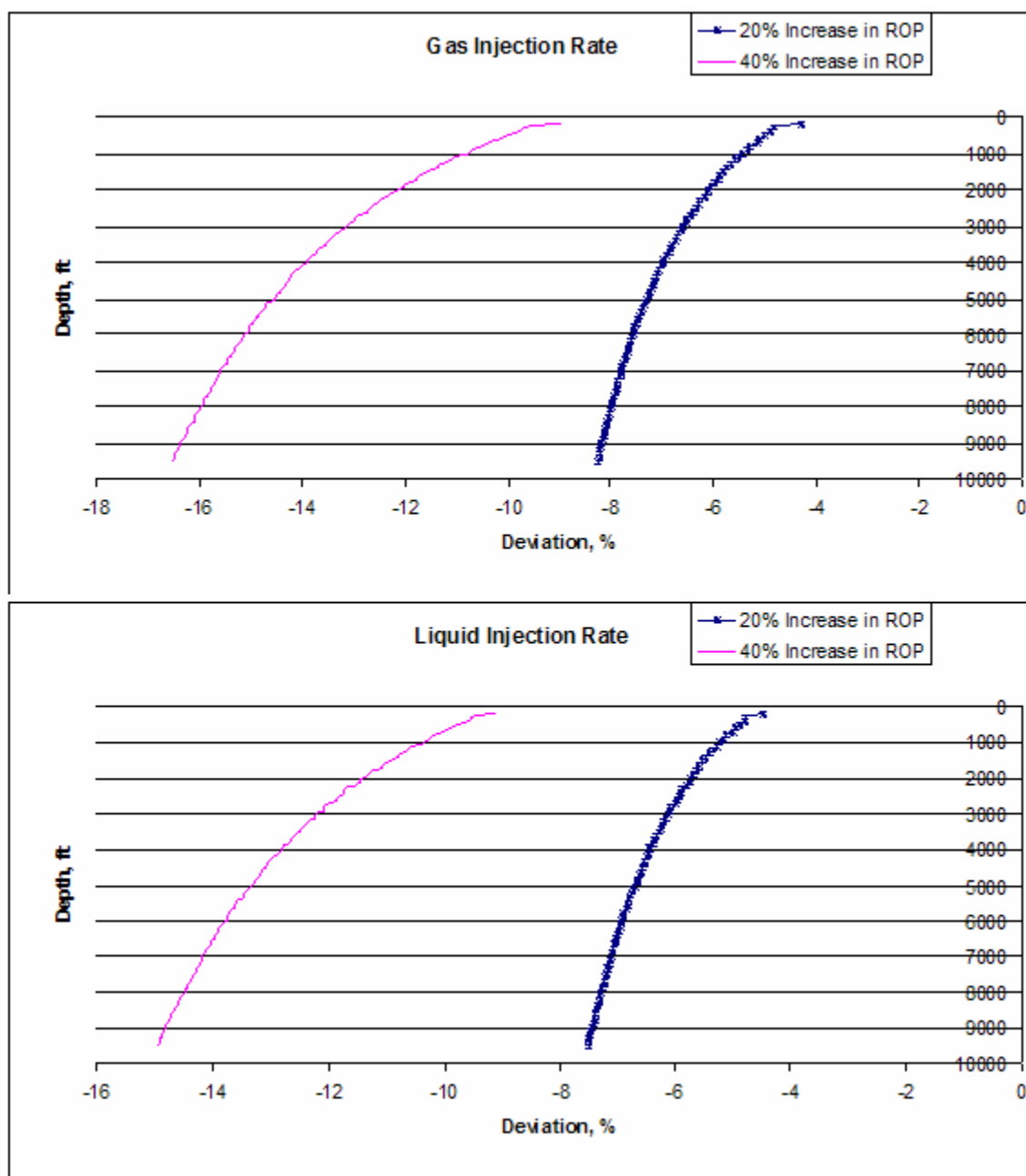


Fig. 3.34-Deviation of Injection Rates vs. Depth (Different ROP)

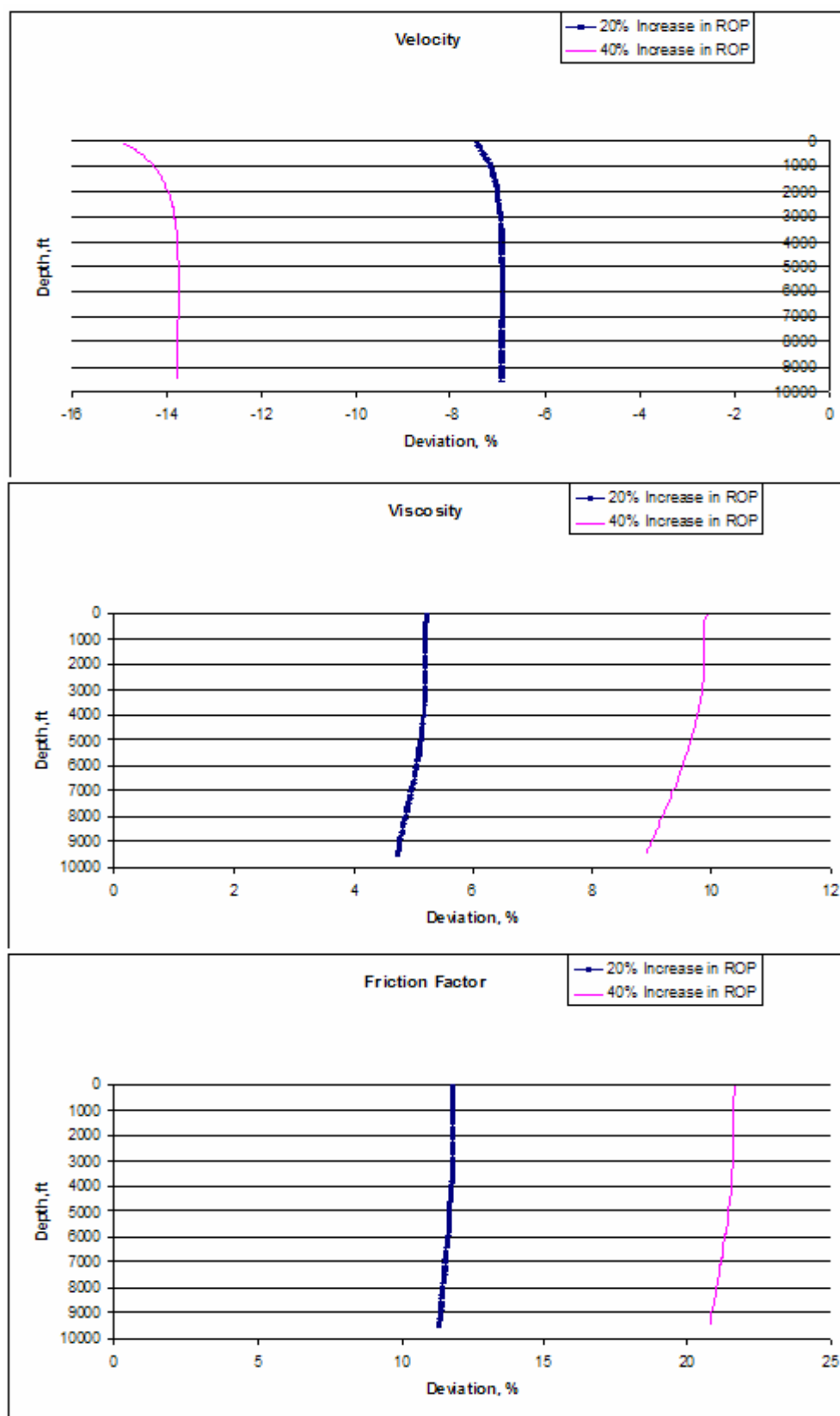


Fig. 3.35-Deviation of Flow Properties vs. Depth (Different ROP)

Table 3.3-Summary of Results (Deviations for ROP)

		Pressure	Gas Injection Rate	Liquid Injection Rate	Velocity	Viscosity	Moody Friction
20% Increase in ROP	<i>% Deviation at Surface</i>	-0.05	-4	-4	-25	5	9
	<i>% Deviation at Bottom</i>	-0.7	-8	-7.5	-7	4.5	9.5
40% Increase in ROP	<i>% Deviation at Surface</i>	-0.1	-9	-9	-15	10	22
	<i>% Deviation at Bottom</i>	-1.4	-17	-14.5	-14	9	21

The summary of the deviation graphs is given in **Table 3.3**. The negative deviation represents an increase in the parameter.

Cuttings concentration

Considering the constant back-pressure of 165 (psia), three different values are assigned to the cuttings concentration. **Fig. 3.36** shows that increasing the cuttings concentration increases the bottom-hole pressure.

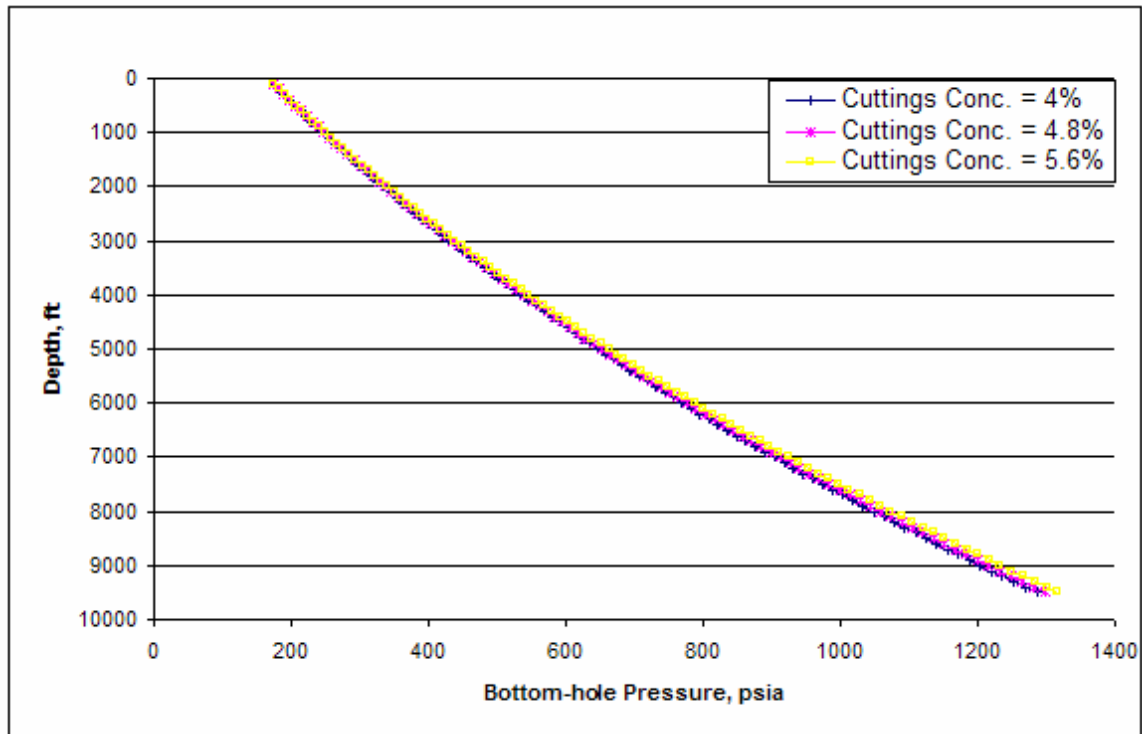


Fig. 3.36-Bottom-hole Pressure vs. Depth at Different Cuttings Concentrations

The higher value of cuttings concentration means more cuttings in the annulus hence higher injection rate is needed for removal of the cuttings. It is shown in **Fig. 3.37** that the increase in cuttings concentration increases the required minimum injection rates.

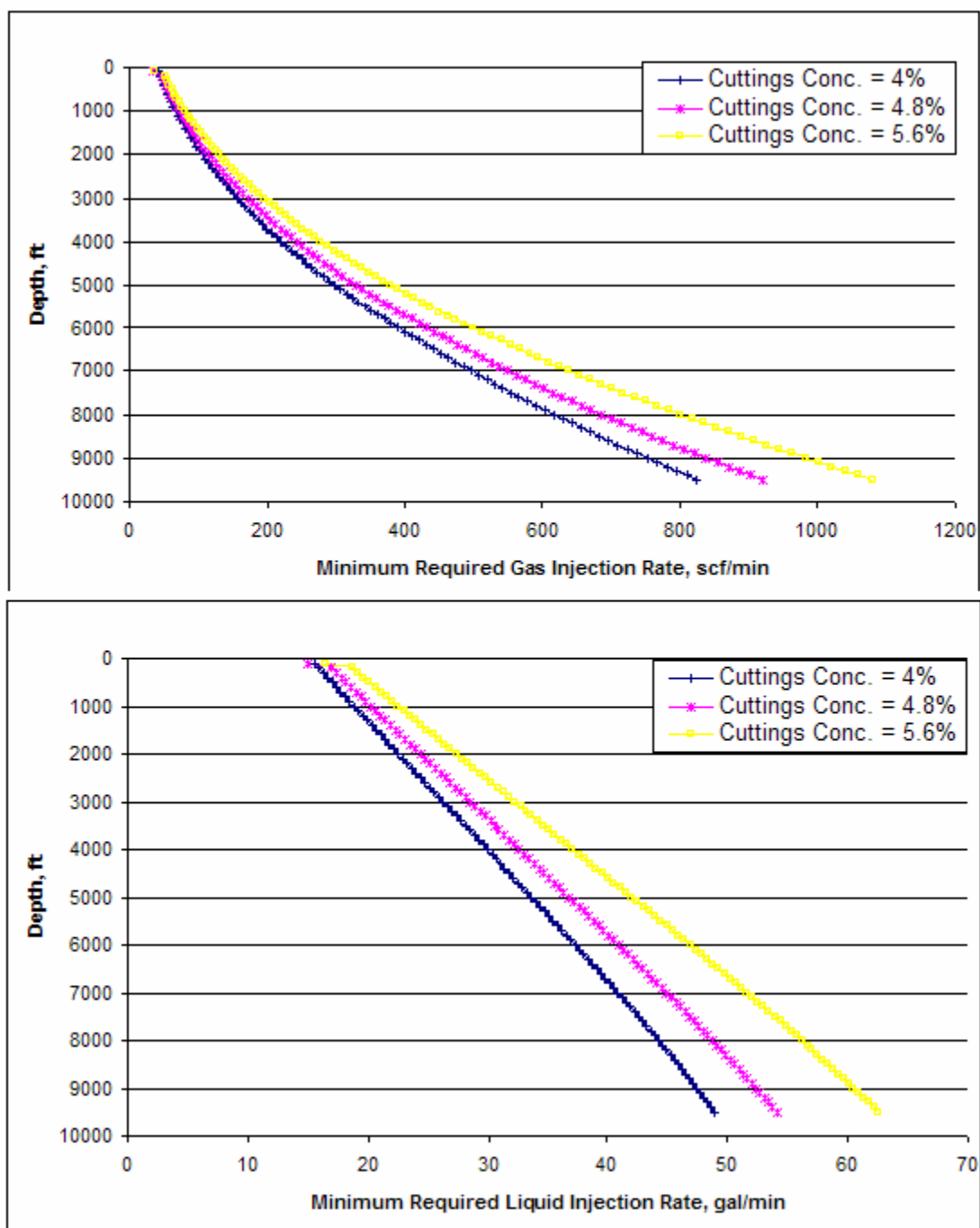


Fig. 3.37-Minimum Injection Rates vs. Depth at Different Cuttings Concentrations

Increasing the cuttings concentration increases the foam velocity and an increase in foam velocity decreases the foam viscosity and consequently the foam friction. **Fig 3.38** clearly shows the effect of increasing the back-pressure on the flow properties.

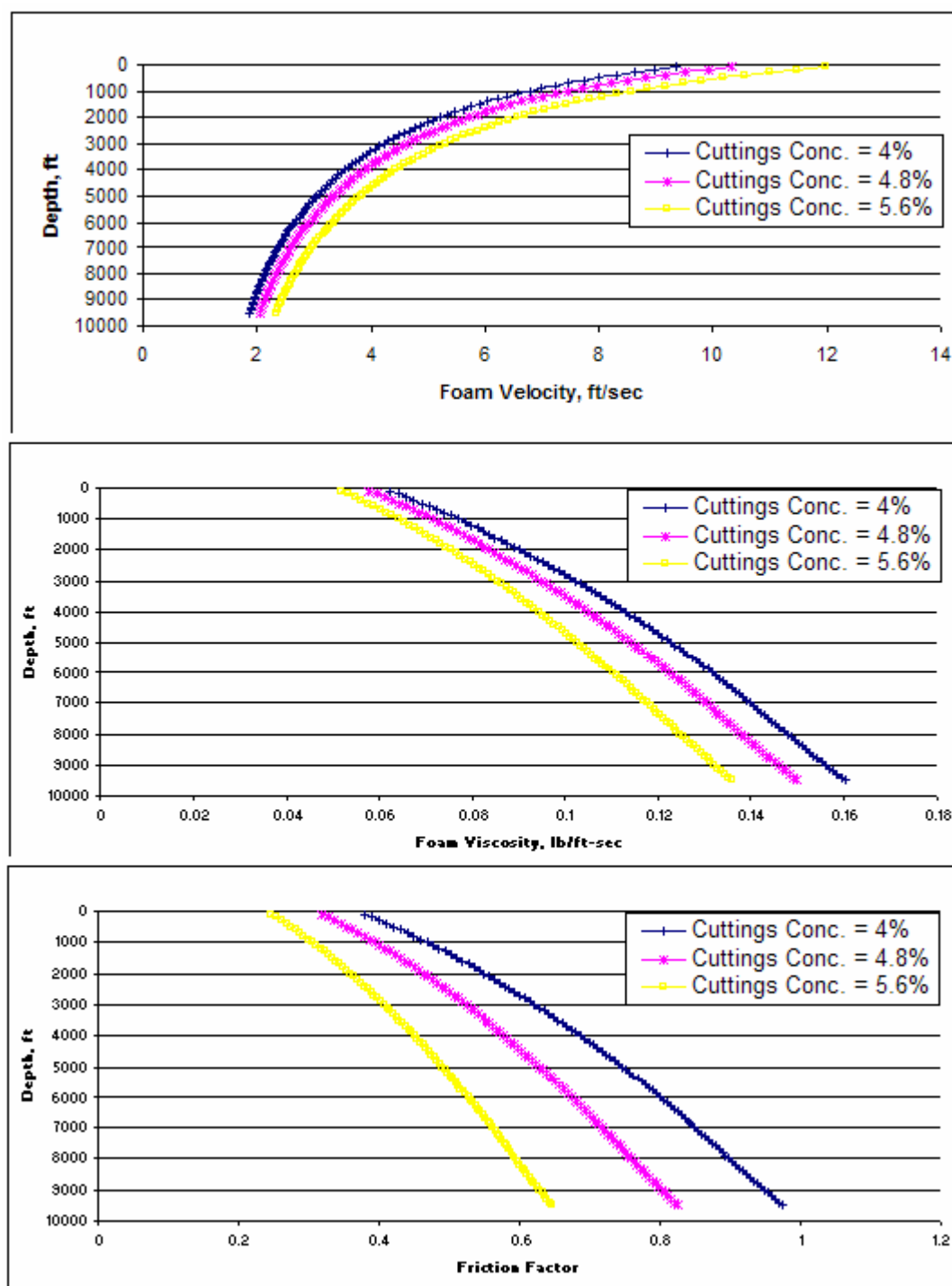


Fig. 3.38-Flow Properties vs. Depth at Different Cuttings Concentrations

A default value of 4% is assumed for the cuttings concentration and then to make the comparison of the results easier, the default value is increased by 20% and 40% respectively. The deviations of properties in these two values are compared with the default value. The effect of increasing the cuttings concentration by 20% and 40% is indicated by the following figures;

Deviation of pressure in **Fig. 3.39**, suggests that increasing cuttings concentration decreases the bottom-hole pressure. Since the graph shows a maximum deviation of 2.5% the increase in pressure is considerable.

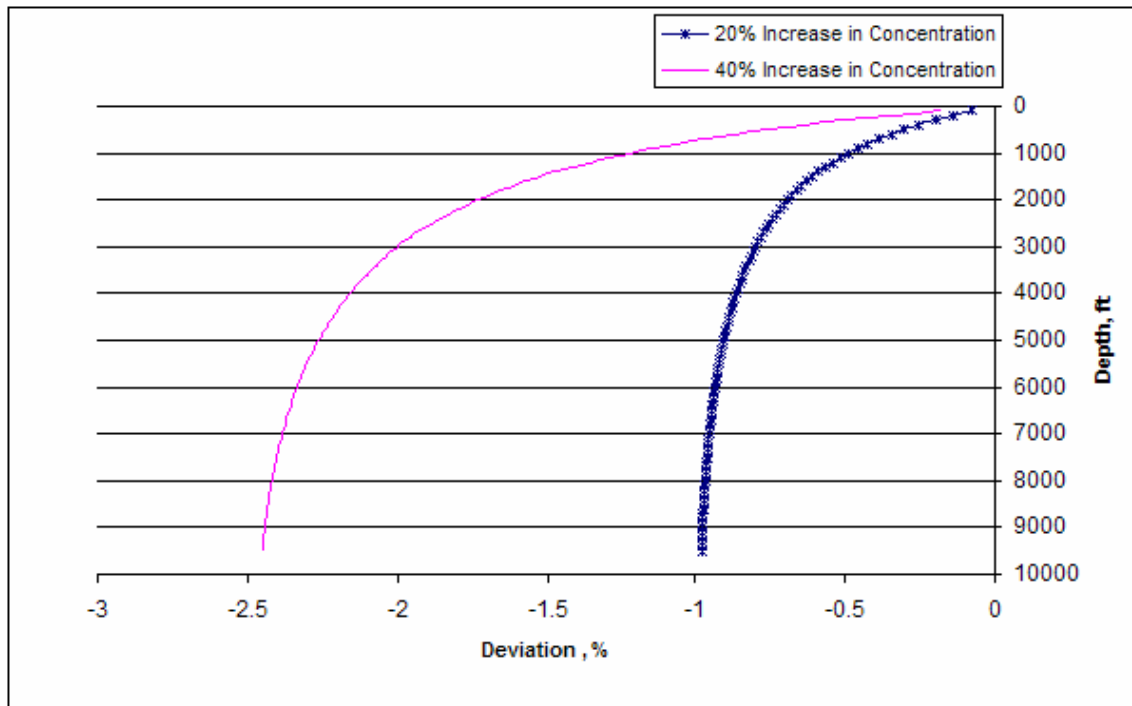


Fig. 3.39-Deviation of Bottom-hole Pressure vs. Depth (Different Concentrations)

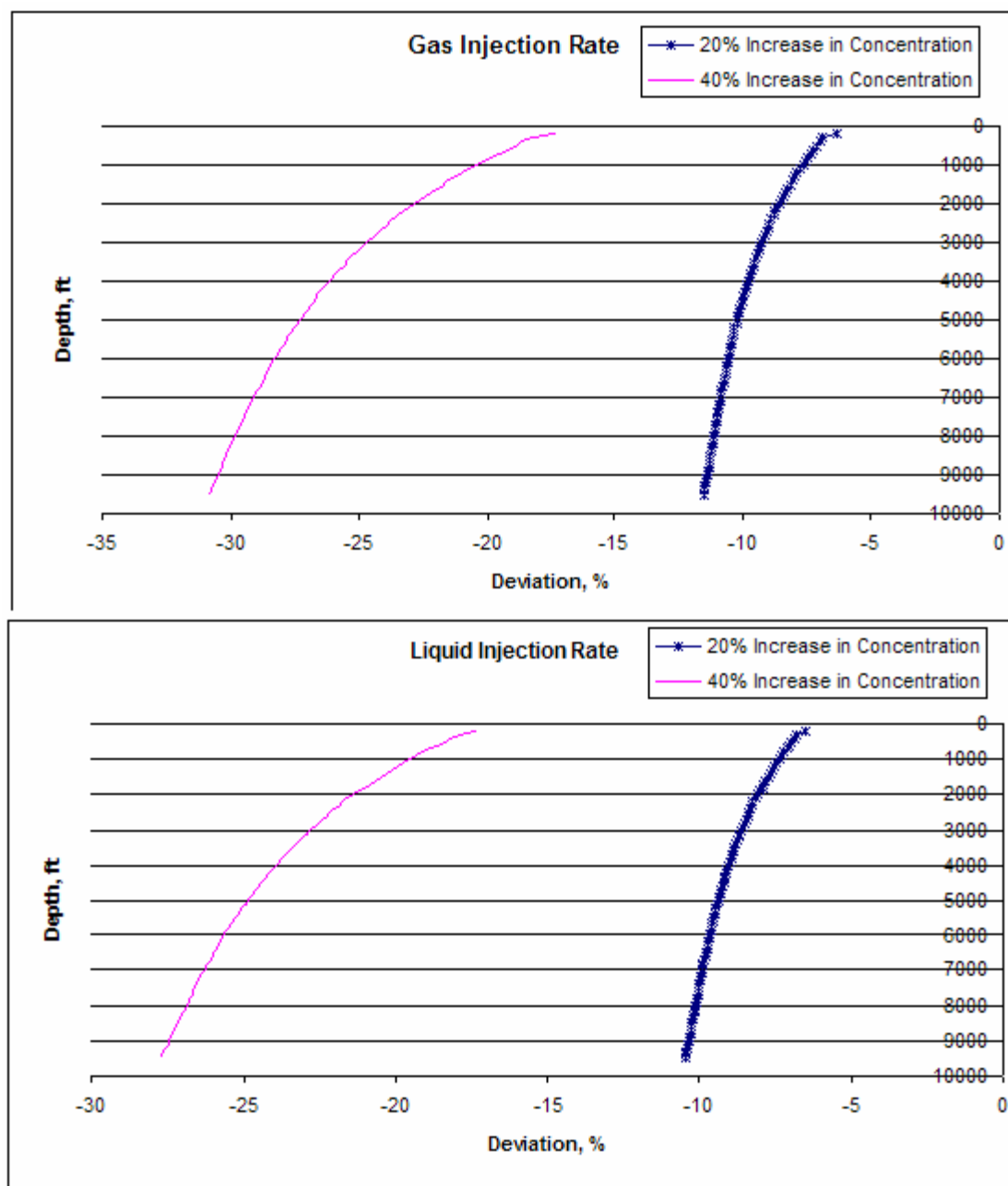


Fig. 3.40-Deviation of Injection Rates vs. Depth (Different Concentrations)

Fig. 3.40 shows that the increase in liquid and gas injection rates are approximately the same. The higher increase in gas injection rate is caused by the increase in the bottom-hole pressure.

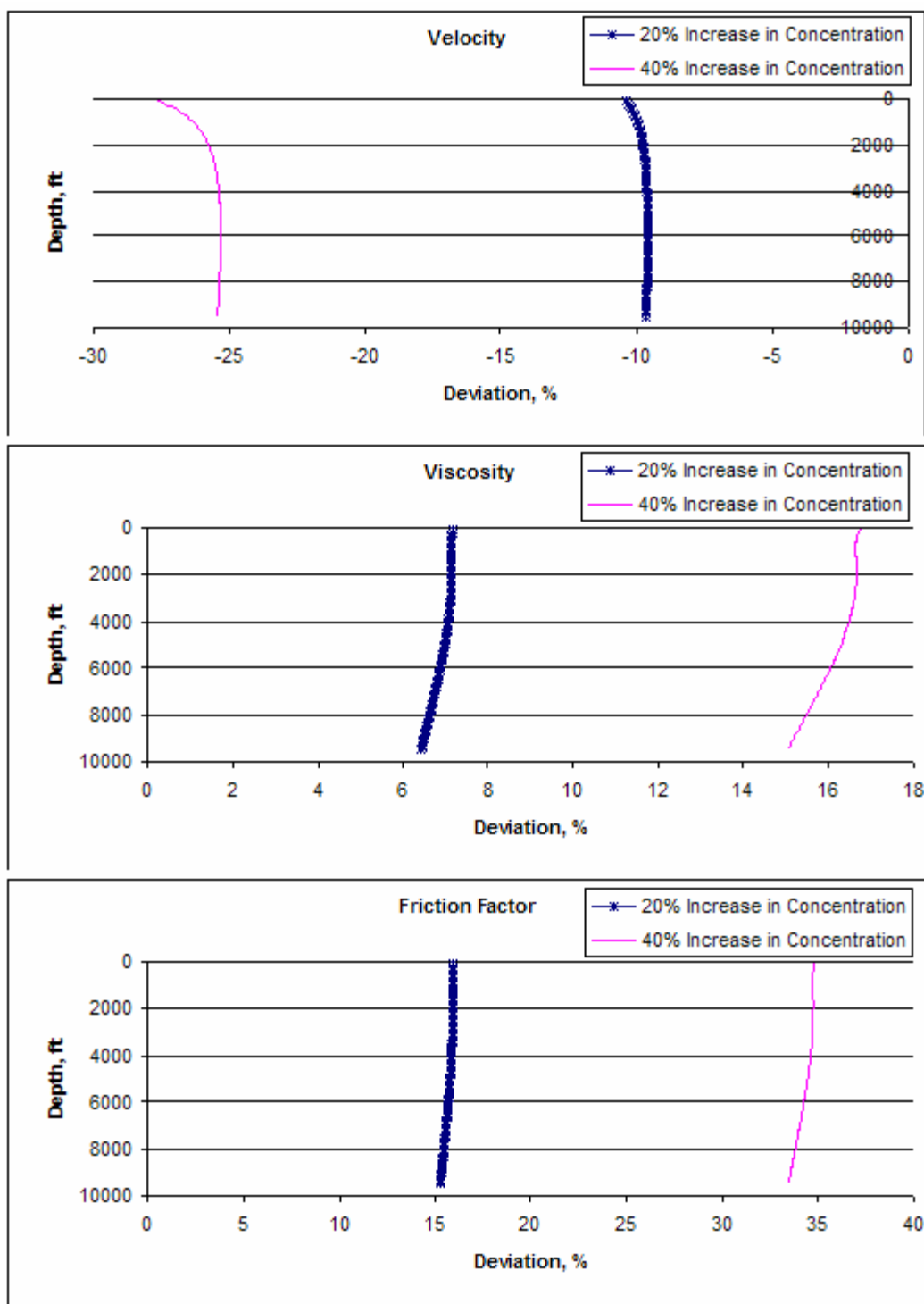


Fig. 3.41-Deviation of Flow Properties vs. Depth (Different Concentrations)

Fig. 3.41 shows that the flow properties are highly affected by the increase in cuttings concentration.

Table 3.4-Summary of Results (Deviations for Cuttings Concentration)

		Pressure	Gas Injection Rate	Liquid Injection Rate	Velocity	Viscosity	Moody Friction
20% Increase in Concentration	<i>% Deviation at Surface</i>	-0.1	-7	-6	-10.5	7	14.5
	<i>% Deviation at Bottom</i>	-1	-12	-10.5	-10	6.5	15
40% Increase in Concentration	<i>% Deviation at Surface</i>	-1	-17	-18	-27	16	35
	<i>% Deviation at Bottom</i>	-2.5	-31	-28	-25	15	34

The summary of the deviation graphs is given in **Table 3.4**. The negative deviation represents an increase in the parameter.

Cuttings size

Considering the constant back-pressure of 165 psia, three different values are assigned to the cuttings diameters. **Fig. 3.42** shows that the pressure slightly increases with increasing the cuttings diameter.

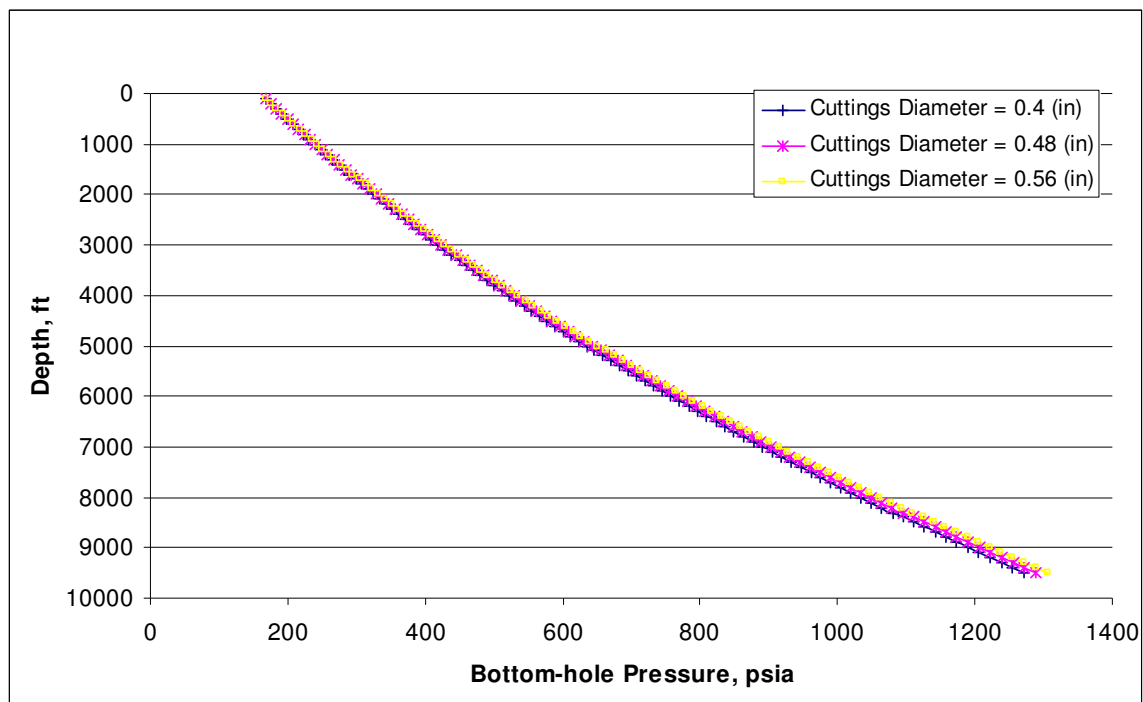


Fig. 3.42-Bottom-hole Pressure vs. Depth at Different Cuttings Diameters

It is shown in **Fig. 3.43** that the increase in cuttings diameter increases the required minimum injection rates. Obviously, as the cuttings get larger, higher injection rates are needed to transport the cuttings to the surface.

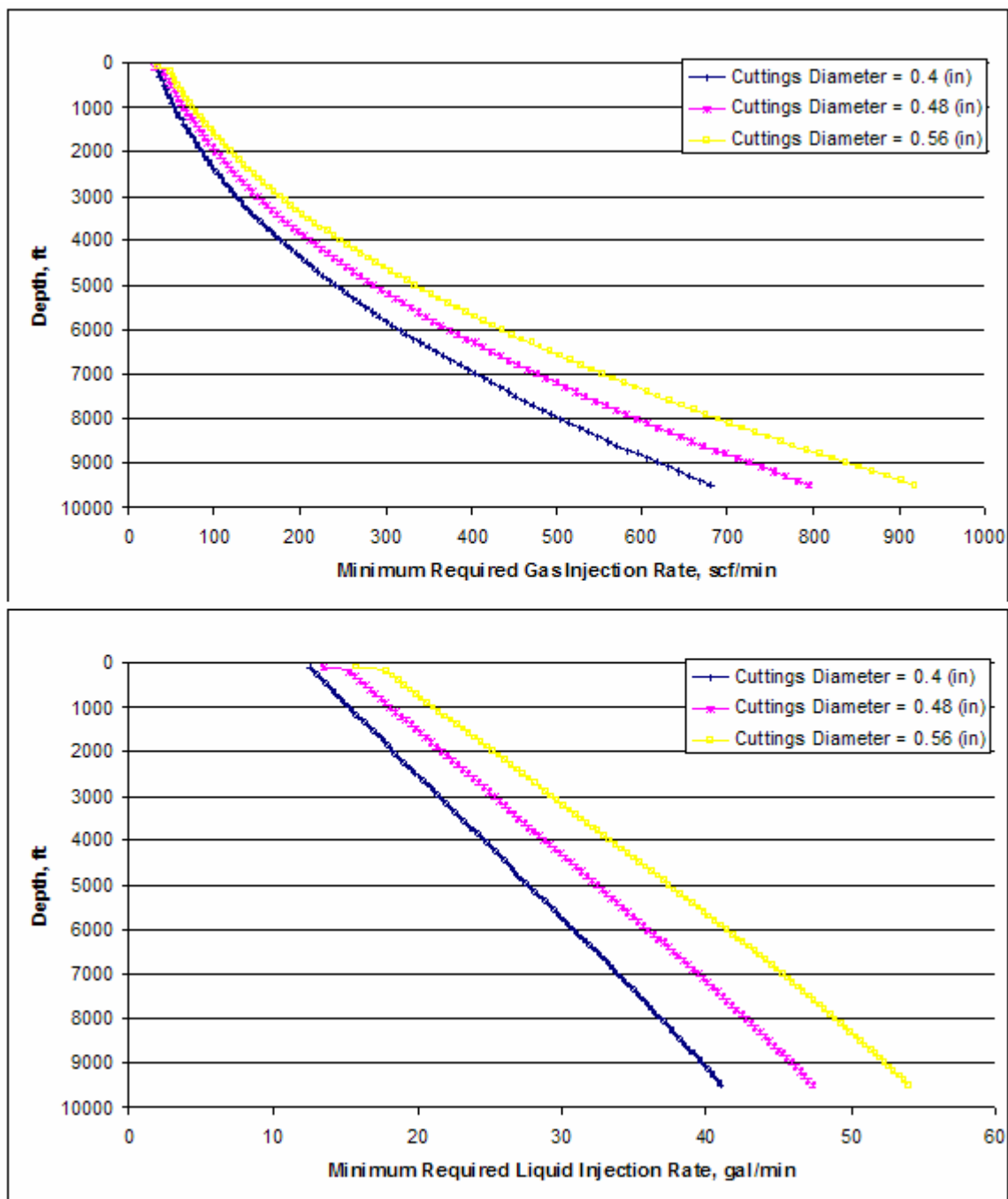


Fig. 3.43-Minimum Injection Rates vs. Depth at Different Cuttings Diameters

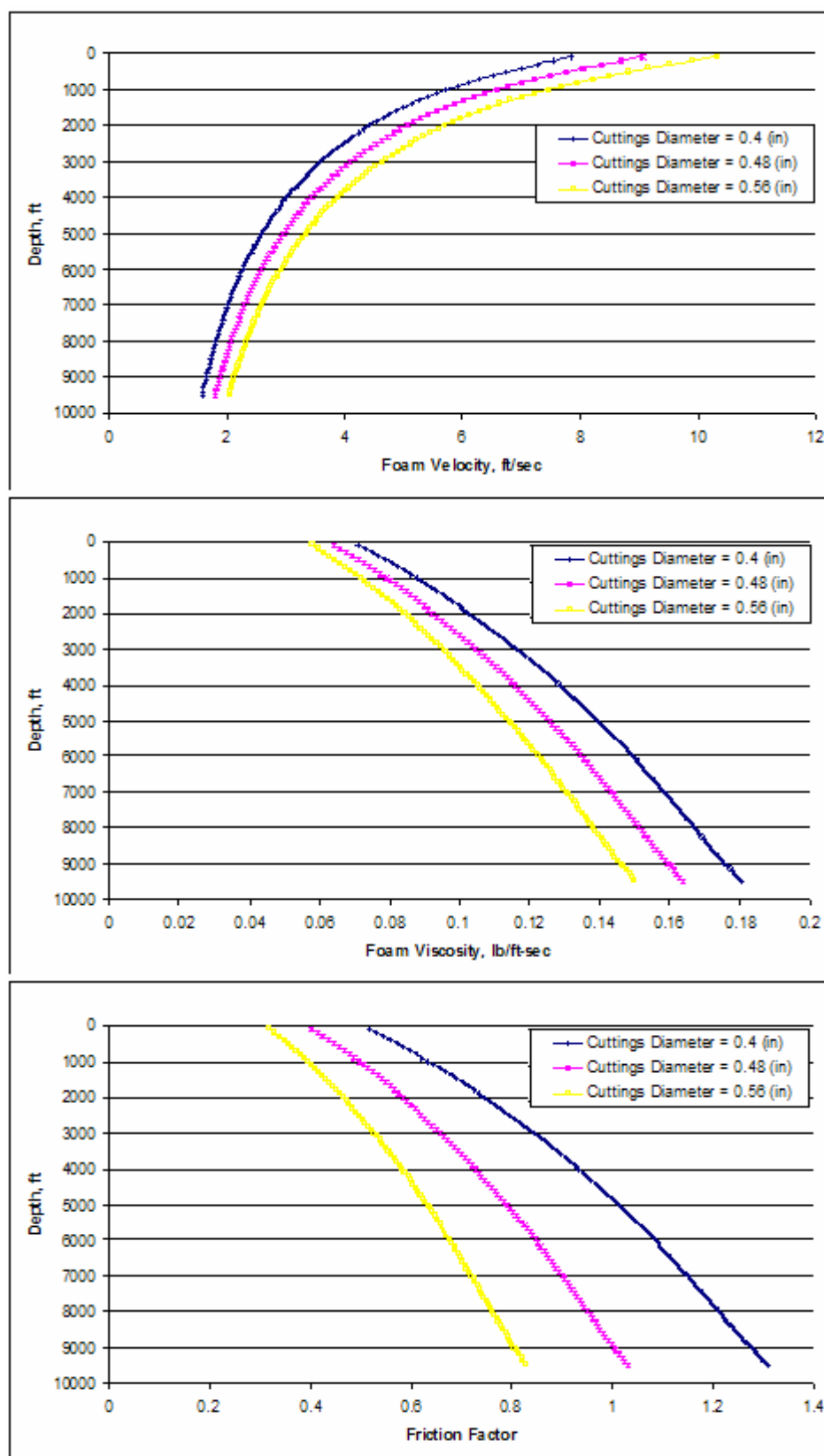


Fig. 3.44-Foam Flow Properties vs. Depth at Different Cuttings Diameters

Increasing the rate of penetration increases the foam velocity and an increase in foam velocity decreases the foam viscosity and consequently the foam friction. **Fig 3.44** clearly shows the effect of increasing the cuttings diameter on the flow properties.

A default value of 0.4 in. is assumed for the cuttings diameter and then to make the comparison of the results easier, the default value is increased by 20% and 40% respectively. The deviations of properties in these two values are compared with the default value. The effect of increasing the cuttings diameter by 20% and 40% is indicated by the following figures;

Deviation of pressure in **Fig. 3.45**, suggests that increasing the cuttings diameter increases the bottom-hole pressure.

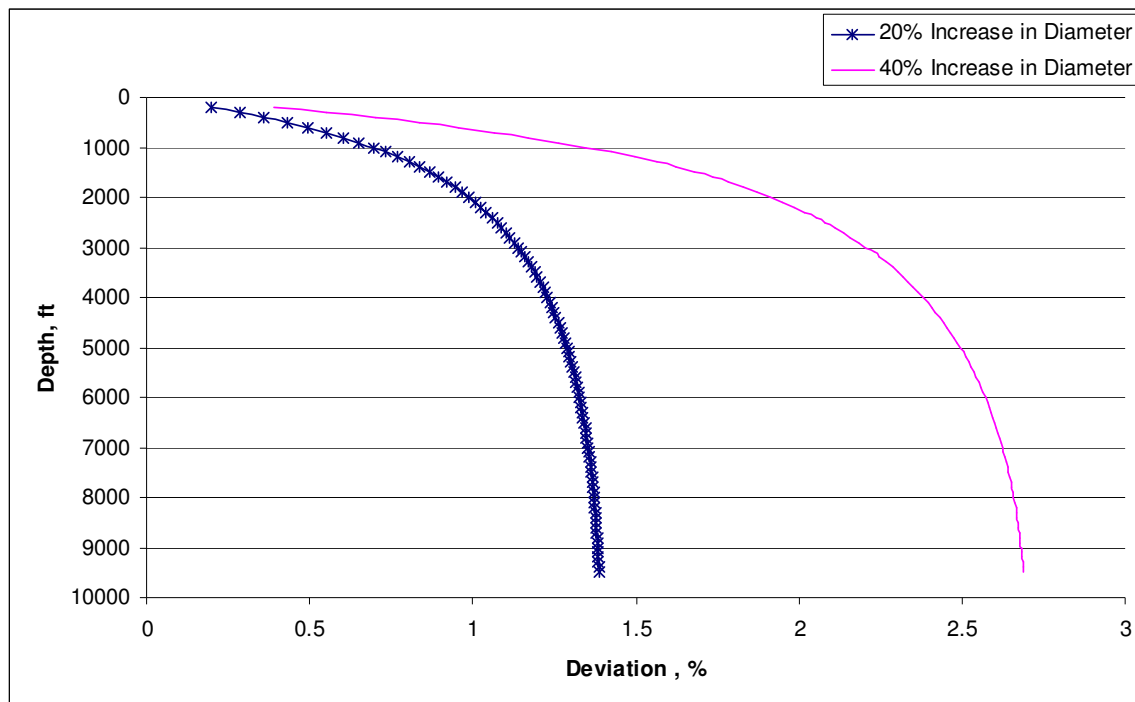


Fig. 3.45-Deviation of Bottom-hole Pressure vs. Depth (Different Diameters)

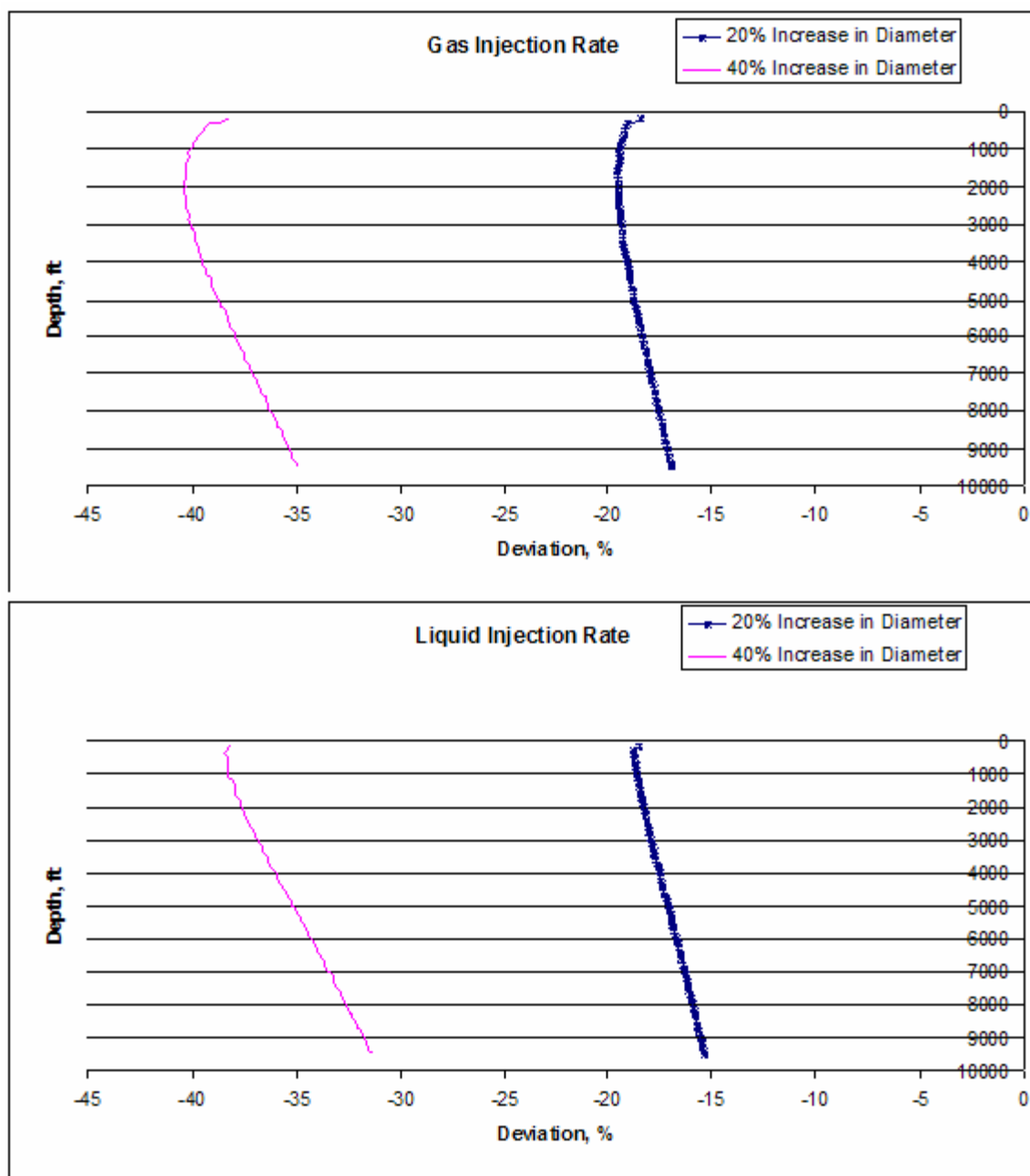


Fig. 3.46-Deviation of Injection Rates vs. Depth (Different Diameters)

Fig. 3.46 shows that increasing the cuttings diameters dramatically increases the minimum required injection rates.

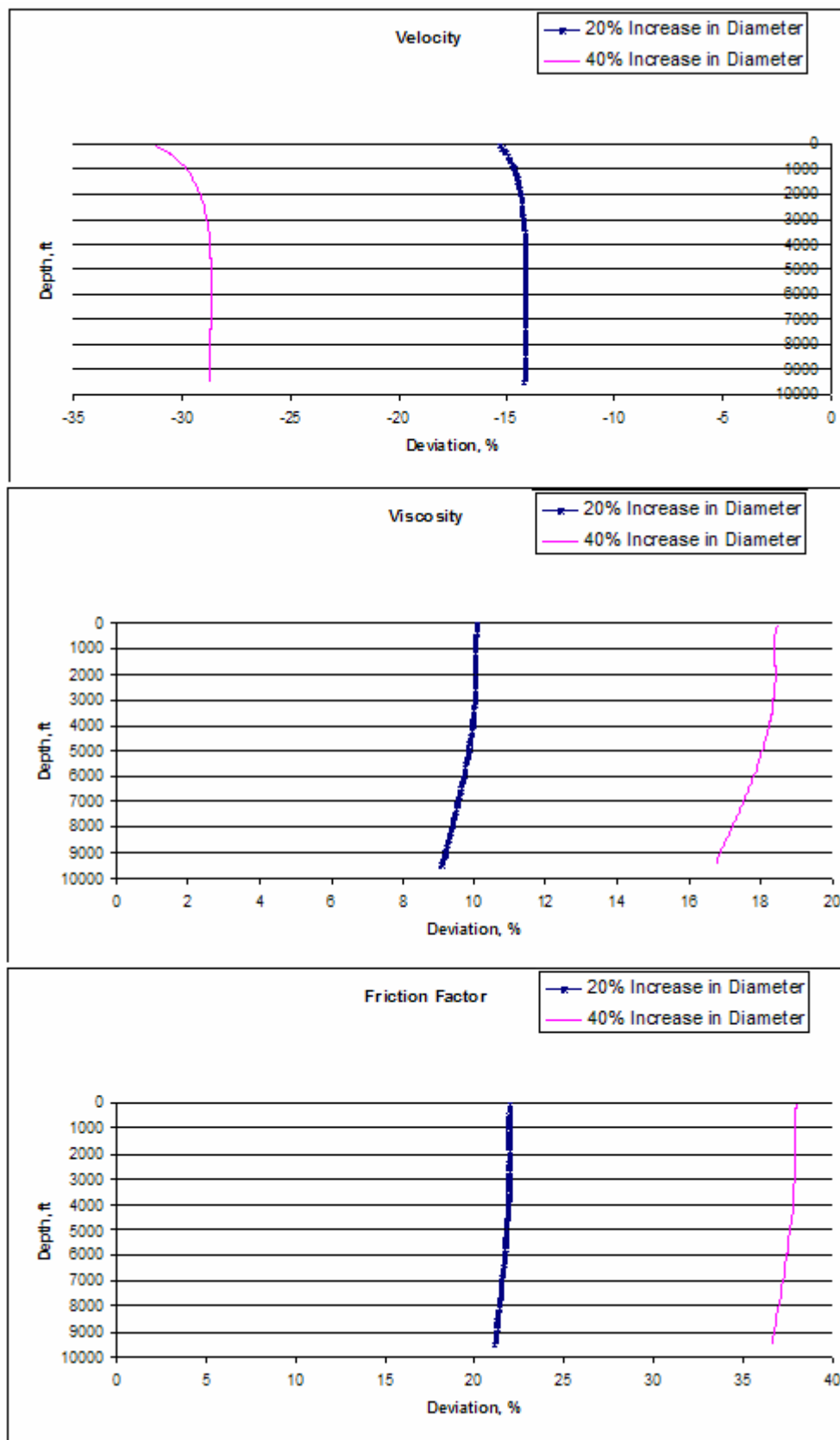


Fig. 3.47-Deviation of Flow Properties vs. Depth (Different Diameters)

Fig. 3.47 shows that the friction factor is highly affected by the increase in cuttings diameter.

Table 3.5-Summary of Results (Deviations for Cuttings Diameter)

		Pressure	Gas Injection Rate	Liquid Injection Rate	Velocity	Viscosity	Moody Friction
20% Increase in Diameter	% Deviation at Surface	-0.2	-18	-18	-15	9.5	22
	% Deviation at Bottom	-1.4	-17	-15	-14.5	9	21
40% Increase in Diameter	% Deviation at Surface	-0.4	-37	-39	-31	18	37
	% Deviation at Bottom	-2.65	-35	-31	-29	17	36

The summary of the deviation graphs is given in **Table 3.5**. The negative deviation represents an increase in the parameter.

Formation water influx

When formation water influx is not zero the simulation of the model is a little different. The difference is, the value of GLR (see **Eq. 2.7**) does not remain constant during the operation. Hence any change in injection rate would result a change in the value of GLR.

Considering the constant back-pressure of 165 psia, three different values are assigned to the water influx rate. **Fig. 3.48** shows that the pressure does not change with any increase in influx rate.

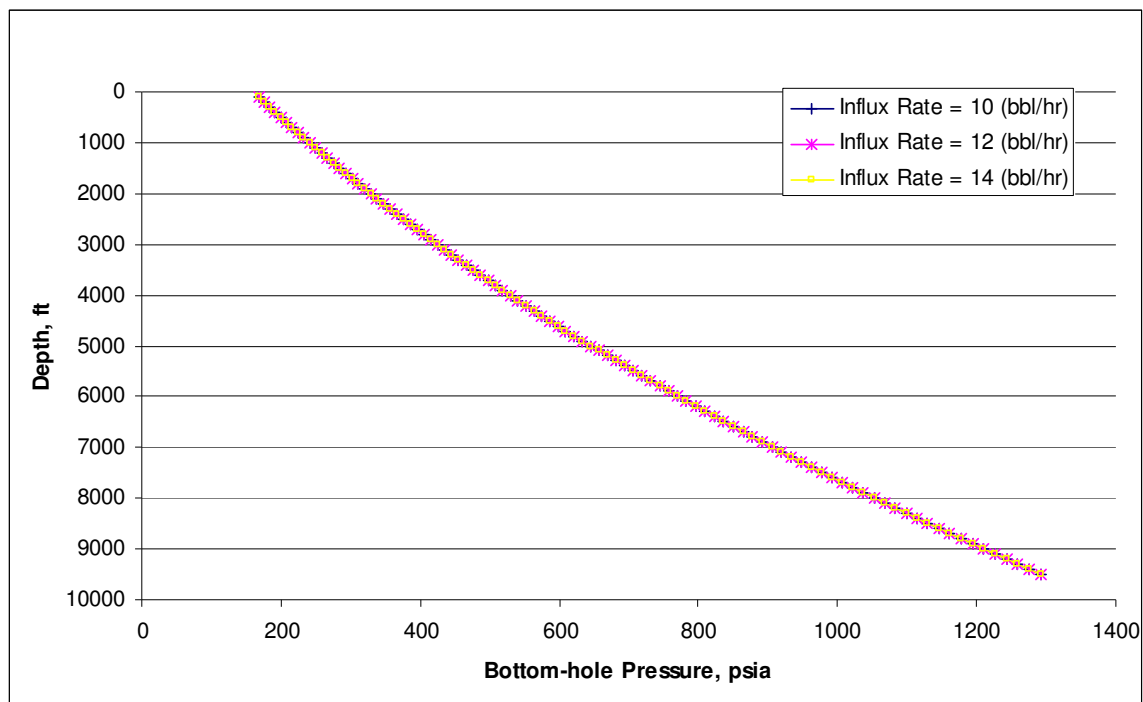


Fig. 3.48-Bottom-hole Pressure vs. Depth at Different Water Influx Rates

Fig. 3.49 shows that increasing the formation influx rate does not change the flow properties. That is because an increase in influx rate decreases the minimum required injection rates and hence the velocity remains constant.

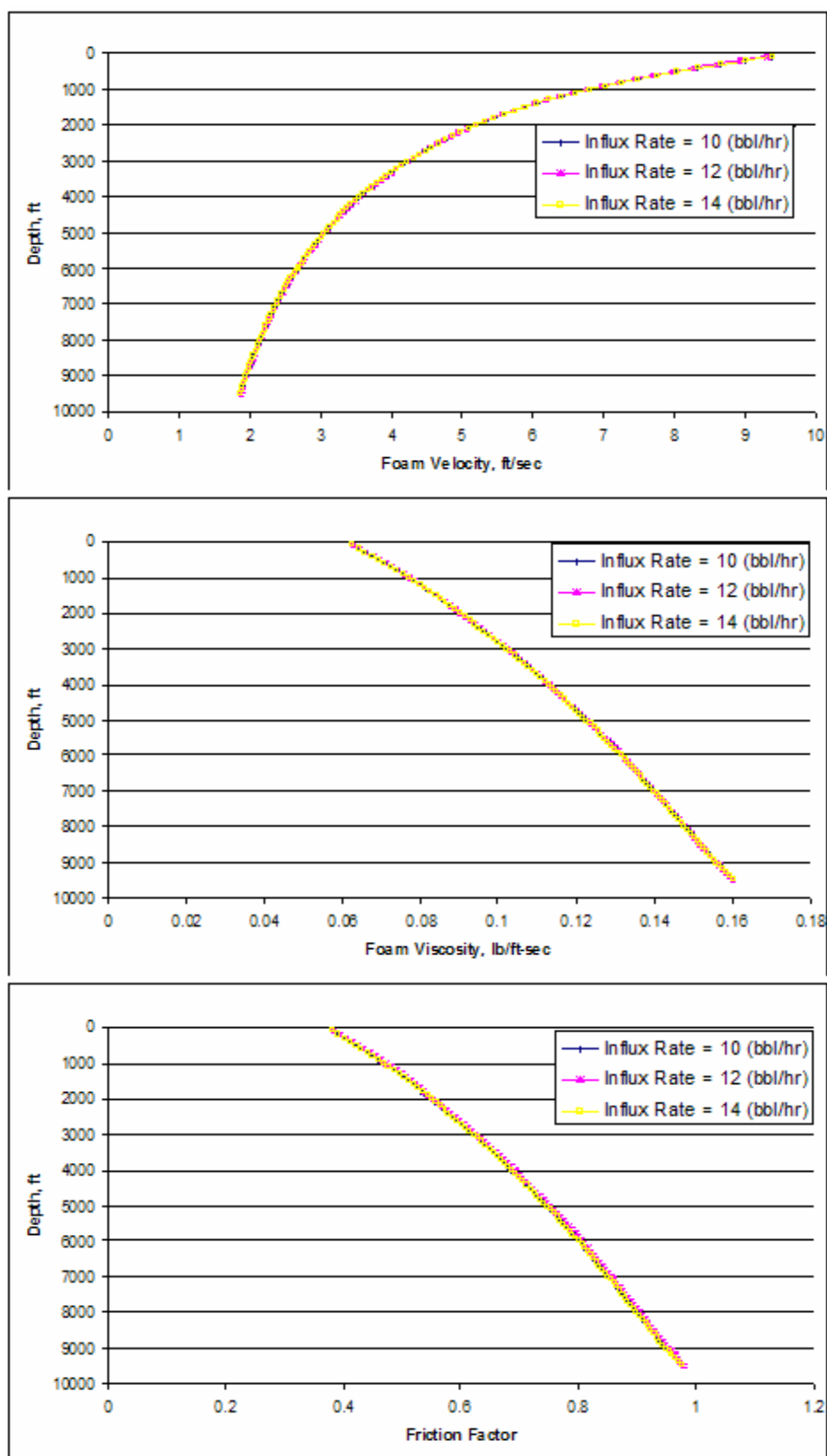


Fig. 3.49-Flow Properties vs. Depth at Different Water Influx Rates

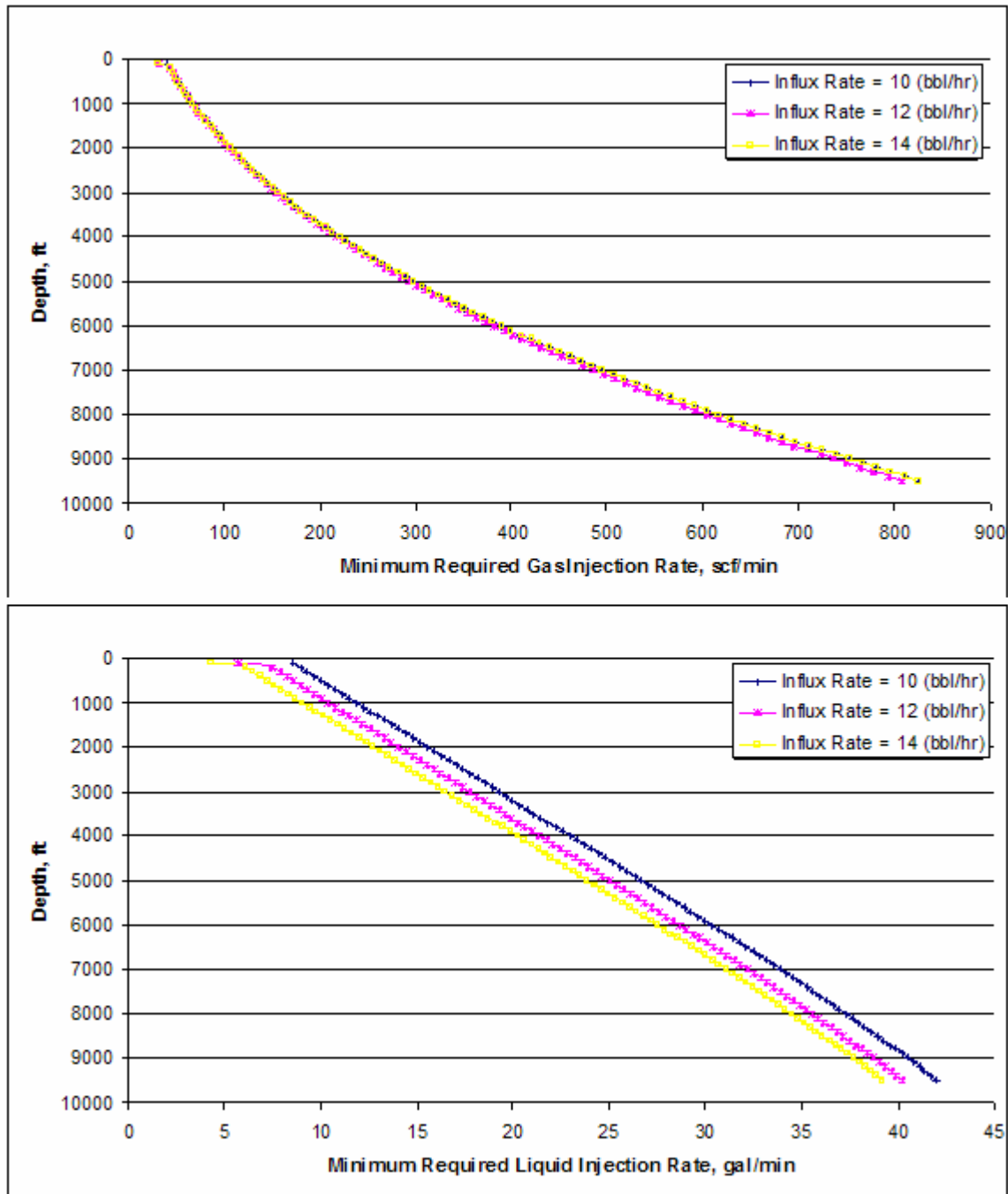


Fig. 3.50-Minimum Injection Rates vs. Depth at Different Water Influx Rates

It is shown in **Fig. 3.50** that the increase in influx rate decreases the required minimum liquid injection rate but the necessity of increasing the GLR with an increase in influx rate (**Fig. 3.51**), increases the minimum required gas injection rate.

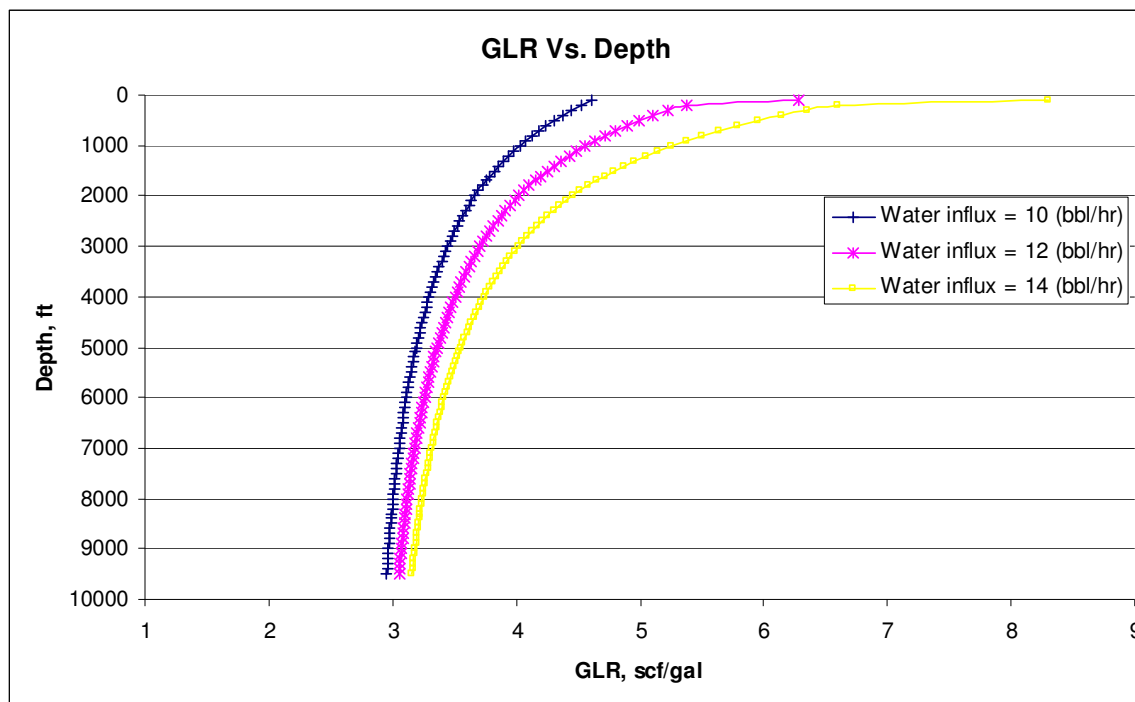


Fig. 3.51-GLR vs. Depth at Different Water Influx Rates

On the other hand, at constant liquid injection rate as it is shown in **Fig 3.52** there would be much more increase in gas injection rate. The increase in the gas injection rate can be explained by the increase in the GLR.

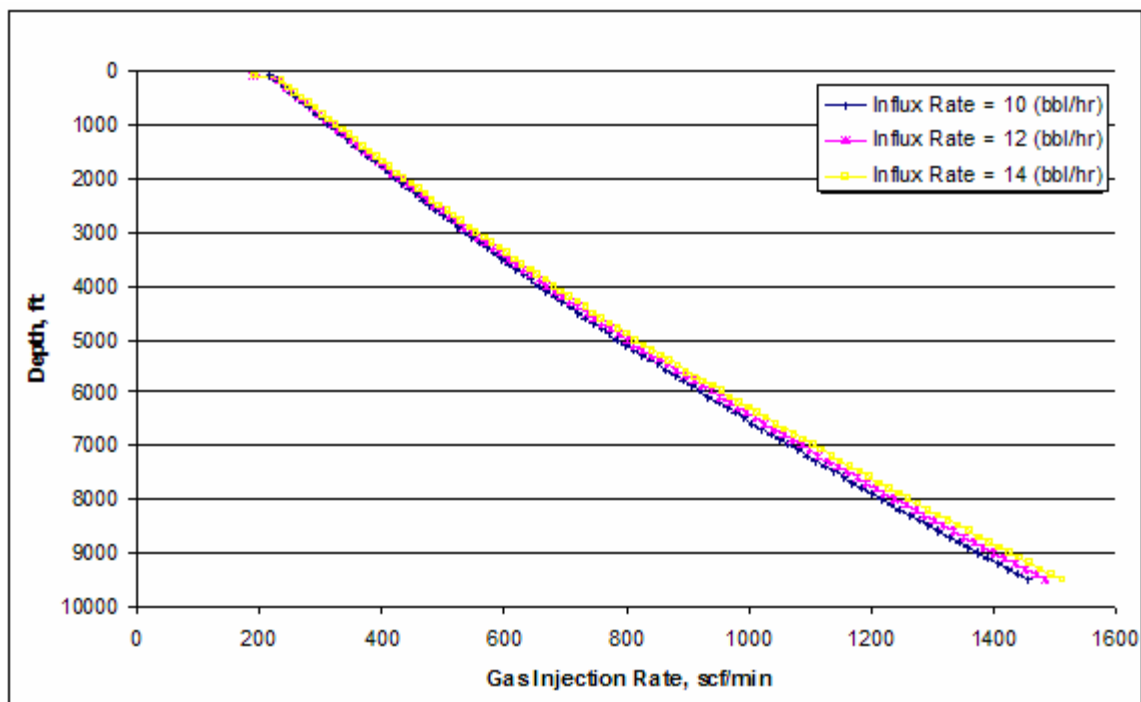


Fig. 3.52-Gas Injection Rate vs. Depth at Different Water Influx Rates

Increasing the influx rate at constant liquid injection rate would also change the flow properties. **Fig 3.53** shows the changes in flow properties in contrast with the flow properties shown in **Fig 3.49**.

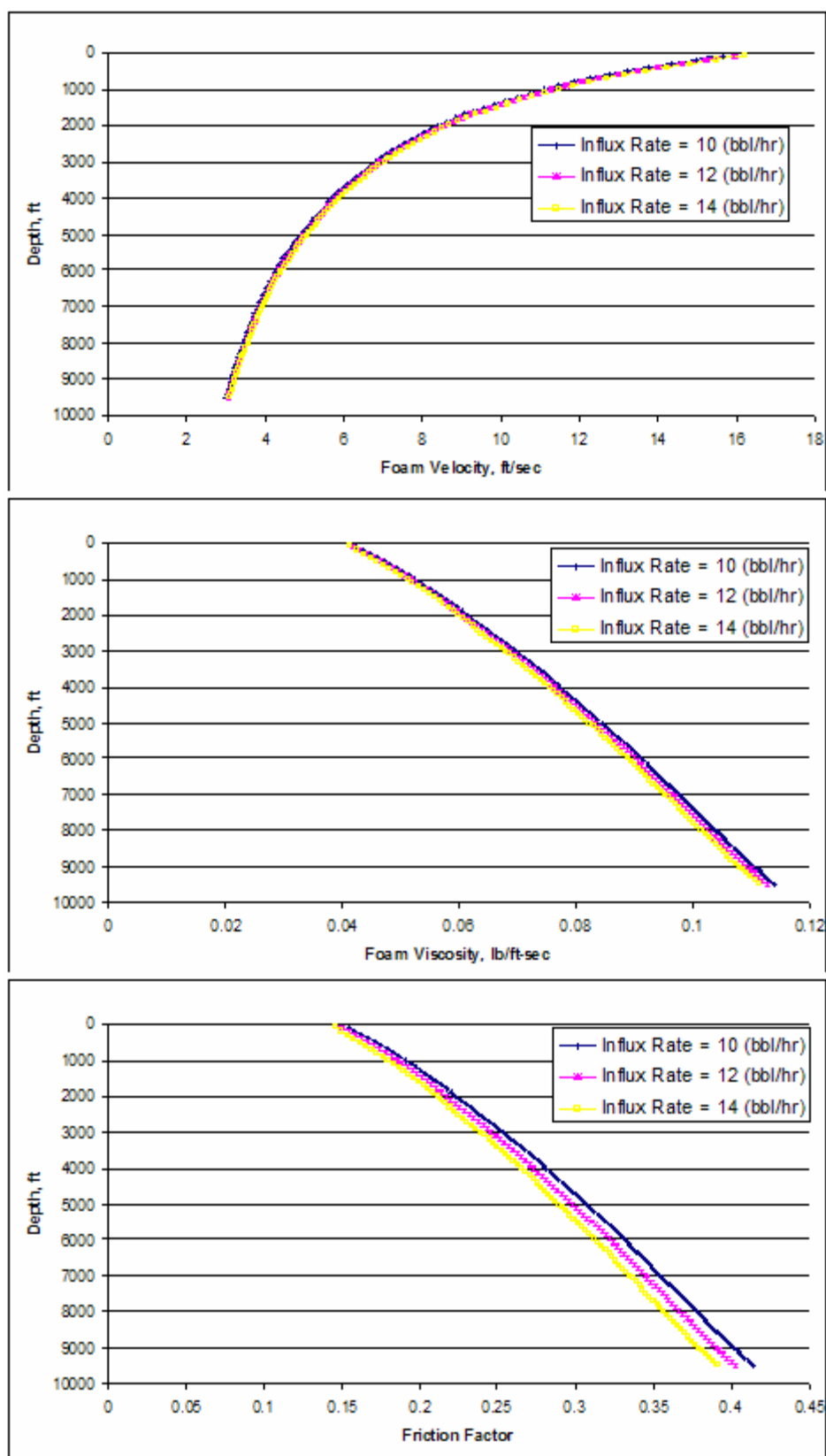


Fig. 3.53-Flow Properties vs. Depth at Different Water Influx Rates (Const. Inj. Rate)

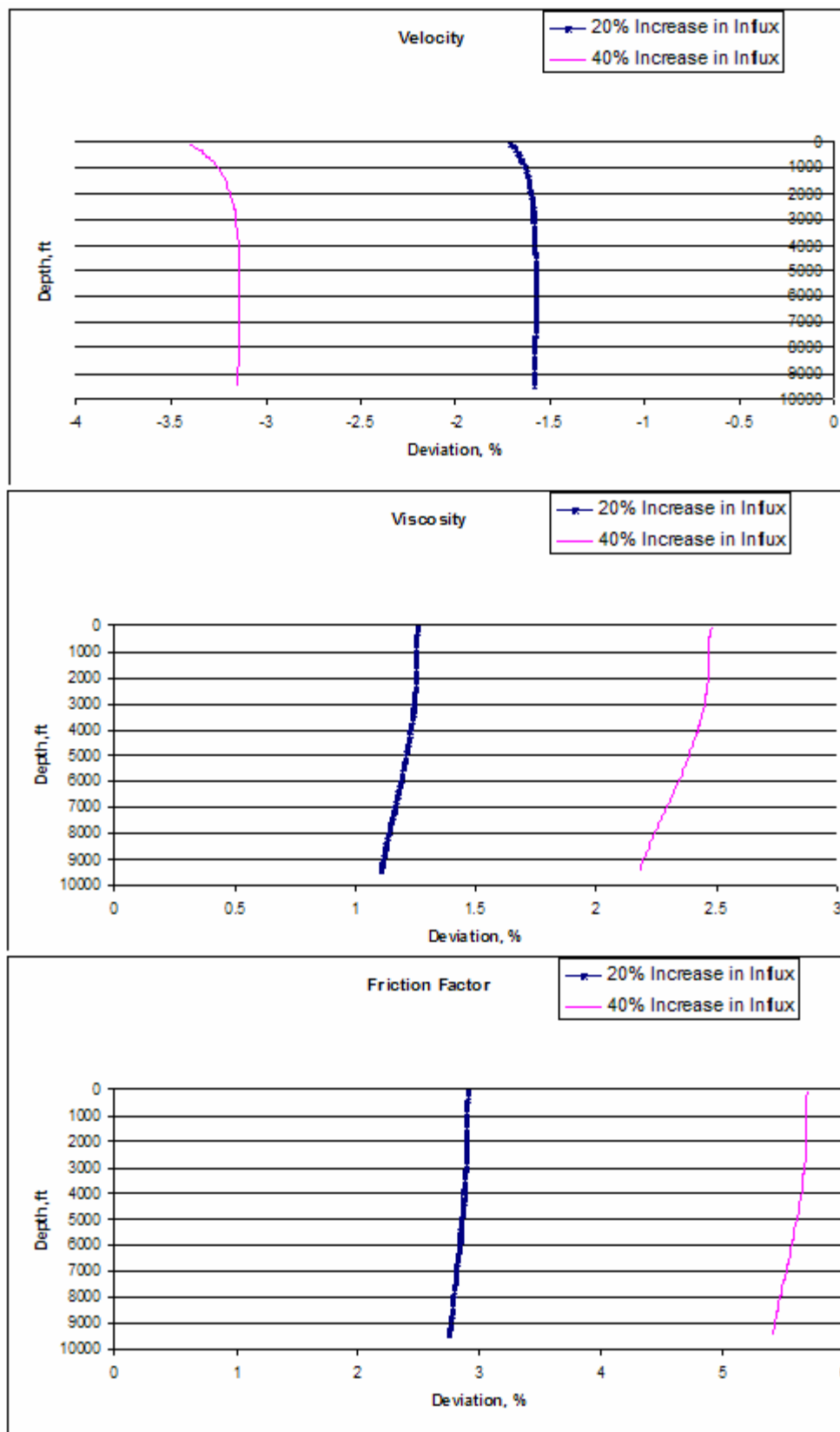


Fig. 3.54-Deviation of Flow Properties vs. Depth (Different Influx Rates)

Fig. 3.54 shows the percent change of each property at constant liquid injection rate and back-pressure.

Table 3.6-Summary of Results (Deviations for Water Influx Rate)

		Pressure	Gas Injection Rate	GLR	Velocity	Viscosity	Moody Friction
20% Increase in Influx	% Deviation at Surface	-0.2	-4	-6	-1.75	1.25	3
	% Deviation at Bottom	-0.2	-2	-10.5	-1.5	1.2	2.9
40% Increase in Influx	% Deviation at Surface	-0.35	-6.5	-18	-3.5	2.5	5.5
	% Deviation at Bottom	-0.35	-4	-28	-3.25	2.2	5.4

The deviation of GLR values is shown in **Table 3.6**. The negative deviation represents an increase in the parameter.

Injection rate

Considering the constant back-pressure of 165 psia, three different values (which are greater than minimum required injection rate) are assigned to the injection rate. **Fig. 3.55** shows that the effect of injection rate on the pressure is significant. As it is shown increasing the injection rate increases the bottom-hole pressure.

It is shown in **Fig. 3.56** that the increase in injection rate decreases the foam quality along the wellbore.

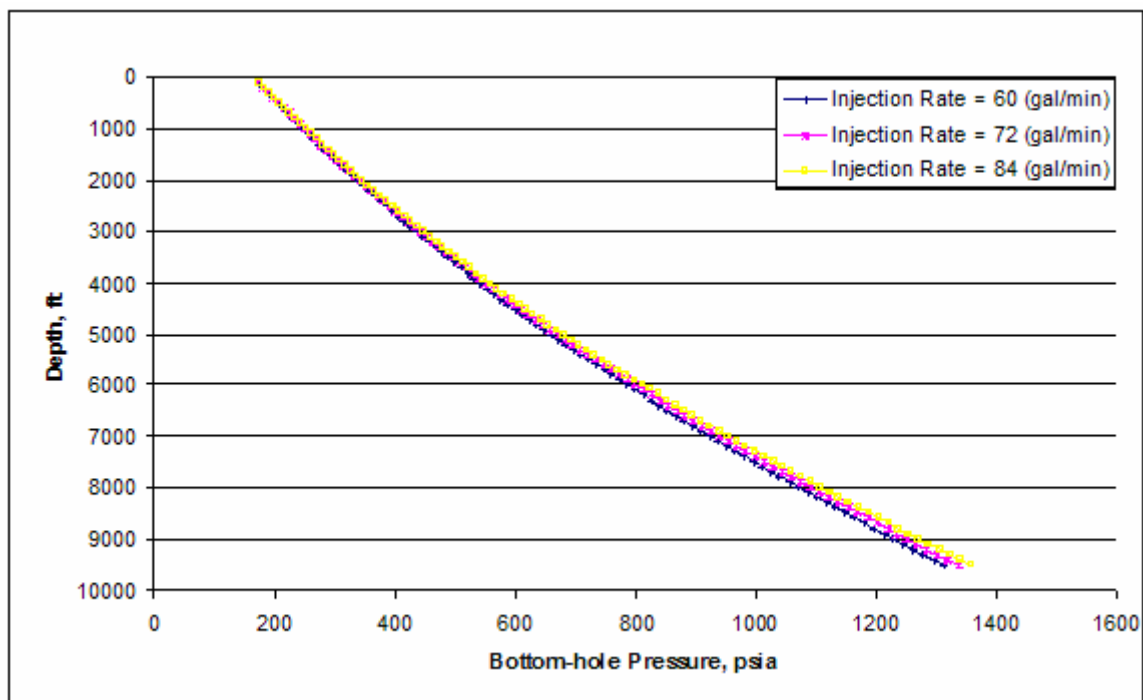


Fig. 3.55-Bottom-hole Pressure vs. Depth at Different Injection Rates

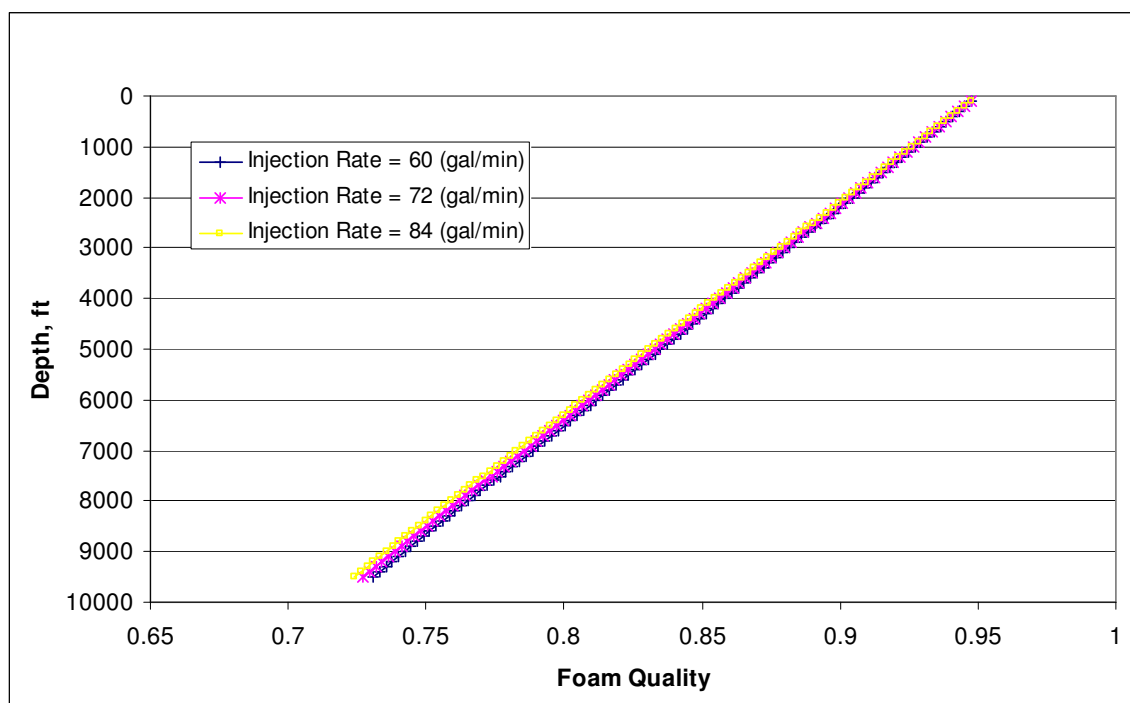


Fig. 3.56-Foam Quality vs. Depth at Different Injection Rates

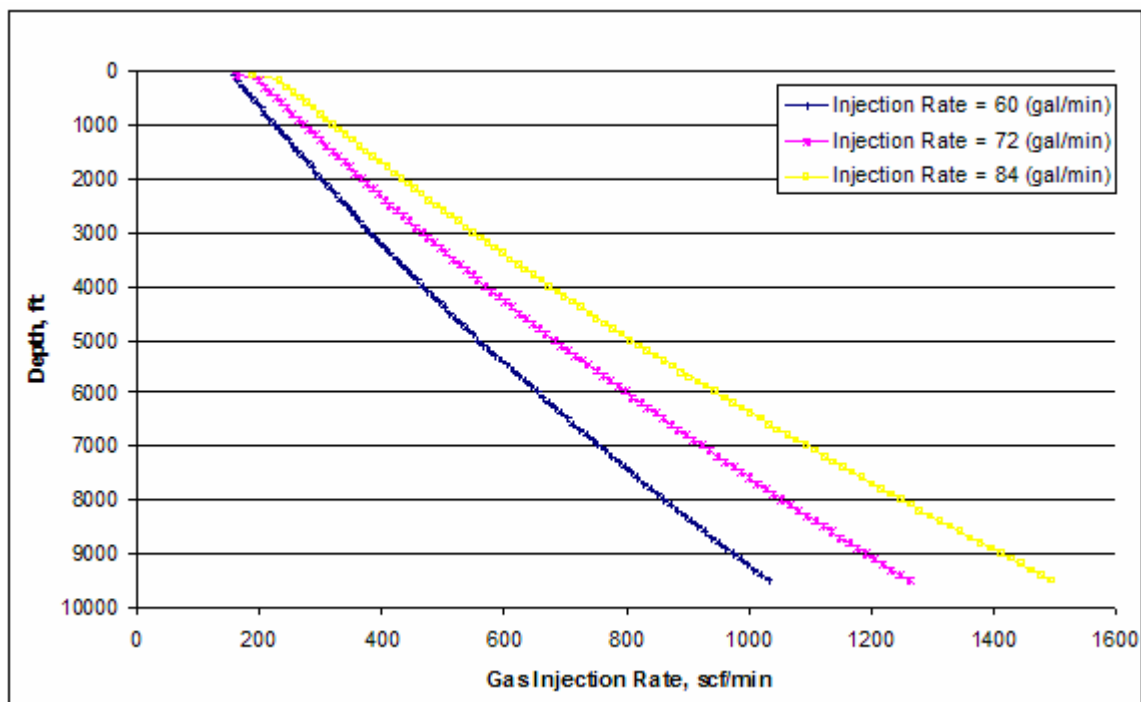


Fig. 3.57-Gas Injection Rate vs. Depth at Different Injection Rates

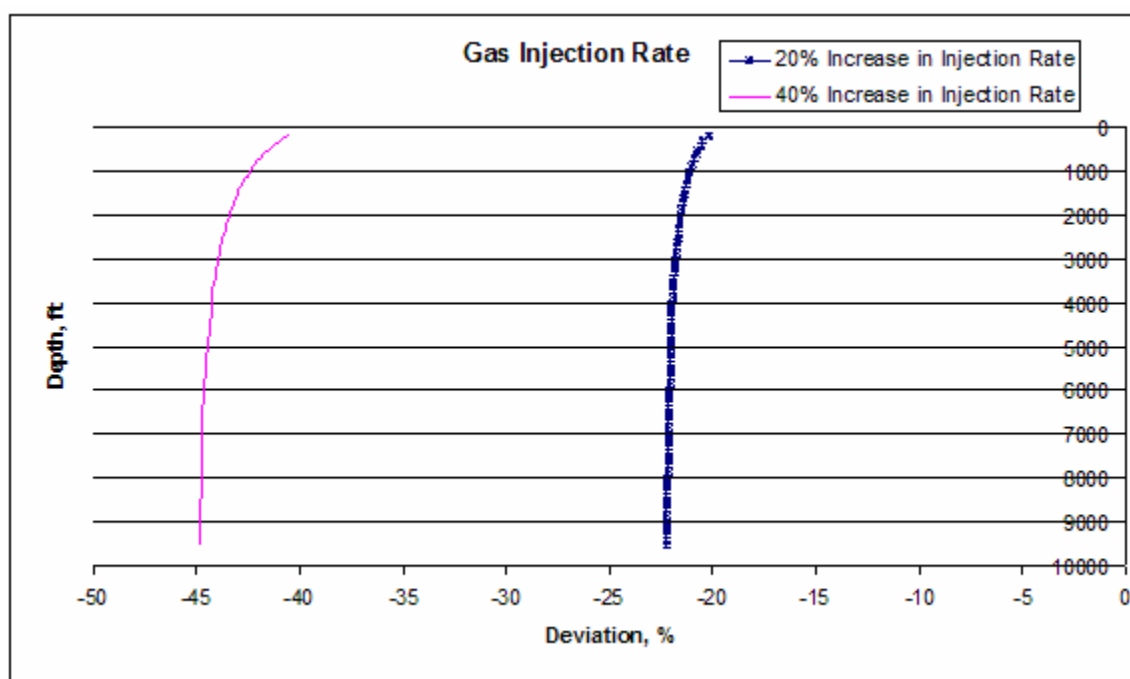


Fig. 3.58-Deviation of Gas Injection Rate vs. Depth (Different Injection Rates)

Fig 3.57 and **Fig 3.58** show that increasing the liquid injection rate by 20% and 40% increases the gas injection rate a little more than 20% and 40% respectively.

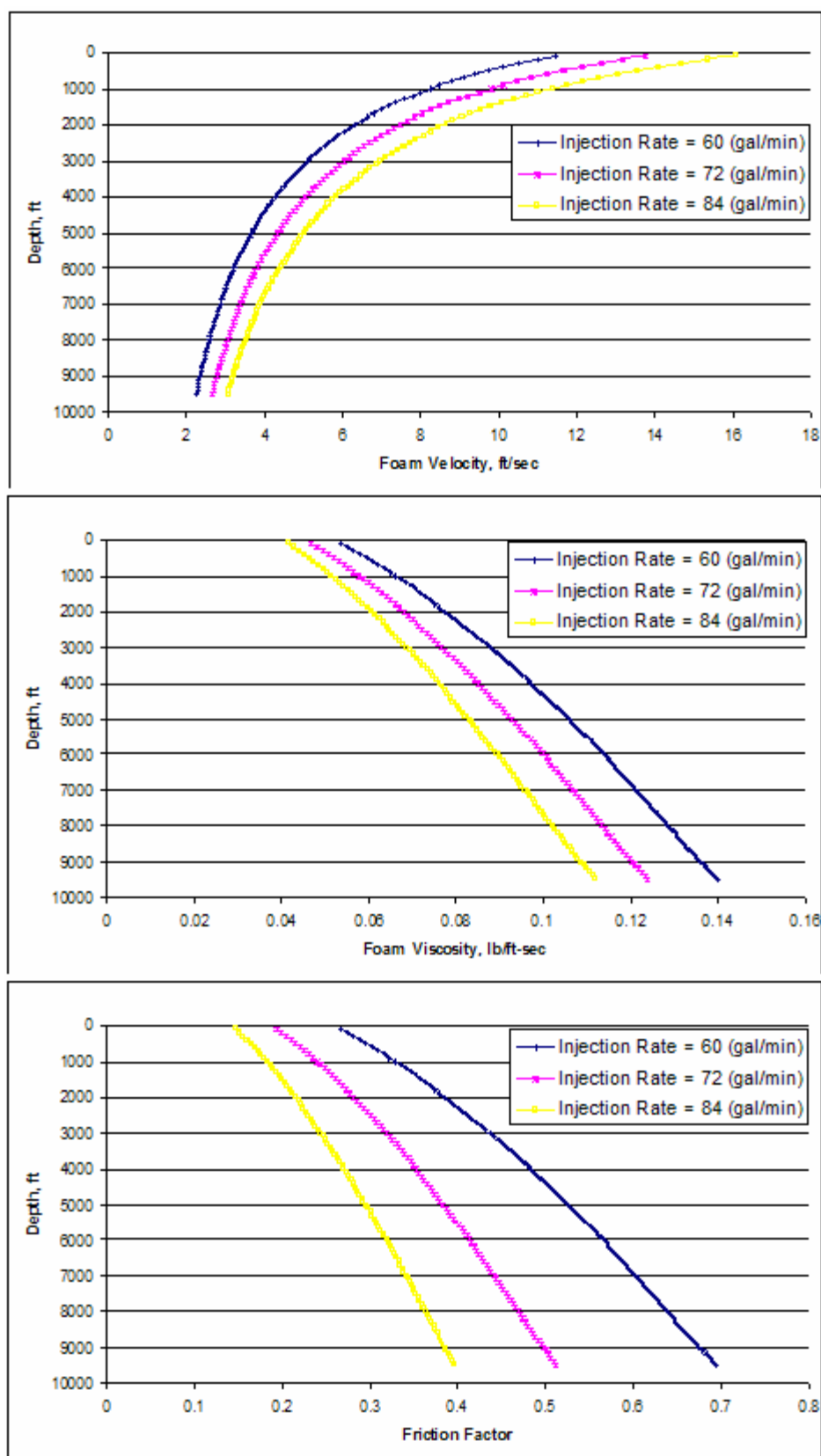


Fig. 3.59-Flow Properties vs. Depth at Different Injection Rates

Increasing the liquid injection rate increases the foam velocity and an increase in foam velocity decreases the foam viscosity and consequently the foam friction. **Fig 3.59** clearly shows the effect of increasing the injection rate on the flow properties.

A default value of 60 (gal/min) is assumed for the injection rate and then to make the comparison of the results easier, the default value is increased by 20% and 40% respectively. The deviations of properties in these two values are compared with the default value. The effect of increasing the liquid injection rate by 20% and 40% is indicated by the following figures;

Deviation of pressure in **Fig. 3.60**, suggests that increasing the liquid injection rate increases the bottom-hole pressure. **Fig. 3.61** shows that increasing the injection rate decreases the foam quality.

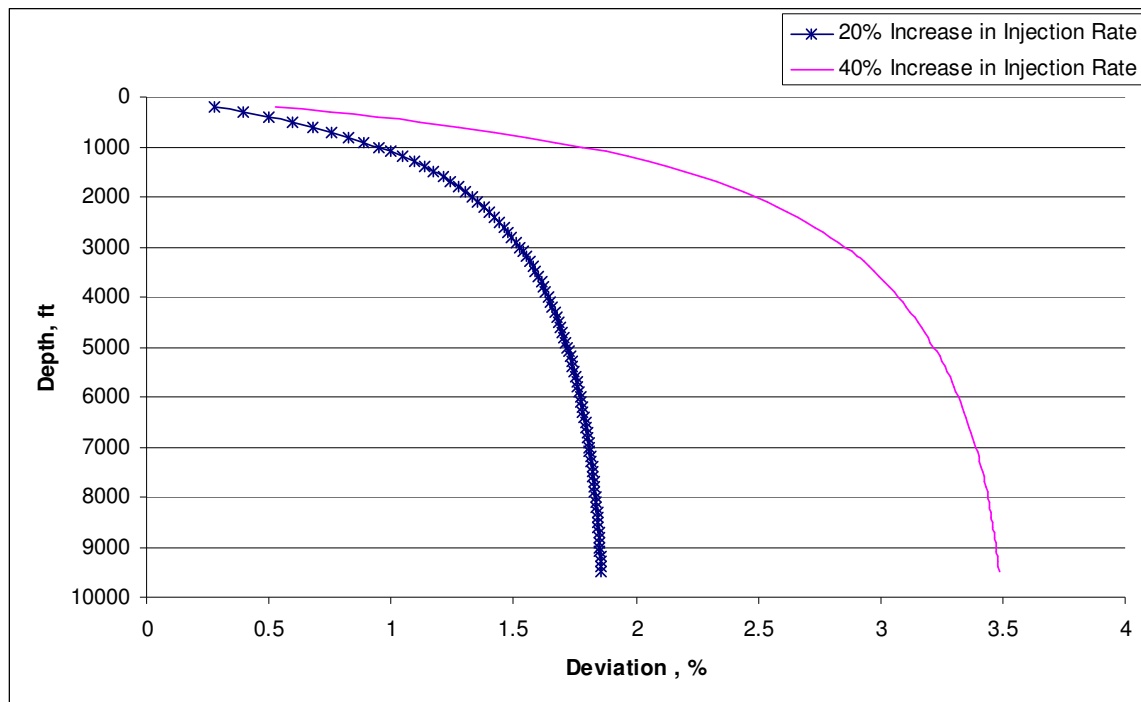


Fig. 3.60-Deviation of Bottom-hole Pressure vs. Depth (Different Injection Rates)

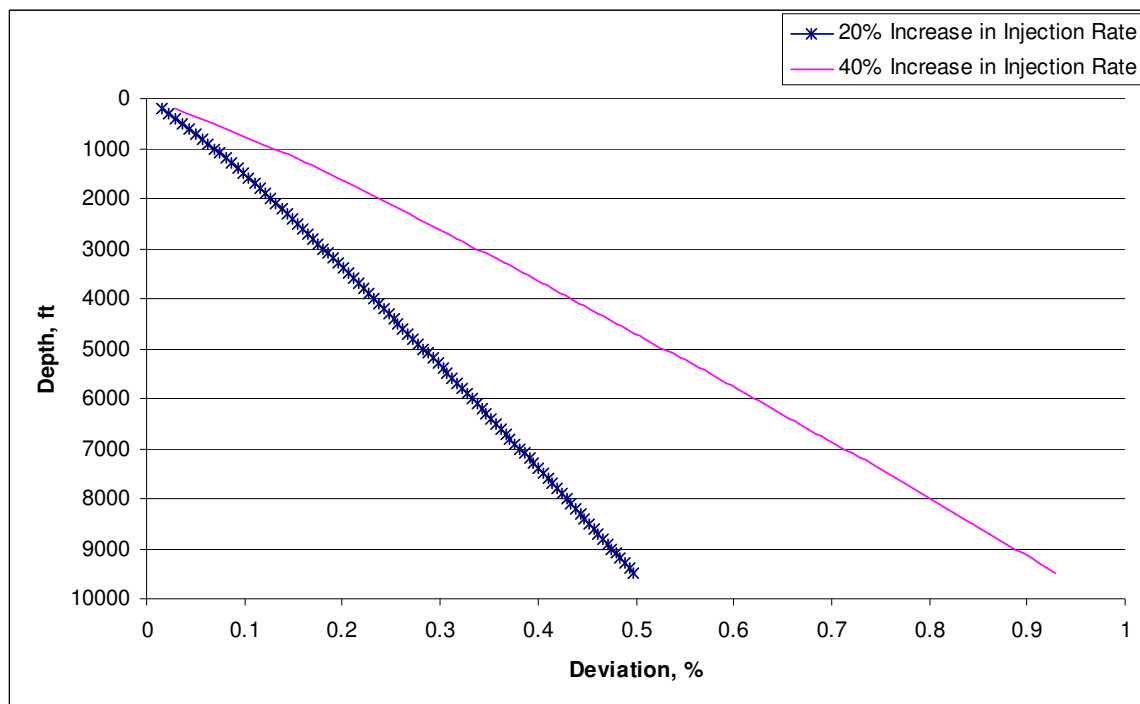


Fig. 3.61-Deviation of Quality vs. Depth (Different Injection Rates)

It can be seen in **Fig. 3.62** that increasing the injection rate dramatically increases the foam velocity and decreases the friction factor.

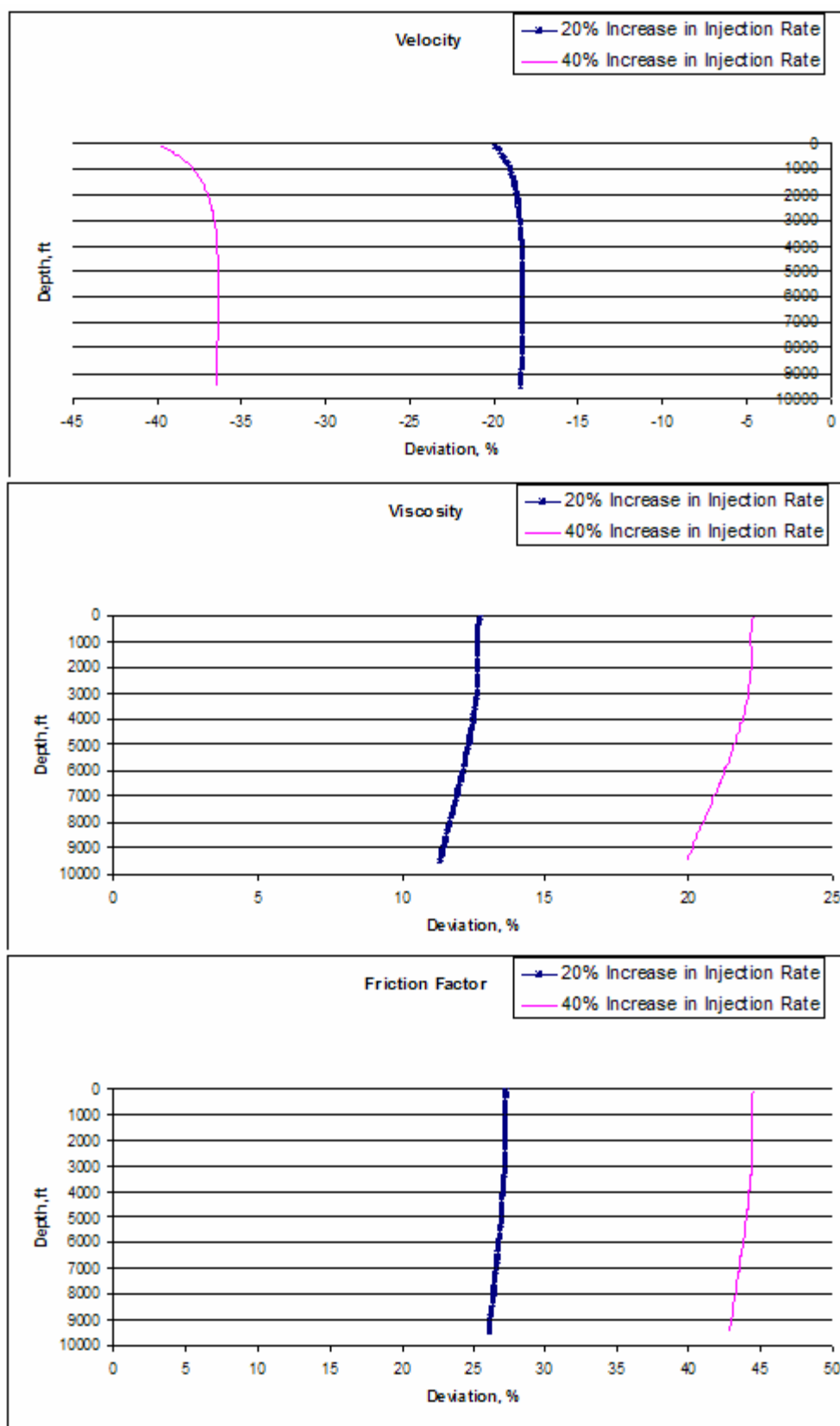


Fig. 3.62-Deviation of Flow Properties vs. Depth (Different Injection Rates)

Table 3.7-Summary of Results (Deviations for Injection Rate)

		Pressure	Gas Injection Rate	Quality	Velocity	Viscosity	Moody Friction
20% Increase in Injection Rate	<i>% Deviation at Surface</i>	-0.3	-20	0	-20	13	27
	<i>% Deviation at Bottom</i>	-1.8	-22	0.5	-19	12	26
40% Increase in Injection Rate	<i>% Deviation at Surface</i>	-0.5	-41	0	-40	22	45
	<i>% Deviation at Bottom</i>	-3.5	-45	0.95	-36	20	44

The summary of the deviation graphs is given in **Table 3.7**. The negative deviation represents an increase in the parameter.

Summary

The effects of some important parameters such as; back-pressure, ROP, cuttings concentration, cuttings size, formation water influx, and injection rate; on pressure, injection rate, and velocity are investigated. The effect of each parameter on the drilling operation conditions is summarized in the tables below;

Table 3.8- Summary of Effects of Parameters on the Pressure

Parameters in order of effectiveness		Back-pressure	Inj. Rate	Cutt. Size	Cutt. Conc.	ROP	Formati on Influx
20% Increase	% Deviation at Surface	(17)	(0.3)	(0.2)	(0.1)	(0.05)	(0.2)
	% Deviation at Bottom	2	(1.8)	(1.4)	(1)	(0.7)	(0.2)
40% Increase	% Deviation at Surface	(38)	(0.5)	(0.4)	(1)	(0.1)	(0.35)
	% Deviation at Bottom	3	(3.5)	(2.65)	(2.5)	(1.4)	(0.35)

Table 3.9-Summary of Effects of Parameters on the Gas Injection Rate

Parameters in order of effectiveness		Inj. Rate	Cutt. Size	Cutt. Conc.	Back-pressure	ROP	Formati on Influx
20% Increase	% Deviation at Surface	(20)	(18)	(7)	2	(4)	(4)
	% Deviation at Bottom	(22)	(17)	(12)	18	(8)	(2)
40% Increase	% Deviation at Surface	(41)	(37)	(17)	3	(9)	(6.5)
	% Deviation at Bottom	(45)	(35)	(31)	20	(17)	(4)

Note that from the parameters discussed above only the back-pressure and the injection rate are controlled by the operator. The best practice for successful foam drilling operation is to follow these steps;

Step I: Run the simulator to determine the minimum required back-pressure.

Step II: Check the bottom-hole pressure;

- If the pressure at the bottom needs to be increased then increase the injection rate or increase the back-pressure by more than 50%.
- If the pressure at the bottom needs to be decreased then decrease the injection rate or increase the back-pressure by less than 50%.

Note:

- The model calculates the minimum required back-pressure hence it is not possible to decrease the back-pressure.
- The minimum required injection rate for successful removal of cuttings varies with the back-pressure.
- At a specific back-pressure the injection rate should not be less than the minimum required injection rate calculated by the model.
- Increasing the injection rate decreases the foam quality. Hence, foam quality should be monitored while increasing the injection rate.

Selection of the optimum back-pressure and injection rate is a very complicated matter. Some restrictions such as; wellbore stability, wellbore washout, and economical considerations play an essential role in optimization of foam drilling operations.

CHAPTER IV

HEAT TRANSFER

Development of Model

Heat transfer in the wellbore takes place in radial and vertical directions. Radial conduction occurs between the fluid inside the drill pipe, annulus fluid, and formation. Vertical convective heat transfer occurs within the flowing drilling fluid. **Fig. 4.1** shows a control volume in the flowing fluid.

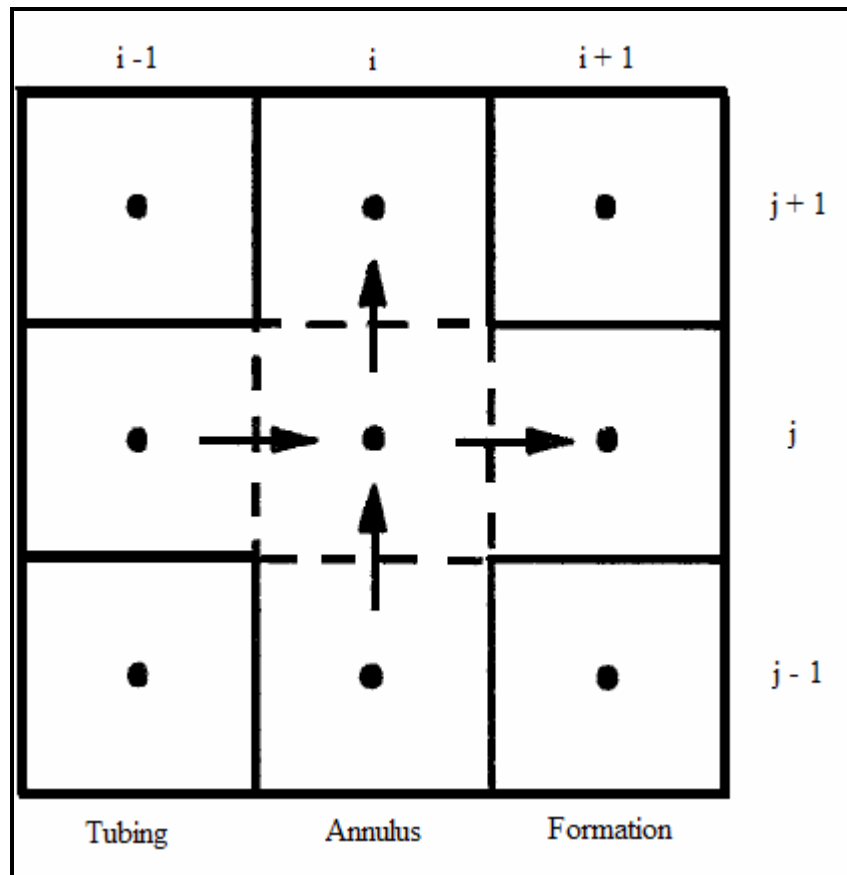


Fig. 4.1-Control Volume in the Flowing Fluid

In the control volume of flowing fluid, the wellbore is divided in three regions. The heat transfer model is formulated by performing an energy balance on a volume in the center. The radial direction is represented by index, i, and index, j, represents the vertical direction along the wellbore. The temperature nodes are located at the center of the cells. The governing heat transfer equations written in discretized form are obtained as;

In radial direction, conductive heat is transferred into and out of the central cell, and the net heat accumulation in the cell (i , j) is expressed as;

$$\Delta E_{i,j}^c = U_{i-\frac{1}{2},j} A_{i-\frac{1}{2},j} (T_{i,j}^{n+1} - T_{i-1,j}^{n+1}) - U_{i+\frac{1}{2},j} A_{i+\frac{1}{2},j} (T_{i+1,j}^{n+1} - T_{i,j}^{n+1}), \dots\dots\dots(4.1)$$

where,

ΔE^c = Net conductive heat accumulation

U = Overall heat transfer coefficient

A = Surface area of borders between the cells

In the vertical direction, the convective heat is transferred into and out of the central cell, and the net heat accumulation in the cell (i , j) is expressed as;

$$\Delta E_{i,j}^f = QC_{p,i,j} (T_{i,j}^{n+1} - T_{i,j-1}^{n+1}) + U_{i,j+\frac{1}{2}} A_{i,j+\frac{1}{2}} (T_{i,j}^{n+1} - T_{i,j+1}^{n+1}) - U_{i,j-\frac{1}{2}} A_{i,j-\frac{1}{2}} (T_{i,j-1}^{n+1} - T_{i,j}^{n+1}), \dots\dots\dots(4.2)$$

where,

ΔE^f = Net forced convective heat accumulation

Q = Fluid flow rate

C_p = Specific heat

The energy accumulation in the central cell is given as;

$$\Delta E_{i,j}^e = \frac{(mC_p)_{i,j}}{\Delta t} (T_{i,j}^{n+1} - T_{i,j}^n), \dots\dots\dots(4.3)$$

where,

ΔE^e = Net energy accumulation

m = Mass

Δt = Time interval

In steady-state conditions there would be no energy accumulation in the cell and the value for **Eq. 4.4** is zero.

Accounting for external heat sources such as; heat generated by flow friction and mechanical work of the bit, the net energy balance at the cell (i , j) is;

$$\Delta E_{i,j}^c + \Delta E_{i,j}^f + \bar{E}^m = \Delta E^e, \dots\dots\dots(4.4)$$

where,

\bar{E}^m = External mechanical and frictional energy

Substituting **Eq. 4.4** for **Eq. 4.1-3** and rearranging yields;

$$\bar{A}T_{i-1,j}^{n+1} + \bar{B}T_{i+1,j}^{n+1} + \bar{C}T_{i,j}^{n+1} + \bar{D}T_{i,j-1}^{n+1} + \bar{E}T_{i,j+1}^{n+1} = T_{i,j}^n + \bar{E}^m, \dots\dots\dots(4.5)$$

where,

$\bar{A}, \bar{B}, \bar{C}, \bar{D},$ and \bar{E} are temperature coefficients in energy balance equations.

The temperature coefficients are calculated from thermal properties and cell dimensions.

Eq. 4.5 gives the heat balance correlation over the entire model along the wellbore.

The first step to solve **Eq. 4.5** is to determine the temperature coefficients. The coefficient \bar{A} which represents the radial conduction between the drill pipe and the annulus is calculated as;

$$\bar{A} = -U_{i-\frac{1}{2},j} A_{i-\frac{1}{2},j} \left(\frac{\Delta t}{mC_p} \right), \dots\dots\dots(4.6)$$

Heat transfer between the downward flow in pipe and the upward flow in annulus can be treated as counter-flow heat transfer in heat exchangers. Hence, the overall heat transfer coefficient is written as;

$$\frac{1}{U_{i-\frac{1}{2},j}} = \frac{r_o}{r_i} \frac{1}{h_{f_{Pipe}}} + \frac{r_o}{k} \ln\left(\frac{r_o}{r_i}\right) + \frac{1}{h_{f_{Ann}}}, \dots\dots\dots(4.7)$$

where,

$h_{f_{Pipe}}$ = Foam heat transfer coefficient in pipe

$h_{f_{Ann}}$ = Foam heat transfer coefficient in annulus

r_o = Pipe outer radius

r_i = pipe inner radius

And the surface area between cell (i-1, j) and cell (i, j) is;

$$A_{i-\frac{1}{2},j} = 2\pi r_{o_{Pipe}} \Delta z, \dots\dots\dots(4.8)$$

where,

$r_{o_{Pipe}}$ = Pipe outer radius

Δz = Vertical length interval

The coefficient \bar{B} represents the radial heat conduction between the annulus and formation through the casing. The coefficient \bar{B} is calculated as;

$$\bar{B} = U_{i+\frac{1}{2},j} A_{i+\frac{1}{2},j} \left(\frac{\Delta t}{mC_p} \right), \dots\dots\dots(4.9)$$

where the overall heat transfer coefficient and the surface area of border between cell (i, j) and cell (i+1, j) are respectively;

$$\frac{1}{U_{i+\frac{1}{2},j}} = \frac{1}{h_{f_{Ann}}} + \frac{r_o}{k} \ln \left(\frac{r_o}{r_i} \right), \dots\dots\dots(4.10)$$

$$A_{i+\frac{1}{2},j} = 2\pi r_i \Delta z, \dots\dots\dots(4.11)$$

where,

r_o = Casing outer radius

r_i = Casing inner radius

The coefficient \bar{C} represents the both radial heat conduction and vertical heat convection into and out of the center cell (i, j). The coefficient \bar{C} is calculated as;

$$\bar{C} = \left[-U_{i-\frac{1}{2},j} A_{i-\frac{1}{2},j} - U_{i+\frac{1}{2},j} A_{i+\frac{1}{2},j} - \rho q C_p - U_{i,j-\frac{1}{2}} A_{i,j-\frac{1}{2}} - U_{i,j+\frac{1}{2}} A_{i,j+\frac{1}{2}} + \frac{mC_p}{\Delta t} \right] \left(\frac{\Delta t}{mC_p} \right), \dots\dots\dots(4.12)$$

where, the overall heat transfer coefficients for vertical heat conduction into and out of the cell (i, j) are written as;

$$U_{i,j-\frac{1}{2}} = U_{i,j+\frac{1}{2}} = k, \dots\dots\dots(4.13)$$

where,

k = Foam heat conductivity

And the surface area of the borders between the central cell and upper or lower cells is expressed as:

$$A_{i,j-\frac{1}{2}} = A_{i,j+\frac{1}{2}} = \frac{\pi(R^2 - r^2)}{\Delta z}, \dots\dots\dots(4.14)$$

where,

R = Casing inner radius

r = Pipe outer radius

Coefficients \bar{D} and \bar{E} are calculated as;

$$\bar{D} = \left[\rho q C_p + U_{i,j-\frac{1}{2}} A_{i,j-\frac{1}{2}} \right] \left(\frac{\Delta t}{m C_p} \right), \dots\dots\dots(4.15)$$

$$\bar{E} = U_{i,j+\frac{1}{2}} A_{i,j+\frac{1}{2}} \left(\frac{\Delta t}{m C_p} \right) \dots\dots\dots(4.16)$$

In order to determine the coefficients \bar{A} , \bar{B} , \bar{C} , \bar{D} , and \bar{E} , it will be necessary to achieve certain values of foam heat transfer coefficient and foam conductivity at any depth along the wellbore. Considering the fact that foam heat transfer coefficient and foam conductivity vary with foam quality, there is a need to establish a correlation between these parameters and foam quality. No guidelines have yet been developed on how to correlate foam heat transfer coefficient and heat conductivity with foam properties. Clearly, further work is required to estimate parameters of heat transfer phenomena when dealing with foam.

Bit Mechanical Energy

Considering the fact that foam has much lower heat capacity compared to conventional mud, bit mechanical energy plays a significant role in foam temperature analysis.

Bit mechanical energy analysis can be categorized in two distinct types: diamond bits and tricone bits. Energy analysis for each type is brought separately in the following text.

Diamond bits

The friction between diamonds and the formation generates significant amounts of heat. The rate of heat generated by the friction between the wear flat surface of the bit and the rock is presented by Memarzadeh and Miska³² as;

$$Q_{bit} = \frac{\mu_b WOB (D^2 + Dd + d^2) N}{74.3(D + d)}, \dots\dots\dots (4.17)$$

where,

Q_{bit} = Heat generated by the bit

μ_b = Coefficient of friction between the bit and the formation

WOB = Weight on bit

D = Bit outside diameter

d = Bit inside diameter

N = Rotary Speed

Tricone bits

Tricone bits are more common in foam drilling operations. Pessier and Fear³³ have developed a model to calculate the bit mechanical energy. The model was designed for tricone bits but, it is also applicable for diamond bits. They presented their model as below;

$$E = 1.285 \times 10^{-3} (E_s - \sigma) ROP * A_b, \dots\dots\dots (4.18)$$

where,

E = Heat loss

E_s = Specific energy

σ = Compressive strength of rock

ROP = Rate of penetration

A_b = Borehole area

Teale³⁴ derived the following equation for specific energy used in **Eq. 4.18**;

$$E_s = \frac{WOB}{A_b} + \frac{120\pi NT}{A_b ROP}, \dots\dots\dots (4.19)$$

where,

N = Rotary speed

T = Torque at the bit

Solution

Once coefficients and heat generated by the bit have been computed, it is time to solve the **Eq. 4.5** by using FDM. **Eq. 4.5** can be presented in the matrix form of:

$$A'x = B', \dots\dots\dots (4.20)$$

where,

A' = Matrix of coefficients

x = Vector of unknown temperatures at the current time-step

B' = Vector of calculated temperatures at the previous time-step

The best approach to solve **Eq. 4.20**, is to solve the system of equations simultaneously using an iterative solution method.

CHAPTER V

CONCLUSIONS AND RECOMMENDATIONS

Conclusions

1. A computer code is developed to process the data and accurately simulate the pressure during drilling a well using foam drilling fluids.
2. The developed model simulates the borehole pressure based on the minimum required back-pressure at the surface.
3. Successful removal of cuttings is guaranteed by the determination of the minimum required injection rates at any surface back-pressure.
4. The results are presented by both the tables and figures.

Recommendations

1. The results of the simulator should be compared with the results of the other available simulators or the real data from foam drilling operations.
2. The foam drilling simulator has the potential to be used as an aerated drilling simulator. Including the aerated mud in the current simulator enables us to combine the temperature model with the pressure model.
3. The Bingham plastic behavior of foams with qualities of more than 85% should be investigated upon the availability of the foam shear stress.
4. The simulation of the foam flow in deviated and horizontal wells can be included in the current simulator.
5. Effect of formation gas influx especially in shallow wells should be investigated.
6. Additional research is required to analyze the foam heat transfer coefficient and thermal conductivity.
7. Foam heat transfer coefficient and thermal conductivity should be determined by either experimental procedures or simulation of the real data obtained by MWD.

8. Some uncertainties about the foam rheology still exist; more investigation on rheological properties of the different types of foams would increase the accuracy of the foam drilling simulators.

NOMENCLATURE

A = Annulus area, in²

A_b = Borehole area, in²

$A_{i,j}$ = Surface area of borders between the cells, ft²

C_p = Cuttings concentration, %

C_p = Specific heat, Btu/ft-hr-°F

$C_{P_{Foam}}$ = Heat capacity of foam, Btu/ft-hr-°F

$C_{P_{Gas}}$ = Heat capacity of gas, Btu/ft-hr-°F

$C_{P_{Water}}$ = Heat capacity of water, Btu/ft-hr-°F

D = Tube inside diameter, in

D_H = Hydraulic diameter, ft

D = Bit outside diameter, in

D_s = Cuttings equivalent diameter, ft

D_H = Conduit hydraulic diameter, ft

d = Pipe inside diameter, in

d = Bit inside diameter, in

d_h = Hole diameter, in

E = Heat loss, Btu/hr

E_s = Specific energy, psi

\bar{E}^m = External mechanical and frictional energy, Btu/hr

f = Moody friction factor, dimensionless

$g = 32.2$, ft/s²

$g_c = 32.2$, ft/s²

$h_{f_{Ann}}$ = Foam heat transfer coefficient in annulus, Btu/ft²-hr-°F

$h_{f_{Pipe}}$ = Foam heat transfer coefficient in pipe, Btu/ft²-hr-°F

K = Consistency index

k = Foam heat conductivity, Btu/hr-ft

L = Conduit length, ft

LVF = Liquid Volume Fraction, dimensionless

M = Gas molecular weight, lb_m

m = Mass, lb_m

m_g = Mass of gas, lb_m

m_l = Mass of liquid, lb_m

N = Rotary Speed, rpm

P = Pressure at any point, lb/ft^2

P_{bh} = Bottom-hole pressure, psia

P_s = Pressure at surface, lb/ft^2

Q = Fluid flow rate, ft^3/sec .

Q_{bit} = Heat generated by the bit, Btu/hr

Q_f = Formation fluid influx rate, bbl/hr

Q_{gs} = Gas injection rate, Sft^3/min

Q_l = Liquid injection rate, gal/min

R = Casing inner radius, in

Re = Reynolds number, dimensionless

ROP = Rate of penetration, ft/hr

R_p = Rate of penetration, ft/hr

r = Pipe outer radius, in

r_i = pipe inner radius, in

r_i = Casing inner radius, in

r_o = Pipe outer radius, in

$r_{o_{Pipe}}$ = Pipe outer radius, in

r_o = Casing outer radius, in

T = Torque at the bit, ft-lbf

T = Temperature at any point, $^{\circ}\text{R}$

T_s = Temperature at surface, $^{\circ}\text{R}$

U = Overall heat transfer coefficient, $\text{Btu/ft}^2\text{-hr-}^{\circ}\text{F}$

V = Gas volume at any point, ft^3

V_f = Formation fluid influx volume, ft^3

V_g = Gas volume, ft^3

V_l = Liquid volume, ft³

V_s = Gas volume at surface, ft³

v = Velocity, ft/sec.

v = Bulk velocity, ft/sec.

\bar{v} = Average foam velocity, ft/sec

v_f = Foam velocity, ft/sec.

v_n = Nozzle velocity, ft/sec.

v_{sl} = Cuttings settling velocity, ft/sec.

v_{tr} = Terminal velocity, ft/sec

WOB = Weight on bit, lbf

\dot{w} = Mass flow rate, lb_m/hr

ΔE^c = Net conductive heat accumulation, Btu/hr

ΔE^e = Net energy accumulation, Btu/hr

ΔE^f = Net forced convective heat accumulation, Btu/hr

ΔP_b = Pressure drop across the bit, psia

Δt = Time interval, hr

Δz = Vertical length interval, ft

Γ = Foam quality, dimensionless

γ = Wall shear rate, sec⁻¹

γ_f = Specific weight of foam, lb/ft³

μ_a = Apparent Viscosity, lb/ft-sec

μ_b = Coefficient of friction between the bit and the formation, lb/ft-sec

μ_e = Effective foam viscosity, lb/ft-sec

μ_e = Effective viscosity, lb/ft-sec

μ_F = Foam viscosity, lb/ft-sec

μ_o = Bingham Viscosity, lb/ft-sec

μ_e = Effective Viscosity, cp

μ_p = Plastic Viscosity, lb/ft-sec

μ_u = Base liquid viscosity, lb/ft-sec

$\bar{\rho}$ = Average foam density, lb/ft³

ρ_f = Foam density, lb/ft³

σ = Compressive strength of rock

τ_w = Wall shear stress, lb/ft²

τ_y = Yield strength, lb/ft²

τ_{yp} = True yield point stress, lb/ft²

REFERENCES

1. Hutchison, S.O.: "Foam Workovers Cut Costs 50%," *World Oil* (January 1969) 33.
2. Medley, G.H., Cohen, J.H., Maurer, W.C., and McDonald, W.J.: "Development and Testing of Underbalanced Drilling Products," final report, Contract No. DE-AC21-94MC31197, U.S. DOE, Morgantown, West Virginia (September 1995).
3. Sibree, J.O.: "The Viscosity of Froth," *Faraday Soc. Trans.* (1934) **30**,325.
4. Grove, C.S.: "Viscosity of Fire Fighting Foams," *Ind. Eng. Chem.* (1951) **43**, 1120.
5. Fried, A.N.: "The Foam Drive for Increasing the Recovery of Oil," U.S.B.M. Report of Investigation No. 5866 (1961).
6. Raza, S.H., and Marsden, S.S.: "The Streaming Potential and the Rheology of Foam," *SPE J.* (1967) **7**, 4.
7. David, A., and Marsden, S.S.: "The Rheology of Foam," paper SPE 2544 presented at the 1969 SPE Annual Meeting, Denver, 28-30 September.
8. Blauer, R.E., Mitchell, B.J., Kohlhaas, C.A.: "Determination of Laminar, Turbulent, and Transitional Foam Flow Losses in Pipes," paper SPE 4885 presented at the 1974 SPE Annual California regional Meeting, San Francisco, 4-5 April.
9. Mitchell, B.J.: "Test Data Fill Theory Gap on Using Foam as a Drilling Fluid," *Oil and Gas J.* (1979).
10. Beyer, A.H., Millhone, R.S., and Foote, R.W.: "Flow Behavior of Foam as a Well Circulating Fluid," paper SPE 3986 presented at the 1972 SPE Annual Conference and Exhibition, San Antonio, Texas, 8-11 October.
11. Reidenbach, V.G., Harris, P.C., Lee, Y.N., and Lord, D.L.: "Rheology Study of Foam Fracturing Fluids Using Nitrogen and Carbon Dioxide," paper SPE 12026 presented at the 1983 Technical Conference and Exhibition, San Francisco, 5-8 October.

12. Sanghani, V.: "Rheology of Foam and its Implications in Drilling and Cleanout Operations," M.S. thesis, U. of Tulsa, Tulsa, Oklahoma (1982).
13. Ozbayoglu, M.E., Kuru, E., Miska, S., and Takach, N.: "A Comparative Study of Hydraulic Models for Foam Drilling," paper SPE 65489 presented at the 2000 Horizontal Well Technology Conference, Calgary, Alberta, Canada, 6-8 November.
14. Krug, J.A, and Mitchell, B.J: "Charts Help Find Volume Pressure Needed for Foam Drilling," *Oil and Gas J.* (February 7, 1972) **61**.
15. Blauer, R.E., and Kohlhaas, C.A.: "Formation Fracturing with Foam," paper SPE 5003 presented at the 1974 SPE Annual Meeting, Houston, 6-9 October.
16. Okpobiri, G.A., and Ikoku, C.U.: "Volumetric Requirements for Foam and Mist Drilling Operations," paper SPE 11723 presented at the 1983 SPE California Regional Meeting, Ventura, 23-25 March.
17. Guo, B., Miska, S., and Hareland, G.: "A Simple Approach to Determination of Bottom Hole Pressure in Directional Foam Drilling," *ASME Drilling Technology*, (February 1988), **65**, 329.
18. Lord, D.L.: "Mathematical Analysis of Dynamic and Static Foam Behavior," paper SPE 7927 presented at the 1979 SPE Symposium on Low Permeability Gas Reservoirs, Denver, 20-22 May.
19. Spoerker, H.F., Trepess, P., Valko, P., Economides, M.J.: "System Design for the Measurement of Downhole Dynamic Rheology for Foam Fracturing Fluids," paper SPE 22840 presented at the 1991 SPE Technical Conference, Dallas, 6-9 November.
20. Liu, G., and Meldy, G.H.: "Foam Computer Model Help in Analysis of Underbalanced Drilling," *Oil and Gas J.* (1996) **94**, No. 27, 114.
21. Gardiner, B.S., Dlugogorski, B.Z., and Jameson, G.J.: "Rheology of Fire Fighting Foams," *Fire Safety J.* (May 1998) 61-75.
22. Guo, B., Sun, K., and Ghalambor, A.: "A Closed Form Hydraulics Equation for Predicting Bottomhole Pressure in UBD With Foam," paper SPE 81640 presented at the 2003 Underbalanced Technology Conference, Houston, 25-26 March.

23. Farris, R.: "A Practical Evaluation of Cements for Oil Wells," *Drilling and Production Practice*, API (1941) 283.
24. Edwardson, M.J., Girner, H.M., Parkinson, H.R., Williams, C.D., Matthews, C.S.: "Calculation of Formation Temperature Disturbance Caused by Mud Circulation," paper SPE 124 presented at the 1961 SPE Annual Meeting, Dallas, 8-11 October.
25. Crawford, P.B., Tragesser, A.F., Crawford, H.R.: "A Method for Calculating Circulating Temperatures," paper SPE 1484 presented at the 1966 SPE Annual Meeting, Dallas, 2-5 October.
26. Holmes, C.S., and Swift, S.C.: "Calculation of Circulating Mud Temperatures," paper SPE 2318 presented at the 1968 SPE Annual Meeting, Houston, September 29-October 2.
27. Keller, H.H., Couch, E.J., Berry, P.M.: "Temperature Distribution in Circulating Mud Columns," *SPE J.* (June 1970) 23-30.
28. Marshall, T.R. and Lie, O.H.: "A Thermal Transient Model of Circulating Wells," paper SPE 24290 presented at the 1992 European Petroleum Computer Conference, Stavanger, Norway, 25-27 May.
29. Guo, B.: "Use of Spreadsheet and Analytical Models to Simulate Solid, Water, Oil and Gas Flow in Underbalanced Drilling," paper SPE 72328 presented at the 2001 Middle East Drilling Technology Conference, Bahrain, 22-24 October.
30. Moore, L.: *Drilling Practices Manual*, Petroleum Publishing Co., Tulsa, Oklahoma (1974) 228-239.
31. Gou, B., Ghalambor, A.: *Gas Volume Requirements for Underbalanced Drilling*, Penn Well Co., Tulsa, Oklahoma (2002).
32. Memarzadeh, F.D., Miska, S.: "Numerical Simulation of Diamond-Bit Drilling With Air," SPE paper 12908 presented at the 1984 SPE Rocky Mountain Regional Meeting, Casper, Wyoming, 21-23 May.
33. Pessier, R.C., and Fear, M.J.: "Quantifying Common Drilling Problems with Mechanical Specific Energy and a Bit-Specific Coefficient of Sliding Friction," paper SPE 24584 presented at the 1992 SPE Technical Conference and Exhibition, Washington, DC, 4-7 October.

34. Teale, R.: "The Concept of Specific Energy in Rock Drilling," *Intl. Rock Mech. Mining Sci. J.* (1965) **2**, 57-73.

VITA

Name: Amir Saman Paknejad

Address: 1100 Hensel Drive. Apt. X4G
College Station, TX, 77840.

Email Address: amirsaman@tamu.edu

Education: B.S., Petroleum Engineering, Petroleum University of
Technology, Iran, 1998
M.S., Petroleum Engineering, Texas A&M University,
2005